CHARACTERIZING THE IMPACT OF HOST AND TUMOR AUTOPHAGY DEFICIENCY ON THE DEVELOPMENT OF ANTI-TUMOR IMMUNITY

by

DANIEL WILLIAR SHARP

A Dissertation submitted to the

School of Graduate Studies

Rutgers, The State University of New Jersey,

in partial fulfillment of the requirements for the degree of

Doctor of Philosophy

Graduate Program in Microbiology and Molecular Genetics

Written under the direction of

Edmund Lattime

And approved by

_____

_____

_____

_____

New Brunswick, NJ

October, 2018

ABSTRACT OF THE DISSERTATION

CHARACTERIZING THE IMPACT OF HOST AND TUMOR AUTOPHAGY DEFICIENCY ON THE DEVELOPMENT OF ANTI-TUMOR IMMUNITY

By DANIEL SHARP

Dissertation Director:

Edmund Lattime

Macroautophagy is an important cellular pathway in cancer metabolism with significant impacts on tumor growth and on the development and maintenance of antitumor immune responses. Clinical trials inhibiting autophagy to control tumor growth have shown promising results, but greater understanding of the role of autophagy in anti-tumor immunity is crucial in order to achieve successful therapies. Using CRISPR-Cas9 technology we targeted the key autophagy gene *Atg7* and generated Atg7+/+ and Atg7Δ/Δ clones of the male murine urothelial carcinoma tumor line MB49 to examine the importance of functional tumor autophagy on anti-tumor immunity. Deletion of *Atg7* led to a number of immune effects in one MB49 clone that generated a significantly stronger anti-tumor immune response compared to Atg7+/+ clones, but the heterogeneity of additional Atg7Δ/Δ clones showed no consistent effects. We next examined the importance of functional host autophagy by using an inducible murine model of *Atg7* deletion, and found that whole body inhibition of autophagy led to immune-mediated rejection of multiple cell lines. MB49 was rejected completely in Atg7-deleted female

mice (Cre.Atg7Δ/Δ)—with significantly decreased growth in male mice—but not in Atg7-competent mice (Cre.Atg7+/+). Depletion of T-cells by intraperitoneal (i.p.) injection of monoclonal antibodies specific to CD4 and CD8 led to complete rescue of MB49 tumor growth, with most of the effect found in CD4 depletion. The male murine melanoma tumor line YUMM1.1 had similar results when grown in female but not male Cre.Atg7Δ/Δ mice. Having previously shown that regulatory T-cells (Tregs) control MB49 growth we investigated whether autophagy dysfunction impacted the Treg population size or function. The number of Tregs was unchanged between Cre.Atg7+/+ and Cre.Atg7Δ/Δ in both the spleen and tumor, but analysis of RNA expression (Nanostring) revealed decreased Treg signal in the MB49 tumors of Cre.Atg7Δ/Δ mice amid a general upregulation of the immune response. Depletion of Tregs by i.p. injection of a monoclonal antibody specific to CD25 (PC61) led to rejection of MB49 in Cre.Atg7+/+ mice similar to the rejection of untreated tumors in Cre.Atg7Δ/Δ mice. These studies demonstrate the significant impact autophagy can have on immunity, and support the hypothesis that autophagy deficiency can improve tumor outcomes by modulating the immune response.

ACKNOWLEDGEMENTS

Firstly, I thank Dr. Edmund Lattime, my mentor, for the support and guidance over the years as I've worked on my PhD. His knowledge, expertise and guidance have been crucial during my studies. I also thank Dr. Claude Monken, lab manager and fellow researcher in the Lattime lab for his support and technical assistance. Special thanks go to past lab member Christiaan de Vries, who taught me several of the key assays described here.

I also wish to acknowledge and thank Joshua Vieth, of the Sant'Angelo lab, and Dr. Andrew Zloza and members of his lab for their assistance and instruction on flow cytometry and other immunology protocols. Special thanks to Praveen Bommareddy of the Zloza lab for his collaboration on our Nanostring experiments, and Salvatore Aspromonte and Jenna Newman of the Zloza lab for their help with antibody selection and flow cytometry protocols.

This research would not have been possible without the excellent collaboration of Dr. Eileen White and many members of her lab. Special thanks go to Laura Poillet Perez for her aid in providing the genetic mice and YUMM1.1 cells needed for our experiments, as well as her assistance with immunoblotting techniques. And many thanks to Xiaoqi Xie for her work in producing the CRISPR-Cas9 MB49 clones.

I thank the members of my research committee: Dr. Lisa Denzin, Dr. Lori Covey, Dr. Eileen White and Dr. Edmund Lattime. Their constructive critiques, experimental ideas and suggestions, and general support were invaluable.

Finally, I thank my wife for her unending support, sacrifice, counsel, and care as I've worked on my PhD. Without her at my side, I could not have accomplished what I have.

This work was made possible by support from the Rutgers Cancer Institute of New Jersey, the Rutgers Graduate School of Biomedical Sciences, and NIH Grant R01CA42908.

TABLE OF CONTENTS

LIST OF ILLUSTRATIONS

LIST OF TABLES

INTRODUCTION

With the development of cutting edge immunotherapies like checkpoint blockade inhibitors showing success in clinical trials, with active research into combining immunotherapy with conventional chemotherapies, basic research into understanding how the immune system interacts with these other therapies is crucial. This dissertation details studies conducted on the interaction of the metabolic process of autophagy and the development of an anti-tumor immune response in a syngeneic murine model of urothelial carcinoma. Herein, we describe the creation of autophagy-deficient tumor cell lines to investigate the impact of tumor-cell autophagy on the development of anti-tumor immune responses. We then utilize an inducible murine model of autophagy-deficiency to characterize the impact of host-autophagy on the development of anti-tumor immunity. Finally, we use monoclonal antibodies to deplete important T cell populations to further characterize the role of host-autophagy on tumor immunity. It is our hope that the findings reported herein will advance the field of cancer immunotherapy and contribute translatable knowledge to inform cancer treatments.

Principles of Autophagy

Autophagy (from the Greek "αυτο + φαgεῖν", meaning self-eating) refers to three distinct intracellular pathways: macroautophagy, microautophagy and chaperone-mediated autophagy. All end in lysosomal degradation of intracellular material, but differ in the functional mechanisms leading up to it. Macroautophagy is the predominant autophagic pathway in mammals, is commonly (and hereafter) referred to as autophagy, and is the focus of this dissertation. Autophagy is a highly conserved catabolic process by which cells can capture and degrade intracellular components, including damaged

organelles, proteins and lipids, and even invading pathogens[1]. It does this by sequestering organelles (such as mitochondria) and cytosol into a double-membraned vesicle called an autophagosome. The autophagosome can then fuse with a lysosome, creating an autolysosome and exposing its contents to hydrolases that will break them down into recyclable macromolecules[2-6].

Autophagy has a basal level of constitutive expression that promotes cellular health and homeostasis by eliminating old and damaged organelles, turning over long-lived proteins, and clearing out protein aggregates. Along with autophagy's general bulk actions, it can also be selective, using ubiquitin tagging or adapter protein binding to target specific substrates to autophagosomes via receptor recognition and binding[7-9]. It can be induced by certain environmental stresses, including starvation, hypoxia, infection by pathogens, radiation, oxidative stress, and certain chemical compounds (such as some anti-cancer drugs)[10-12]. This upregulation of autophagy is normally cytoprotective, as it provides substrates for synthesis pathways and energy production during starvation, and can remove cellular components damaged by the stressors[13,14]. Dysfunction and dysregulation of autophagy is associated with a variety of pathologies including cancer[15], neurodegeneration[16], autoimmune disorders[17], microbial infections[18], and even heart disease[19].

The mechanisms of autophagy are quite complex, requiring dozens of proteins to facilitate the formation of the autophagosome and subsequent conjugation with lysosomes[5]. One of these proteins, ATG7, is required for the formation of the core autophagy machinery, where it functions to enable the conjugation of ubiquitin-like proteins that act during the expansion of the phagophore membrane[20]. While alternative

autophagy pathways that do not require ATG7 exist[21-23], ATG7 is required for the more common canonical pathway[24], and deletion of the *Atg7* gene in mice prevents autophagy's functions[25].

Autophagy and Cancer

Paradoxically, autophagy can have both tumor preventative and tumor promoting effects[26,27]. By clearing out damaged and defective proteins and organelles, autophagy prevents toxicity to cells and tissues, and helps block the development of a tumorigenic inflammatory state[15,28,29]. Autophagy also helps prevent genomic instability and subsequent tumorigenesis[30,31]. Autophagy's roles in the adaptive immune response (to be discussed in more detail below) can also affect tumor development[32,33]. In established tumors, however, it is clear that autophagy can improve tumor survival[34,35], and several tumors have been shown to require autophagy[36-38]. Tumors exist in metabolically stressful envinronments of starvation and hypoxia, and have increased metabolic demand due to their rapid proliferation[15]. Autophagy can provide the energy and substrates needed for tumor survival in these stressful conditions[10]. It is also believed that autophagy may have both pro- and anti-metastatic functions depending on the situation[39]. In accordance with these contradictory roles, both autophagy inhibitors and inducers have been studied as cancer therapeutics, with promising results in each category[34,40]. Multiple trials combining autophagy modulation with chemotherapeutics have been performed[41], with some showing very promising synergistic results[42]. Most of the tested combination treatment regimens have focused the combination of autophagy inhibition with cytotoxic chemotherapeutics, but the best results will likely require accounting for the impact of autophagy on the immune system[43].

Principles of Autophagy and Immunity

One specific way in which autophagy may contribute to tumor suppression is via its role in the immune system[33]. Autophagy is involved in innate immunity[44-46], where it can be induced by pattern recognition receptors[47,48], eliminate intracellular pathogens[18,49,50], and regulate inflammatory signaling[51-54]. Autophagy also has significant roles in adaptive immunity, including anti-cancer immunity. It has been shown that functional autophagy in tumor and other antigen donor cells is crucial for efficient uptake and presentation by antigen presenting cells (APCs) like dendritic cells (DCs), likely through the pathway of autophagic cell death[50,52]. Autophagy is also important for DCs to be able process and present antigen[55-57], especially for cross presentation[58-60]. This is important in developing an immune response because MHC-I canonically only presents endogenous antigens derived from the cell itself (like viral antigens), and MHC-II presents exogenous antigens taken up by APCs (like bacterial and tumor antigens). Since MHC-I activates CD8+ T-cells, and MHC-II activates CD4+ T-cells, efficient anti-tumor immunity requires presenting tumor antigens on both molecules via cross presentation[61,62]. Autophagy has been shown to be part of pathways cross-presenting both endogenous and exogenous antigens onto MHC-II and MHC-I proteins, respectively[58,63]. Efficient cross presentation of antigen in DCs also requires type I IFN signaling[64], which has been shown to be affected by autophagy[51,59,65].

Along with antigen presentation, autophagy is known to be required for the maintenance, function and long-term survival of immune cell populations, including T-cells[66] and B-cells[67-69], but not DCs[56,59]. This necessity was seen primarily after activation, when the immune cells adopted a long-lasting memory phenotype[70]. In mature

memory T-cells, the requirement for autophagy is believed to be due to their switch from aerobic oxidative phosphorylation to anaerobic glycolysis, a metabolic change that depends on functional autophagy[66,71]. Autophagy also affects a variety of other essential metabolic processes in mature T cells[72,73]. Since functional autophagy has beneficial homeostatic effects, long term inhibition of autophagy in cells may lead to accumulation of toxic byproducts that can prove lethal to cells[74].

Of specific import to this dissertation is the role of functional autophagy in regulatory T cells (Tregs). Tregs are a subset of CD4+ T cells that function as potent suppressors and inhibitors of the immune response, and have been shown to be recruited and activated by tumors as a mechanism of immune escape[75]. Other groups have shown that not only do Tregs have significantly upregulated autophagy compared to naïve CD4+ cells[76], but congenic disruption of *Atg7* within Tregs led to a profound loss of Tregs in mice[77]. Wei et al. showed that when activated, Tregs require autophagy to maintain cellularity and survival, and that deletion of *Atg7* in Tregs actually led to suppression of key Treg transcription factor FoxP3[76]. Modulation of Treg function by inhibition of autophagy can thus have profound impacts on cancer immunity.

Oncolytic virus cancer therapy

A growing field of cancer research and therapy makes use of oncolytic viruses (OVs) in both pre-clinical animal models and clinical trials with patients[78,79]. OVs were of interest initially because of their preferential infection and lysis of tumors[80], but research has shown that in addition to direct killing of tumor cells, OVs can induce an anti-tumor response in the host[81] This anti-tumor response is mediated by a range of pro-inflammatory signals released by active viral infection in the tumor microenvironment[80],

as well as OV subjecting tumor cells to immunogenic cell death[82]. In addition, OVs are amenable to recombinant technology, allowing "arming" with both pro-inflammatory cytokines like GM-CSF as well as tumor associated antigens (TAAs), improving their ability to direct anti-tumor immune responses[83-85]. One OV therapeutic has even received FDA approval for cancer treatment[86,87].

The OV pertinent to this dissertation is vaccinia virus (VV), a member of the poxvirus family and the active constituent of the smallpox vaccine[88,89]. VV is amenable to genetic engineering to produce recombinant vaccines encoding a variety of proteins[90] , including GM-CSF[91]. It has also been used successfully in clinical cancer trials[92-94], where it has been tolerated rather well and has successfully induced immune responses[95-97]. VV can induce a variety of immunogenic cell death pathways in tumor cells[98], including autophagic cell death[82]. Pertinent to the work presented here, previous work by our lab found that VV does not require functional cellular autophagy in order to replicate[99].

HY, a strong surrogate antigen

In order to study the immunological mechanisms behind anti-tumor immune responses, researchers often make use of surrogate antigens, or "non-self" tumor antigens, instead of "self" TAAs. Surrogate antigens generally induce stronger and more reliable responses than self TAAs, allowing study of the mechanisms involved in immunity[100,101]. However, studies and therapies developed using surrogate antigens do not translate as well to self TAAs, as surrogate antigens are often xenogeneic, hyper-immunogenic proteins instead of the mutated or overexpressed "self" proteins that are actually TAAs[102 103]. Despite this weakness, surrogate antigens are still useful.

In our lab we make use of the male murine minor histocompatibility antigens known as HY as a surrogate antigen for our research. The term HY is used to signify the collection of genes on the Y-chromosome of mice that are strongly immunogenic[104,105] and mediate the rejection of male murine tissue upon transplantation into female mice[106-108]. Several of the immunodominant epitopes that constitute the HY have been discovered[109], including the MHC-I associated peptide Uty[110], and the MHC-II associated peptide Dby[111]. Priming of female mice to HY has proven effective at inducing an anti-HY immune response and subsequently rejecting a tumor of male origin[112]. Previous work by our lab generated VVs expressing Uty and Dby for use in the MB49 tumor model[113].

The MB49 tumor model and Tregs

The MB49 tumor was derived from male C57BL/6 murine bladder epithelial cells treated with the carcinogen 7,12-dimethylbenz(a)anthracene. It is a heterogenous cell line containing many mutations, and also expresses HY, making it a good candidate for our work. Previous work by our lab has shown that despite expression of HY, female C57BL/6 (fB6) mice are unable to reject MB49 or prime an HY-specific IFN-γ response, because of MB49's ability to induce the generation of IL-10 by infiltrating immune cells[114]. When grown in IL-10 knockout female mice, however, MB49 did prime for a specific anti-tumor immune response. Earlier work had demonstrated that MB49 can be induced to express MHC-II *in vitro* via stimulation by IFN-γ, indicating a possible means by which MB49 could interact with IL-10 producing immune cells[115]. Further work characterized how this IL-10 signaling induced by MB49 prevented DCs from stimulating and activating both CD4+ and CD8+ T cell responses[116]. Intratumoral—but

not systemic—vaccination with a cocktail of VVs expressing the dominant immunoepitopes of HY, as well as GM-CSF, in combination with the immune adjuvant keyhole limpet hemocyanin (KLH)—hereafter termed VV-HY—was shown to be able to overcome the immune inhibition of MB49 and generate a HY-specific response that significantly prolonged survival[112]. Finally, our lab showed that the inhibitory effects of Tregs were the mechanism by which MB49 evaded the immune response[113]. Treatment with a monoclonal antibody to CD25 (PC61) to deplete Tregs *in vivo* significantly reduced MB49 growth (**Figure 1A**) and allowed the generation of specific anti-HY CD8 CTL responses (**Figure 1B**). Infiltrating Tregs from the tumors of untreated mice were shown to produce significant amounts of IL-10 upon stimulation with the MHC-II immunodominant epitope of HY, Dby (**Figure 1C**), and suppressed the proliferation of effector T cells (**Figure 1D**). Together these data indicate that MB49 is capable of immune evasion via the specific action of Tregs, and that depletion of Tregs is sufficient for the successful immune-mediated rejection of MB49.

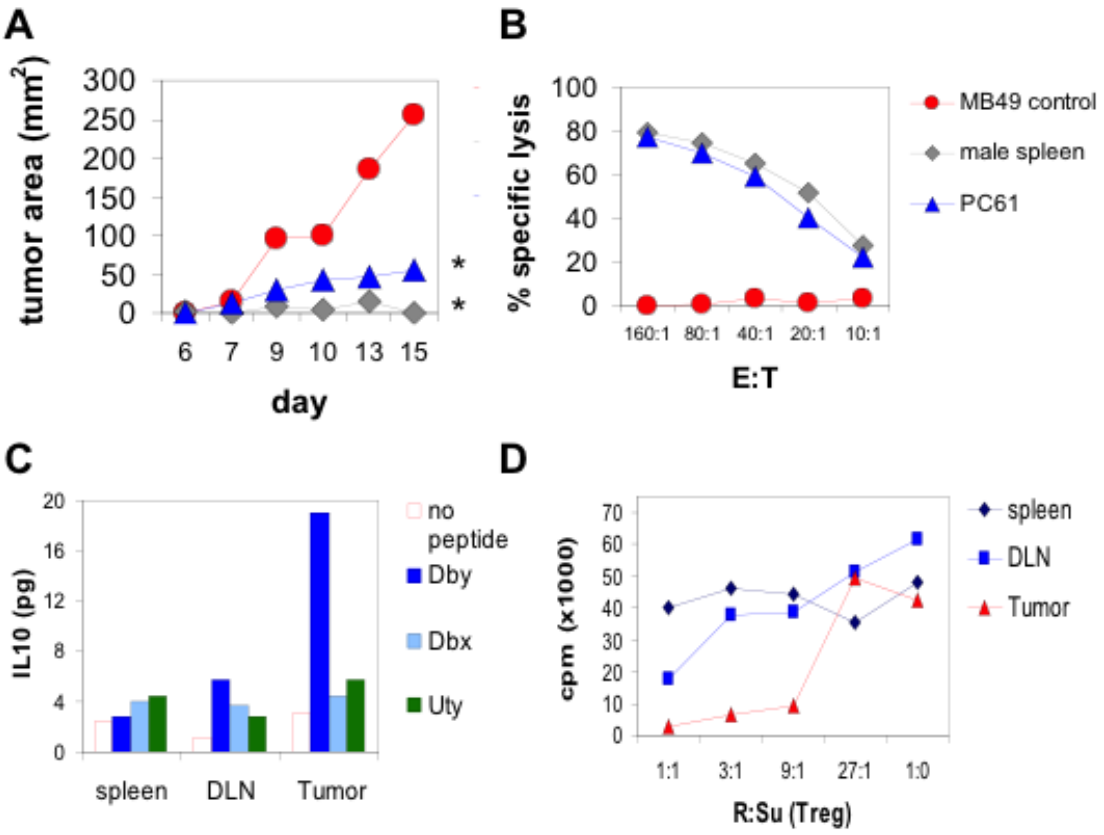

Figure 1. Tregs are crucial to MB49 immune escape. Prior to being inoculated with MB49, fB6 mice were treated with PC61 or immunized with irradiated male splenocytes. Tumor area was measured over time (**A**), and splenocytes from the mice were restimulated with irradiated male splenocytes *in vitro* and used in a CTL assay against MB49 (**B**). Tregs isolated by a CD25+ magnetic bead kit were stimulated with the indicated peptides and IL-10 expression measured by ELISA (**C**). Splenocytes from MB49 bearing fB6 were cultured with irradiated BALB/c splenocytes, with Tregs isolated from the indicated tissues of MB49-bearing fB6 added in and a ^{3}H suppression assay performed (**D**). Data from Figure 1 was provided by previous work in our lab[113]. (Student's T-test * $P<0.05$)

The Ubc-CreERT2/+;Atg7flox/flox mouse construct

The work in this dissertation relies on the Ubc-CreERT2/+;Atg7flox/flox and Ubc-CreERT2/+;Atg7WT/WT mouse lines developed and provided by our collaborators in the White lab[117]. With the addition of Tamoxifen (TAM), the Cre-rcombinase is activated to delete a large section of the key autophagy gene *Atg7* globally within the mice and generate Cre.Atg7Δ/Δ mice (**Figure 2**). TAM treatment of the Ubc-CreERT2/+;Atg7WT/WT generated Cre.Atg7+/+ mice that can be used as wild-type controls for the autophagy-deficient mice. Previous work by the White lab has used these mice to successfully model the metabolic impacts of autophagy on glucose homeostasis and lung tumor maintenance [117]. In collaboration with them we here use it to study the impact of autophagy disruption on the development of anti-tumor immune responses.

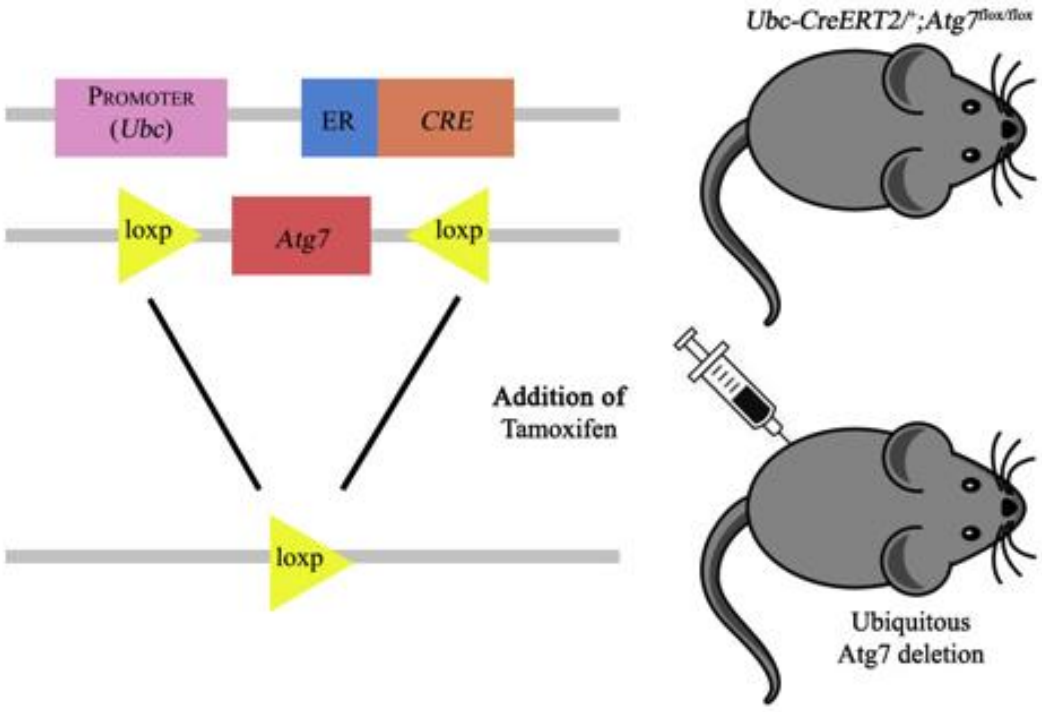

Figure 2. Ubc-CreERT2/+;Atg7flox/flox mouse construct. Crossbreeding of Ubc-CreERT2/+ and Atg7flox/flox mice as described in the methods generates an inducible model of autophagy disruption. The addition of TAM deletes *Atg7* throughout the entire host, including immune cell populations.

RATIONALE

Though autophagy is primarily a metabolic process, a growing body of evidence points to an often-contradictory role in the context of cancer and immunity. While functional autophagy can help prevent the development of cancer, it can also support cancer growth and metabolism, leading to the chemotherapeutic targeting of autophagy in ongoing clinical trials. Furthermore, autophagy has shown to be both an indirect and direct regulator of immunity, impacting the health and survival of multiple immune cell populations, the presentation of antigen, and production of immune modulating cytokines. Given prior studies demonstrating the efficacy of autophagy inhibition on cancer treatment and the hypothesis that such inhibition could impact the development of anti-tumor immune responses, it is reasonable to specifically disrupt autophagy via the deletion of a key autophagy gene like *Atg7* and measure the effect this has on the development of a specific immune response. Therefore, the experiments described in this dissertation had the following specific aims:

1) Determine the importance of tumor cell autophagy by deleting *Atg7* with CRISPR-Cas9 in the well-characterized MB49 urothelial carcinoma and determine the impact on the generation of specific anti-HY T cell responses.

2) Evaluate how global disruption of *Atg7* in host tissues modulates the development of anti-tumor immune responses against MB49 and other tumor lines, with specific focus on CD4+ and CD8+ T cell responses and the induction of inhibitory Tregs.

We hypothesized that specific deletion of *Atg7* in the MB49 tumors line would result in a systemic immune response by altering the presentation of antigen to immune cells. Furthermore, we hypothesized that acute deletion of *Atg7* globally would alter the composition of tumor infiltrating immune cells and overcome immune escape mechanisms such as Tregs.

MATERIALS AND METHODS

Cell Culture

Splenic cell cultures were maintained in T cell media (TCM) composed of RPMI-1640 (Sigma-Aldrich, St. Louis, MO) supplemented with 10% FBS, 2mM L-glutamine, 1mM Na pyruvate, 50 IU/mL penicillin/streptomycin, 50μM 2-mercaptoethanol (2-ME), 0.5x MEM amino acids solution, and 100μM MEM nonessential amino acids solution (Sigma-Aldrich). The MB49 tumor [7,12-dimethylbenz(a)anthracene-induced urothelial cell line derived from male C57BL/6 murine bladder epithelial cells] was provided to Dr. Edmund Lattime by Dr. Timothy Ratliff when at Washington University (St. Louis, MO). MB49 was maintained in a 37ºC, 5% CO2 incubator in RPMI 1640 (Life Technologies, Inc., Rockville, MD) supplemented with 10% fetal bovine serum (FBS), 2 mM L-glutamine, and 50 IU/ml penicillin/streptomycin. YUMM 1.1 and YUMM1.7 cells (derived from BrafV600E/WT, Pten-/-, Cdkn2-/- C57Bl/6J mouse melanomas)[118] were cultured in Dulbecco's minimum essential medium and Ham's F12 (DMEM-F12) (10-092-CV, Corning) supplemented with 10% FBS (F0926, Sigma) in a 5% CO2 incubator at 37°C.

Recombinant vaccinia virus treatment

VV-βGal, VV-GMCSF, VV-Uty and VV-Dby were created by our lab previously and grown and maintained by Dr. Claude Monken as previously described[112]. A treatment cocktail (designated VV-HY) consisting of 2.5x10^6 plaque-forming units (PFUs) of VV-GMCSF, 2.5x10^6 PFUs of VV-Uty and 2.5x10^6 PFUs VV-Dby, along with 7.5 μg of KLH (Sigma, St. Louis, MO) was used in animal experiments, with 100 μL of VV-HY in PBS injected intratumorally within 1 week of tumor inoculation, with a second dose administered intratumorally 2 weeks later.

Animal Models

All animal care and treatments were carried out in compliance with Rutgers University Institutional Animal Care and Use Committee guidelines. Four to 6-week old male and female C57BL/6 (B6) mice syngeneic to the MB49 and YUMM1.1 and YUMM1.7 tumors (Jackson Labs, Bar Harbor, ME) were maintained in a HEPA-filtered cage system for at least 1 week prior to use. Ubc-CreERT2 mice[119] (Jackson Laboratory, Bar Harbor, ME) and Atg7flox/flox mice[25] (provided by Dr. M. Komatsu, Tokyo Metropolitan Institute of Medical Science) were cross-bred by Dr. Eileen White's lab to generate Ubc-CreERT2/+;Atg7flox/flox mice[117]. Acute deletion of *Atg7* throughout the mouse is achieved after injection of Tamoxifen (TAM). TAM (T5648, Sigma) was suspended at a concentration of 20 mg/ml in a mixture of 98% sunflower seed oil and 2% ethanol, and 200 ml per 25 g of body weight and was injected intraperitoneally into 8 to 10 week old male and female Ubc-CreERT2/+;Atg7+/+ or Ubc-CreERT2/+;Atg7flox/flox mice once per day for 4 days to generate groups of *Atg7* deleted (Cre.Atg7Δ/Δ) and wild type (Cre.Atg7+/+) mice.

MB49 (2.5x10^5 cells), YUMM1.1 (1x10^6 cells) and YUMM1.7 (1x10^5 cells) cells were resuspended in 100 mL PBS and injected subcutaneously (s.c.) into the left groin or the dorsal flanks of mice. Depending on experimental design tumors were measured for two to for weeks before mice where sacrificed and tissues collected.

Monoclonal antibody for T cell depletion

A week post TAM, two days before tumor injection and every five days, 200 μg of CD4 (clone GK1.5; BE003-1, BioXCell) and CD8 (clone 2.43; BE0061, BioXCell) antibodies were injected intraperitoneally into Cre.Atg7Δ/Δ and Cre.Atg7+/+ mice. For Treg-

specific depletion, four days before tumor injection and every 7 days, 250 μg of anti-CD25 (clone PC61.5.3; BE0012, BioXCell) antibody was injected intraperitoneally into Cre.Atg7Δ/Δ and Cre.Atg7+/+ mice.

Restimulation and CTL Assays

CTL assays were performed as previously described[112,120]. Briefly, spleens from mice were removed and homogenized, with red blood cells lysed using ammonium chloride buffer (ACK buffer, 0.15M NH4Cl, 1.0mM KHCO3, 0.1mM EDTA), washed with TCM and filtered through a 70 μm nylon mesh (BD Biosciences, San Jose, CA). Effector cells were then resuspended at 7x10^6 cells/mL and cultured with 3x10^6 irradiated (25 Gray) splenocytes from naïve male C57BL/6 mice. Restimulation culture was in a total of 2mL of TCM + 2-ME in 24-well plates for 5 days at 37°C, 5% CO2. On day 3 of restimulation, supernatant was harvested and used in a n IFN-γ ELISA. On day 5, stimulated effector cells were collected and cultured for 4 hours with $_{51}$Cr-labeled target MB49 or YUMM1.7 cells. Samples were spun down briefly and 100 μL of supernatant was removed and $_{51}$Cr release from target cells was measured wit ha gamma counter (Packard Bioscience, Meriden, CT). Percent specific cytotoxicity was calculated with the formula:

$$\frac{Experimental\ release\ -\ Spontaneous\ release}{Maximum\ release\ -\ Spontaneous\ release} * 100\%$$

Where “Spontaneous release” is defined as the count when target cells were not cultured with any effector cells, and “Maximum release” when target cells were cultured with Triton X-100.

IL-10 production by Tregs

Tregs were isolated from splenocytes and tumors using a mouse CD4+CD25+ Regulatory T Cell Isolation Kit (Miltenyi Biotec, Auburn, CA) according to manufacturers instructions. Isolated Tregs were cultured with PMA (20 ng/mL), Ionomycin (1 μg/mL), and Brefeldin A (10 μg/mL) for 4-6 hours, then stained for intracellular IL-10 accumulation via flow cytometry.

IFN-γ ELISA

ELISA was performed as previously described[121]. Briefly, rat anti-mouse IFN-γ monoclonal antibody (BD Biosciences, San Jose, CA was suspended in coating buffer (NaHCO3) at 2 μg/mL and incubated overnight at at 4°C in 96 well immunoplates (Nalgene-Nunc, Penfield, NY). Wells were blocked with 200μL PBS/10%FBS for 2 hours at room temperature. Standards and sample were added at 100μL per well in PBS/10%FBS and incubated overnight at 4°C. Wells were washed with PBS/0.05% Tween-20 (Thermo Scientific, Waltham, MA) and biotinylated anti-mouse IFN-γ (BD Biosciences) was suspended at 1μg/mL in PBS/10% FBS and incubated at room temperature for 45min. Wells were washed and incubated with 100 μL avidin-peroxidase (Sigma-Aldrich) at 2.5μg/mL in PBS/10% FBS for 30 minutes at room temperature. Enzymatic activity was determined using O-phenylenediamine dihydrochloride substrate (OPD, Sigma-Aldrich) dissolved at 1mg/mL citrate buffer (pH 4.5) with 3% H_2O_2. Color reaction was stopped with 3M HCl and read at 492 nm using a Victor plate reader (Perkin-Elmer, Waltham, MA).

Flow Cytometry analysis

Tumors were homogenized in PBS in a gentleMACS Octo Dissociator (Miltenyi Biotec Inc) according to manufacturer's protocol, and passed through a 70 mm cell restrainer. Spleens were ground with a rubber grinder through steel mesh, treated with ACK Lysis

Buffer to remove erythrocytes and passed through a 70 mm cell restrainer. Nonspecific binding of antibodies to cell Fc receptors was blocked using 20 mL/107 cells of FcR blocker (Miltenyi Biotec Inc). Cell surface immunostaining was performed with the following antibodies purchased from eBioscience: CD25-PE, CD11c-PE-eFluor610, NK1.1-PerCP-Cy5.5, CD4-APC, CD3-AF700, CD11b-APC-Cy7; and the following antibodies from BioLegend: CD45-FITC, MHC-II-BV605, Ly6G-BV650, Ly6C-BV711, CD8-BV785. Aqua Live/Dead (Invitrogen) was included to determine live cells. After staining of surface markers, cells were fixed and permeabilized using BD Bioscience's Transcription Factor staining kit and stained with FoxP3-eFluor450 from eBioscience. Cell staining data were acquired using a LSR-II flow cytometer (BD Biosciences) and analyzed with FlowJo software (Tree Star). Live lymphocytes were gated using forward scatter area (FSC-A) versus side scatter area (SSC-A), followed by FSC-A versus forward scatter height (FSC-H), SSC-A versus side scatter height (SSC-H) plots, forward scatter width (FSC-W) versus side scatter width (SSC-W), and Aqua Live/Dead. Populations were gated as follows: CD45 (%CD45+ of total live lymphocytes), CD3 (%CD3+ of CD11b-, CD11c-, CD45+), CD8 (%CD8+ of CD3), CD4 (%CD4+ of CD3), Treg (%FoxP3+ of CD4), DC (%CD11c+ of MHC-II+, CD45+), MDSC (%Ly6G, CD11b+ of MHC-II-, CD45+).

Immunohistochemistry Staining

Mouse tissues were fixed in 10% buffer formalin solution overnight and then transferred to 70% ethanol for paraffin-embedded sections. Tissue sections were deparaffinized, rehydrated and boiled for 45 min in 10 mM pH 6 Citrate buffer. Slides were blocked in 10% goat serum for an hour and then incubated at 4˚C overnight with primary antibody

against CD4 (1:1,000, Ab183685, Abcam), CD8 (1:100, 14-0808-82, Invitrogen), or FoxP3 (1:100, 14-5773-82, eBiosciences). The following day, tissue sections were incubated with biotin-conjugated secondary antibody for 15min (Vector Laboratories), 3% hydrogen peroxide for 5 min, horseradish peroxidase streptavidin for 15 min (SA-5704, Vector laboratories) and developed by 3,3-diaminobenzidine (Vector Laboratories) followed by hematoxylin staining (3536-16, Ricca). Sections were then dehydrated, mounted in Cytoseal 60 mounting medium (8310, Thermo Scientific) and analyzed using Nikon Eclipse 80i microscope. For quantification of IHC, at least 15 images were analyzed at 60X magnification for each genotype.

Western Blotting

Tissues and tumor samples were ground in liquid nitrogen, lysed in Tris lysis buffer (50 mM Tris HCl, 150 mM NaCl, 1 mM EDTA, 0.1% NP40, 5 mM MgCl2, 10% glycerol), separated on 12.5% SDS-PAGE gel and then transferred on PVDF membrane (Millipore). Membranes were blocked with 5% non-fat milk for 1 hour and probed overnight at 4˚C with antibodies against ATG7 (1:2000, A2856, Sigma), LC3 (1:3000, NB600-1384, Novos Biological) and β-actin (1:5000, A1978, Sigma). Immunoreactive bands were detected using peroxidase-conjugated antibody (GE Healthcare) and enhanced chemiluminescence detection reagents (NEL105001EA, Perkin Elmer) and were analyzed using the ChemiDoc XRS+ system (Biorad).

CRISPR-Cas9

CRISPR-Cas9 deletion of *Atg7* was performed according to established protocols[122]. Briefly, primers were designed to target the following underlined regions of Atg7 and delete a significant portion of the exon:

CCCTGGACGTTGGCTTCTGGCACGAACTGACCCAGAAGAAGTTGAACGAGTACCGCCTGG
GGGACCTGCAACCGAAGACCGTGCTTGACTGGGTCTTCTTCAACTTGCTCATGGCGGACC

Transfected cells were selected for and sorted into single cells by fluorescent assisted cell sorting, and productive colonies were isolated for further growth and analysis. Disruption of *Atg7* was confirmed by sequencing of the gene and Western blot against the ATG7 protein.

Nanostring

Tumors were harvested total RNA was isolated using Qiagen RNAeasy kit. Gene expression analysis was performed using NanoString PanCancer Immune Profiling Panel (XT-CSO-MIP1-12, NanoString). For each sample 50 ng of total RNA in a final volume of 5 μl was mixed with a 3′ biotinylated capture probe and a 5′ reporter probe tagged with a fluorescent barcode from the custom gene expression code set. Probes and target transcripts were hybridized overnight at 65°C for 12-16 hours. Hybridized samples were run on the NanoString nCounter preparation station using the recommended protocol, in which excess capture and reporter probes were removed and transcript-specific ternary complexes were immobilized on a streptavidin-coated cartridge. The samples were scanned at maximum scan resolution on the nCounter Digital Analyzer. Data were processed using nSolver Analysis Software and the nCounter Advanced Analysis module. For gene expression analysis data was normalized using the geometric mean of housekeeping genes selected by the GeNorm algorithm[123].

Statistical Analysis

All statistical analyses were performed using Prism 7 software version 7.0c. Experimental data were compared as appropriate using one-way and two-way ANOVA with Turkey's Multiple Comparison tests and Sidak's Multiple Comparison tests, unpaired t tests, unpaired Welch's t test (two-tailed) and paired ratio t tests. P values of less than 0.05 were considered significant.

EXPERIMENTAL RESULTS

Chapter 1: Characterization of the immune phenotype of Atg7+/+ and Atg7Δ/Δ CRISPR-Cas9 MB49 tumor clones

Atg7Δ/Δ MB49 tumors generated with CRISPR-Cas9 technology

In collaboration with the White Lab, we utilized CRISP-Cas9 technology as described in MATERIAL AND METHODS to delete *Atg7* from the MB49 tumor line and derived single cell clones. The clone MB49-XD1 retained *Atg7* expression, MB49-XD2 was not fully deleted (either due to only losing a single allele or the clone being a mixed population), and MB49-XD3 fully lost *Atg7* expression, with no ATG7 protein production as confirmed by Western Blot (**Figure 3A**). Knowing the important role of *Atg7* in tumor metabolism, we compared the *in vitro* growth of the Atg7Δ/Δ clone MB49-XD3 with that of clones MB49-XD1 and MB49-XD2 to ensure that no gross disruption of growth had occurred (**Figure 3B**). Having observed that the 3 clones grew at similar rates *in vitro* with no difference based on *Atg7* status, we injected 250,000 cells from each clone s.c. into the left groin of female C57BL/6j mice (fB6) to evaluate any changes in *in vivo* growth. In contrast to their *in vitro* growth, the *Atg7*-deficient clones MB49-XD2 and MB49-XD3 grew significantly smaller than the parent strain MB49 and the Atg7+/+ clone MB49-XD1 (**Figure 3C**). Since MB49-XD3 grew at a slightly elevated rate compared to MB49-XD1 *in vitro*, this difference in *in vivo* growth rate was not likely due to an inherent metabolic deficiency, opening the possibility that the difference in growth was immunogenic in nature.

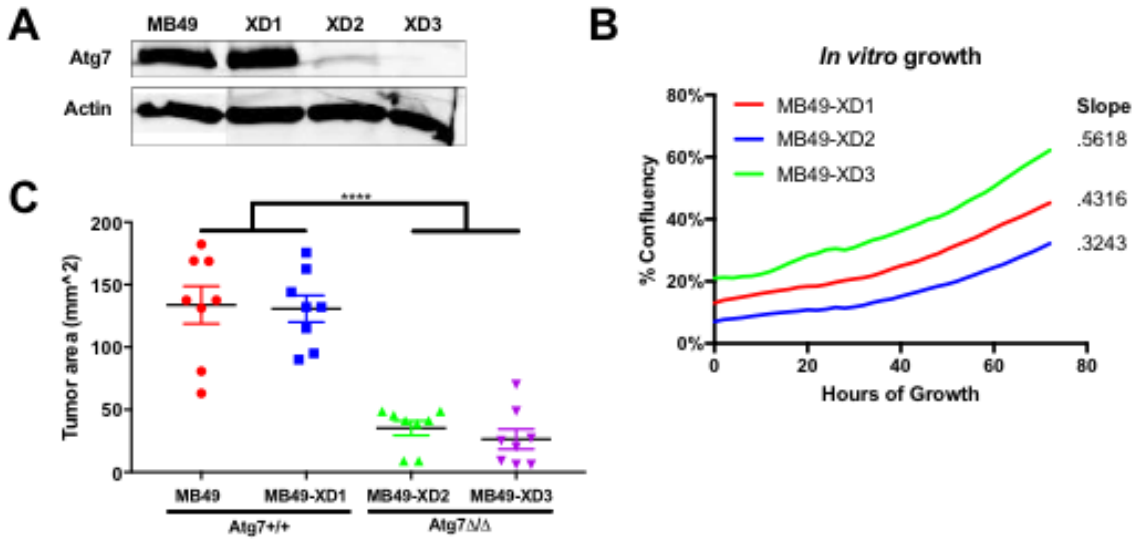

Figure 3. Atg7Δ/Δ clones XD1-XD3 of MB49 grow at similar rates in vitro but differ in vivo. *Atg7* status of the indicated MB49 clones and the parent MB49 strain was determined via Western Blot (**A**). *In vitro* cell culture confluency of the CRISPR clones was tracked over 72 hours in an IncuCyte system, and rate of growth determine via linear regression (**B**). 2.5x10^5 tumor cells of parent MB49 and the indicated CRISPR clones were injected s.c. into the left groins of fB6 mice (n=8 per group), with tumor area measured at 14 days of growth (**C**). (Turkey's multiple comparisons test; **** P <0.0001).

The decreased growth of MB49-XD3 is mediated by the immune response

To determine if the decreased *in vivo* growth of clone MB49-XD3 was due to cellular metabolic differences or immunogenic causes, we injected MB49-XD1 and MB49-XD3 s.c. into the left groins of female and male C57BL6/j mice (fB6 and mB6, respectively), and immunodeficient male NOD scid (NS) mice. While there was a

significant reduction in size of MB49-XD3 compared to MB49-XD1 when grown in mB6 for two weeks, there was no reduction in size when grown in NS mice (**Figure 4A**). The significant rescue of MB49-XD3 tumor growth in NS mice compared to fB6 and mB6 mice indicated that the suppression of MB49-XD3's growth in fB6 is mediated by the adaptive immune response.

Knowing that MB49-XD3's growth was suppressed via an adaptive immune response based on our results in NS mice, we next endeavored to determine if the adaptive response was specific to the HY antigen. Multiple independent experiments growing MB49-XD1 and MB49-XD3 in fB6 for three weeks showed that MB49-XD1 continued to grow while MB49-XD3 tumors completely regressed (**Figure 4B**). Splenocytes from tumor-bearing mice were harvested and restimulated *in vitro* with irradiated male splenocytes and used in a CTL assay against parent MB49 target cells, with effector cells from MB49-XD3-bearing mice showing consistently elevated cytotoxicity (**Figure 4C**). Supernatant from the restimulated splenocyte culture showed that MB49-XD3 lead to significantly elevated IFN-γ production compared to MB49-XD1 (**Figure 4D**). These results together indicated that fB6 generated a more effective specific anti-HY immune response against MB49-XD3 than to MB49-XD1.

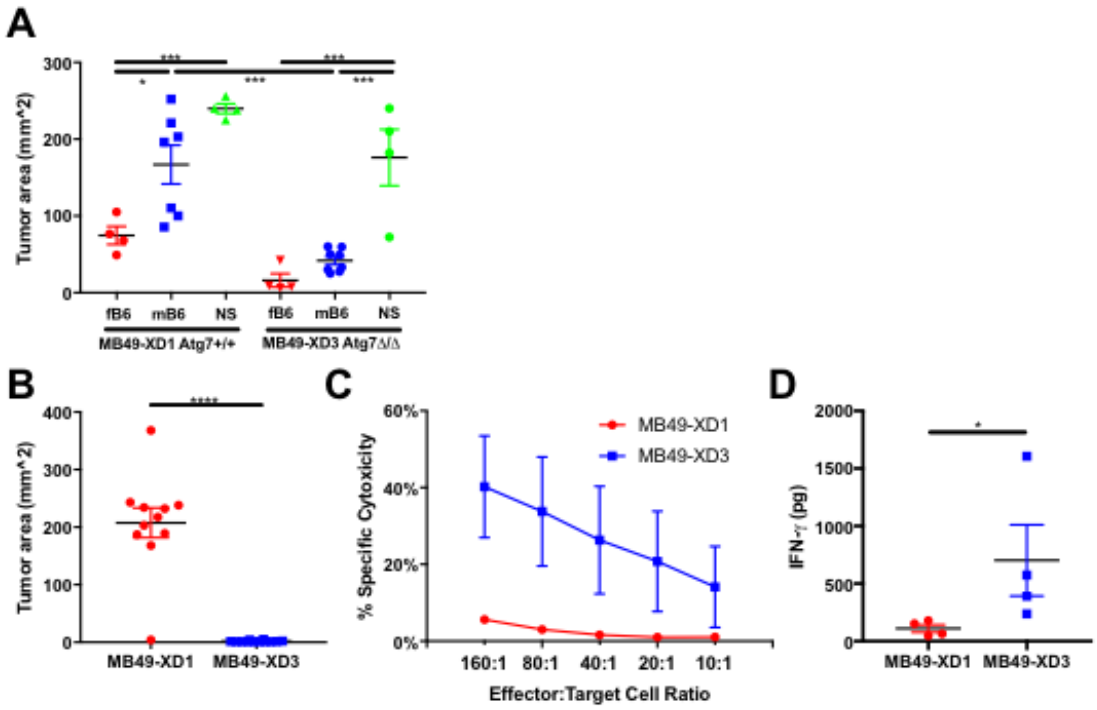

Figure 4. The decreased growth of MB49-XD3 is immunogenic. MB49-XD1 and MB49-XD3 were injected into the left groins of fB6, mB6 and NS mice and tumor area measured at two weeks of growth (**A**). Cumulative tumor area from three repeated experiments injecting MB49-XD1 (n=11) and MB49-XD3 (n=12) into the left groins of fB6 (**B**). The CTL activity of splenocytes from the three experiments in (**A**) restimulated *in vitro* with irradiated male splenocytes (**C**), and their IFN-γ production (**D**). (Turkey's multiple comparisons test (**A**), Welch's t test (**B**) and Ratio paired t test (**C**); * $P < 0.05$, *** $P < 0.001$. **** $P < 0.0001$)

Flow cytometry reveals significant differences in MB49-XD3 infiltrating lymphocytes.

Having shown that the decreased rate of growth of the Atg7Δ/Δ MB49-XD3 clone was immunogenic in nature, and that MB49-XD3 generated significant specific anti-HY immunity, we next sought to determine if this increased immunity was driven by a

change in the tumor-infiltrating-lymphocytes (TILs). Comparative analysis of MB49-XD3 compared to MB49-XD1 by flow cytometry revealed significant changes in multiple immune cell populations within the tumor microenvironment (**Figure 5A**). The ratio of CD4+ T cells in MB49-XD3 tumors was increased, while Tregs, CD8+ T cells, myeloid-derived suppressor cells (MDSCs) and DCs were significantly decreased. In addition, because of previous work by our lab showing that MB49 tumor cells are capable of expressing MHC-II when stimulated *in vitro* with IFN-γ [115], we analyzed whether MB49-XD1 and MB49-XD3 (the CD45- fraction by flow cytometry) expressed MHC-II *in vivo*, and discovered that MB49-XD1 expressed significantly more MHC-II than MB49-XD3 (**Figure 5A**).

To confirm that the lack of MHC-II expression was not simply due to the decreased size of MB49-XD3 tumors *in vivo,* we tested injecting three times the amount of MB49-XD3 cells. As expected, the tumors grew slightly larger, but growth changes did not reach significance (**Figure 5B**), and despite being slightly larger, there was no change in the *in vivo* MHC-II expression (**Figure 5C**). To determine if the decreased *in vivo* MHC-II expression by MB49-XD3 clone was due to lost genetic capacity to express MHC-II, we cultured it with IFN-γ *in vitro,* previously shown by our lab to effectively induce expression[115]. We showed that while MB49-XD3 has low MHC-II expression *in vivo*, when cultured with IFN-γ it expresses MHC-II at similar levels to MB49-XD1 (**Figure 5D**). This suggests that MB49-XD3 retains the capacity to express MHC-II, but that *in vivo,* the MB49-XD3 tumor microenvironment is such that tumor MHC-II expression is not stimulated. Given our previous and above presented work showing *in vitro* expression upon IFN-γ stimulation, we hypothesized that growth of MB49-XD3 *in*

vivo failed to generate the same signaling milieu in the tumor microenvironment, leading to the lack of MHC-II tumor expression.

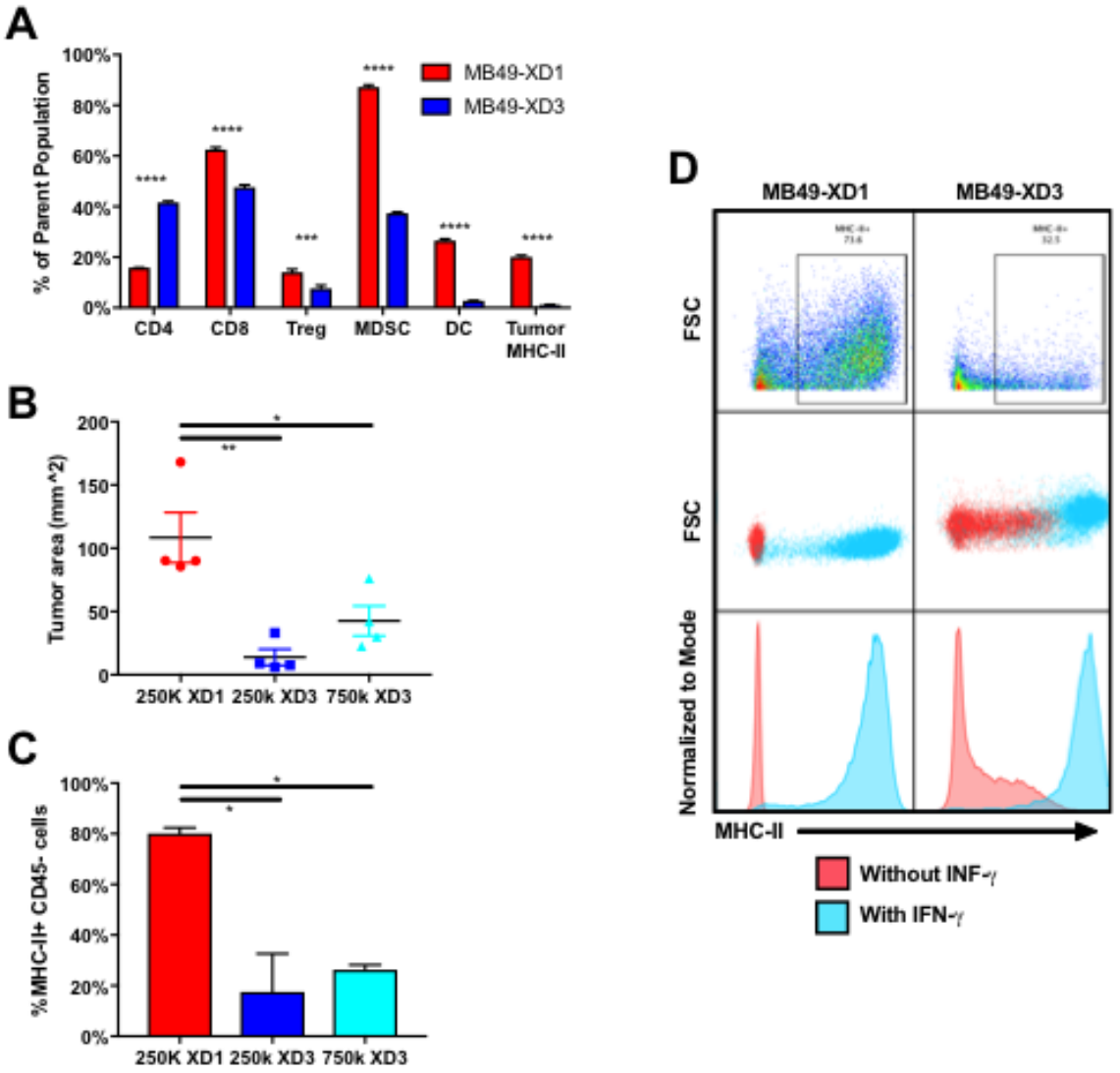

Figure 5. Flow cytometry reveals significant differences in MB49-XD3 infiltrating lymphocytes. Immune populations from MB49-XD1 and MB49-XD3 tumors grown in fB6 mice were analyzed by flow cytometry (**A**). MB49-XD1, MB49-XD3 and three times the number of MB49-XD3 cells were injected into fB6 mice, and tumor growth measured (**B**). The expression of MHC-II on CD45- tumor cells was quantified by flow cytometry, with two groups of tumors pooled from two mice each (**C**). Histograms of MHC-II

expression from MB49-XD1 and MB49-XD3 i*n vivo* (top panel) and *in vitro* (bottom panels) with and without IFN-γ stimulation (**D**). (Turkey's multiple comparisons test; * P < 0.05, ** P < 0.01, *** P < 0.001. **** P < 0.0001)

Intratumoral vaccinia treatment is effective against Atg7+/+ MB49 clone XD1 but not Atg7Δ/Δ clone XD3.

Previous work in our lab had shown that VV-HY (a cocktail of 2.5x10^6 PFUs of recombinant vaccinia viruses expressing the Y chromosome genes Uty and Dby, as well as GMCSF, with 10 ug KLH) therapy could effectively overcome a suppressive tumor microenvironment and inhibit MB49 growth and induce specific anti-tumor immunity[112]. To determine if *Atg7* deletion had any impact on the effectiveness of the viral immunotherapy, we tested the effect of VV-HY therapy on clones MB49-XD1 and MB49-XD3. We discovered that while VV-HY decreased the growth (**Figure 6A**) and increased the cytotoxicity (**Figure 6B**) of Atg7+/+ MB49-XD1 in fB6, it had no effect on Atg7Δ/Δ MB49-XD3's already decreased growth, and actually decreased the induction of specific anti-HY cytotoxicity (**Figure 6C**). These findings demonstrated added complexity of immune regulation of the tumor microenvironment and the impact of VV treatment for future study.

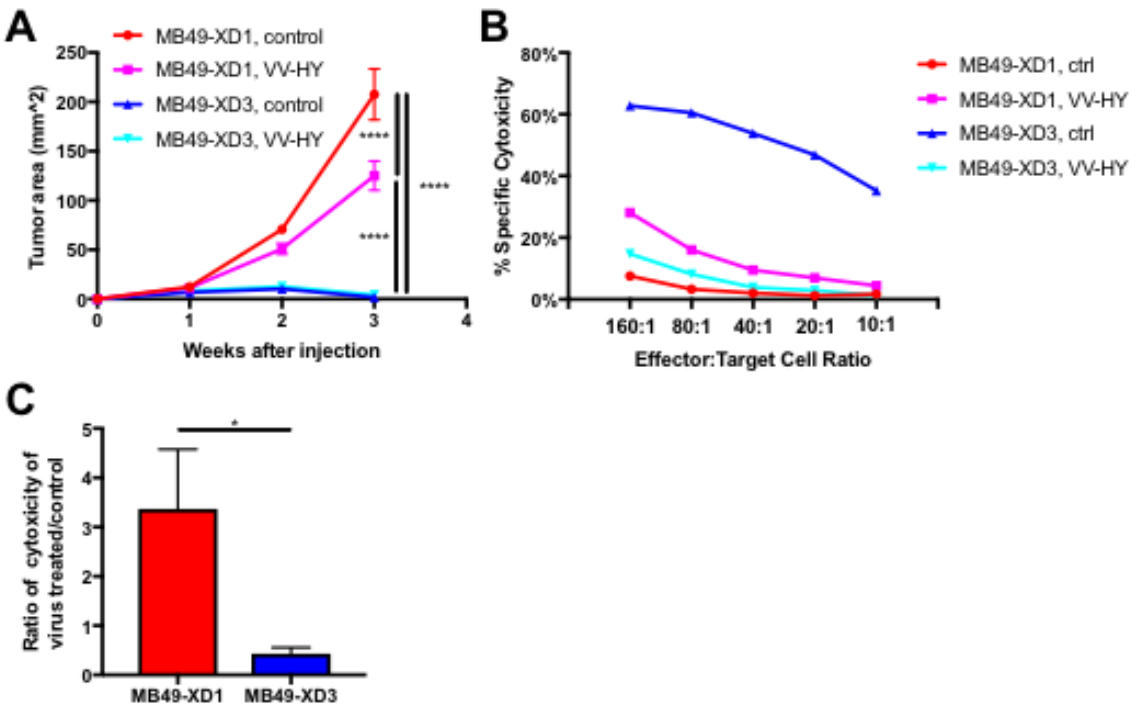

Figure 6. Intratumoral vaccinia treament decreases the anti-HY cytotoxicity generated by MB49-XD3. 2.5x10^5 MB49-XD1 and MB49-XD3 tumor cells were injected s.c. into the left groin of fB6 mice and treated intratumorally with two doses of VV-HY cocktail as described in MATERIALS AND METHODS (**A**). A representative CTL assay of splenocytes from the indicated groups, restimulated with irradiated male splenocytes and targeting uncloned MB49 cells (**B**). The ratio of the cytotoxicity of treated to untreated samples from three repeated experiments at an Effector:Target ratio of 80:1 (**C**). (Turkey's mutiple comparisons test (**A**) and Unpaired t test (**C**); * $P < 0.05$, **** $P < 0.0001$)

Heterogeneity among Atg7Δ/Δ CRISPR-Cas9 MB49 clones.

To determine if the differences between MB49-XD1 and MB49-XD3 are based on *Atg7* status or simply clonal variation, we generated additional CRISPR-Cas9 clones.

We confirmed that *Atg7* was both deleted and functionally suppressed in the Atg7Δ/Δ clones by evaluating ATG7 and LC3-II protein levels (**Figure 7A**), and that the *in vitro* growth rate of these new clones was unaffected by *Atg7* deletion (**Figure 7B**). When tested *in vivo* we found significant heterogeneity in tumor growth between Atg7+/+ and Atg7Δ/Δ clones regardless of *Atg7* status, with all the clones but one growing at similar sizes at three weeks (**Figure 7C**). There was no significant difference in growth between clones based on *Atg7* status, nor was there a consistent relationship between *Atg7* status and inducible CTL activity (**Figure 7D**). These findings demonstrated clonal variability and heterogeneity beyond simple *Atg7* status, supporting the hypothesis that the differences seen earlier in MB49-XD3 were not *Atg7* specific.

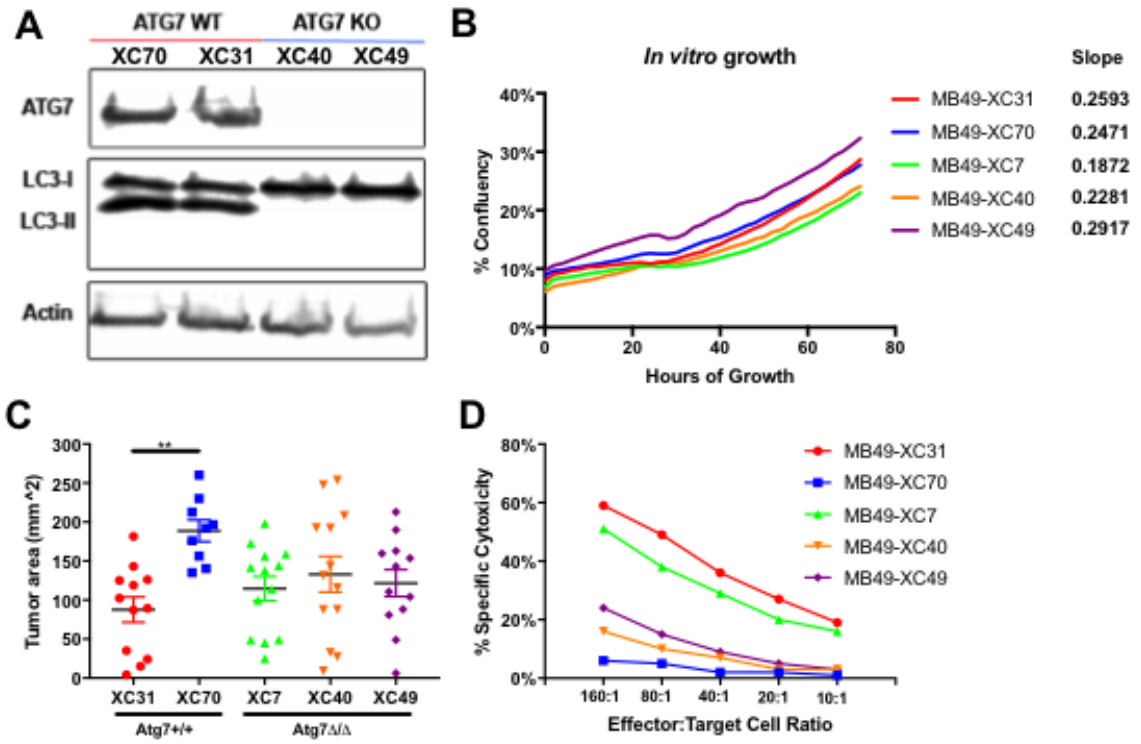

Figure 7. Testing of additional CRISPR-generated clones reveals no clear pattern of growth based on *Atg7* status. ATG7 and LC3 protein expression of four additional CRISPR generated MB49 clones (**A**). *In vitro* cell culture confluency of the CRISPR clones was tracked over 72 hours in an IncuCyte system, with rate of growth determined by linear regression (**B**). 2.5x10^5 of the indicated MB49 clones were injected s.c. into the left groin of fB6 mice and measured over time, with tumor area at three weeks of growth shown (cumulative data from 3 repeat experiments) (**C**). Splenocytes were harvested and re-stimulated with irradiated male splenocytes for 5 days as part of a CTL assay against MB49 tumor cells (one representative experiment shown) (**D**). (Turkey's multiple comparisons test; ** $P < 0.01$)

Atg7Δ/Δ MB49 clones grow differently in male compared to female C57BL/6 mice

Knowing that when MB49 clones express the highly immunogenic HY antigen that cannot be recognized by mB6, but having shown that MB49-XD3's growth was still suppressed in mB6, we decided to further test if these additional Atg7Δ/Δ MB49 clones grew differently in mB6 compared to fB6. We injected each of the five MB49 clones into the left groins of both fB6 and mB6. We saw no difference based on *Atg7* status when grown in fB6 (**Figure 8A**), but found that the Atg7Δ/Δ MB49 clones grew larger than the Atg7+/+ MB49 clones when grown in mB6 (**Figure 8B**). We also found that only the Atg7Δ/Δ MB49 clones grew significantly larger in mB6 compared to fB6 (**Figure 8C**). We hypothesize that the differences were due to inherent changes in antigenicity, since fB6 immune cells can target the highly immunogenic HY antigens and mB6 cannot.

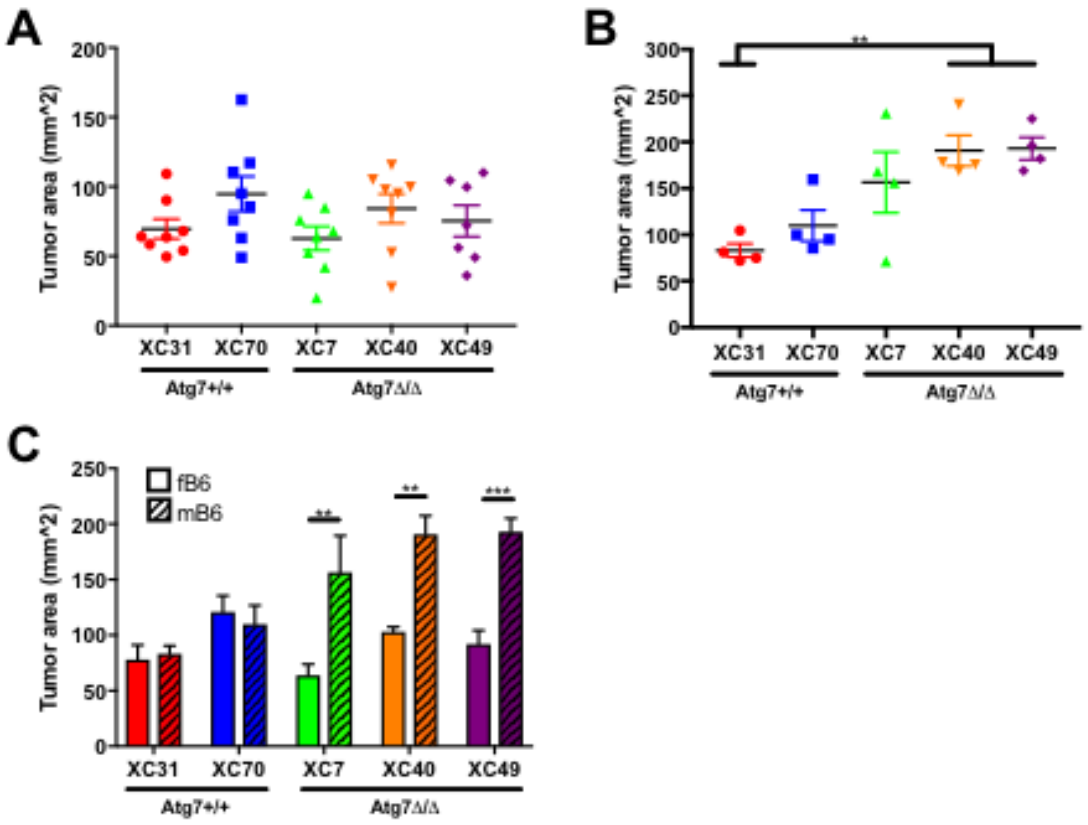

Figure 8. Atg7Δ/Δ MB49 clones grow significantly larger in male C57BL/6 mice. 2.5x10^5 of the indicated MB49 clones were injected s.c. into the left groin of fB6 (**A**) and mB6 (**B**) mice with tumor area at two weeks of growth shown. Tumor area of CRISPR clones grown in fB6 and mB6 as part of the same experiment (**C**). (Turkey's multiple comparisons test; ** P<0.01, *** P<0.001).

All additional tested MB49 clones express large amounts MHC-II in vivo

Having seen that the additional CRISPR clones did not recapitulate the growth or immune effects seen in MB49-XD3, we decided to test their tumor MHC-II expression as we had with MB49-XD1 and MB49-XD3 (**see Figure 5**). All of the clones, regardless of *Atg7* status, expressed significant levels of MHC-II, both *in vivo* as well as *in vitro* when

cultured with IFN-γ (**Figure 9A**). Further analysis of various infiltrating immune cell populations revealed no pattern of differences between Atg7+/+ and Atg7Δ/Δ MB49 clones for any of the tested MB49 clones (**Figure 9B**). This suggests that the decreased MHC-II expression seen in MB49-XD3 was due to clonal heterogeneity and not an effect of *Atg7* deletion.

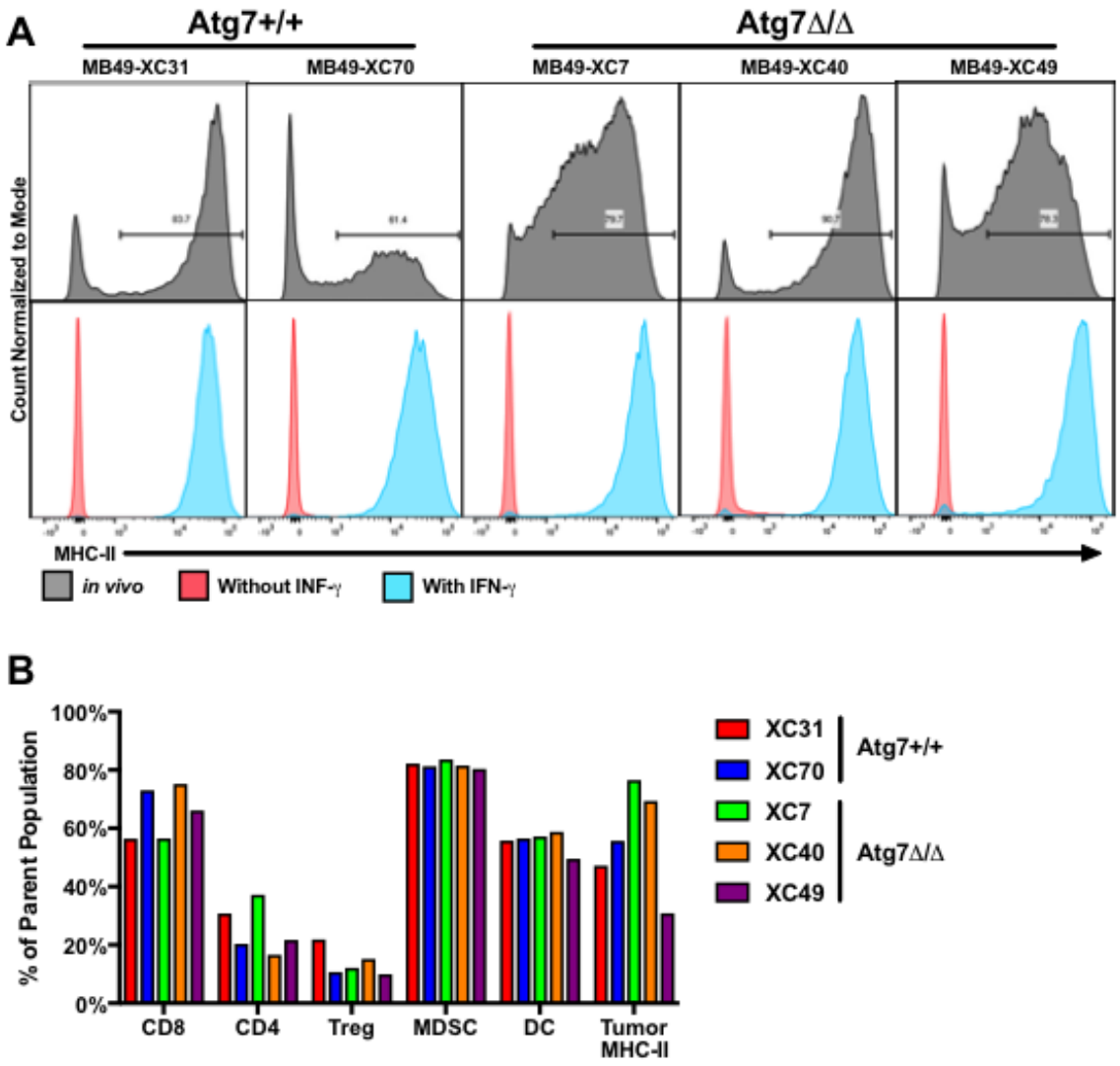

Figure 9. Flow cytometry analysis of additional CRISPR-generated clones reveals no difference in MHC-II expression or immune cell infiltration. *In vivo* (top row) and

in vitro (bottom row, with and without IFN-γ stimulation) MHC-II expression of CD45- tumor cells from of the indicated clones analyzed by flow cytometry (**A**). Infiltrating immune populations from each clone grown in fB6 mice were analyzed by flow cytometry (**B**).

No significant effect of VV-HY therapy based on Atg7 status of two MB49 clones

While there was no apparent difference in *in vivo* growth of this new group of CRISPR MB49 clones, we questioned whether they might respond to VV-HY treatment differently depending on their *Atg7* status. MB49-XD3 had not, but we had already determined that there was significant clonal variability at work in that clone, so we decided to test additional clones to see if a phenotype based on *Atg7* status might emerge. One Atg7+/+ clone (MB49-XC31) and one Atg7Δ/Δ clone (MB49-XC49) were selected randomly for further testing with VV-HY. Multiple experiments treating intratumorally with two doses two weeks apart yielded no significant difference in tumor growth based on treatment or *Atg7* status (**Figure 10A**), with wide variability from mouse to mouse and repeat to repeat. Each of three times this experiment was conducted, we harvested spleens from the treated mice and measured anti-MB49 CTL activity after five days of *in vitro* restimulation with irradiated male splenocytes, with each experiment yielding conflicting results and no consistent pattern of cytotoxicity based on *Atg7* status or viral treatment (**Figures 10B-D**). Analysis of infiltrating immune cell populations by flow cytometry likewise revealed no clear pattern based on *Atgy7* or treatment status **(Figure 10E**).

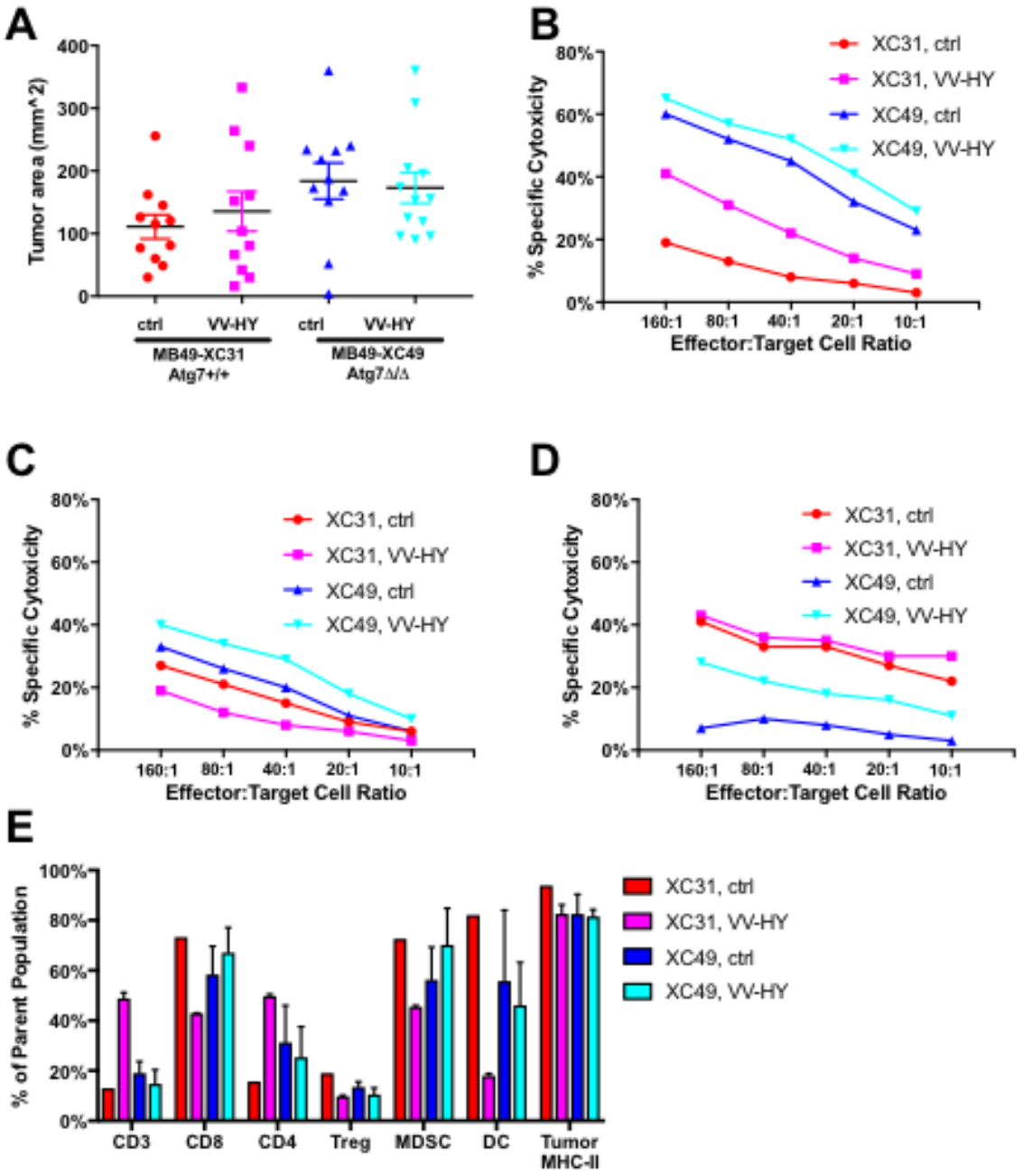

Figure 10. No significant effect of VV-HY treatment based on *Atg7* status. 2.5x10^5 cells of the indicated MB49 clones were injected s.c. into the left groin of fB6 mice and treated intratumorally with two doses of VV-HY. Tumor area at four weeks of growth shown (**A**). Splenocytes were harvested and re-stimulated for 5 days as part of a CTL assay against MB49 tumor cells, with results from three separate experiments shown (**B-**

D). Infiltrating immune populations from each treatment group were analyzed by flow cytometry, with representative data from one of the experiments shown (**E**).

Tumor growth site does not decrease experimental or clonal variability of tumor growth

Given the significant clonal variability evident in the MB49 CRISPR clones, we sought to determine if switching tumor growth site might improve the variability between experiments and uncover differences based on *Atg7* status. We injected 2.5x10^5 cells of parent strain MB49 and several of the CRISPR clones bilaterally into the flanks of C57BL/6 mice, and measured their growth over time (**Figure 11A**). At three weeks of growth, we continued to observe significant clonal variability regardless of *Atg7* status was still noted (**Figure 11B**). These findings, along with the previous results, confirmed that we could make no conclusions as to the effects of *Atg7* deletion in MB49 until we controlled for clonal heterogeneity in the future with new CRISPR-Cas9 clones.

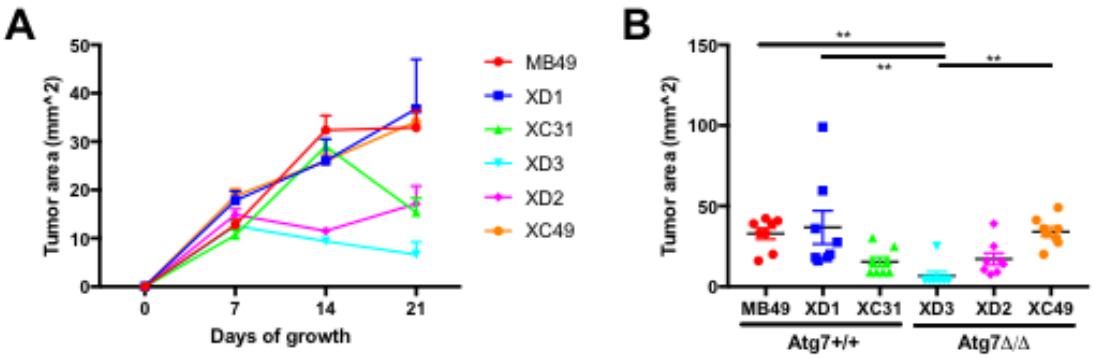

Figure 11. Significant clonal variability exists even when MB49 clones are grown in the flank of mice. 2.5x10^5 cells of the indicated clones were injected s.c. into the bilateral flanks of fB6 mice, and tumor area was measured over time (**A**). Individual

tumor areas shown at 21 days of growth (**B**). (Turkey's multiple comparisons test; ** $P<0.01$).

Chapter 2: The role of host *Atg7* status on growth and the development of anti-MB49 immune responses.

Cre.Atg7Δ/Δ mice maintain capacity to be immunized against HY antigens

To ensure that global *Atg7* deficiency in the Cre.Atg7Δ/Δ mouse model does not prevent the generation of an immune response against the HY antigen as previously shown in C57BL/6 mice, we primed Cre.Atg7+/+ and Cre.Atg7Δ/Δ mice with three different sources of antigen. First, we injected VV-HY cocktail i.p. in both male and female Cre.Atg7+/+ and Cre.Atg7Δ/Δ mice, as well as fB6, with a boost administered two weeks later. As expected, male Cre.Atg7+/+ and Cre.Atg7Δ/Δ mice were unable to generate a specific anti-HY CTL response against MB49 target cells, while female Cre.Atg7+/+ and Cre.Atg7Δ/Δ mice were (**Figure 12A**). There was no apparent difference between the CTL activity of virally-primed female Cre.Atg7+/+ and Cre.Atg7Δ/Δ mice, but both were elevated compared to fB6, leading us to use Cre.Atg7+/+ mice as the control group in all future experiments. Immunizing with irradiated male splenocytes similarly induced HY-specific CTL activity in both female Cre.Atg7+/+ and Cre.Atg7Δ/Δ mice (**Figure 12B**). Mice injected with MB49 syngrafts also generated CTL activity against both MB49 (**Figure 12C**) and the genetically induced male murine melanoma line YUMM1.7[118] (**Figure 12D**), demonstrating that the response was specific to the common HY antigens found in both tumors. The MB49 tumors appeared to have decreased growth in Cre.Atg7Δ/Δ compared to Cre.Atg7+/+, but did not reach statistical significance in this experiment (**Figure 12E**). There was, however a significant survival advantage in MB49-bearing female Cre.Atg7Δ/Δ mice compared to

Cre.Atg7+/+ (**Figure 12F**). We hypothesized that this difference in survival was based on a change in the anti-MB49 immune response.

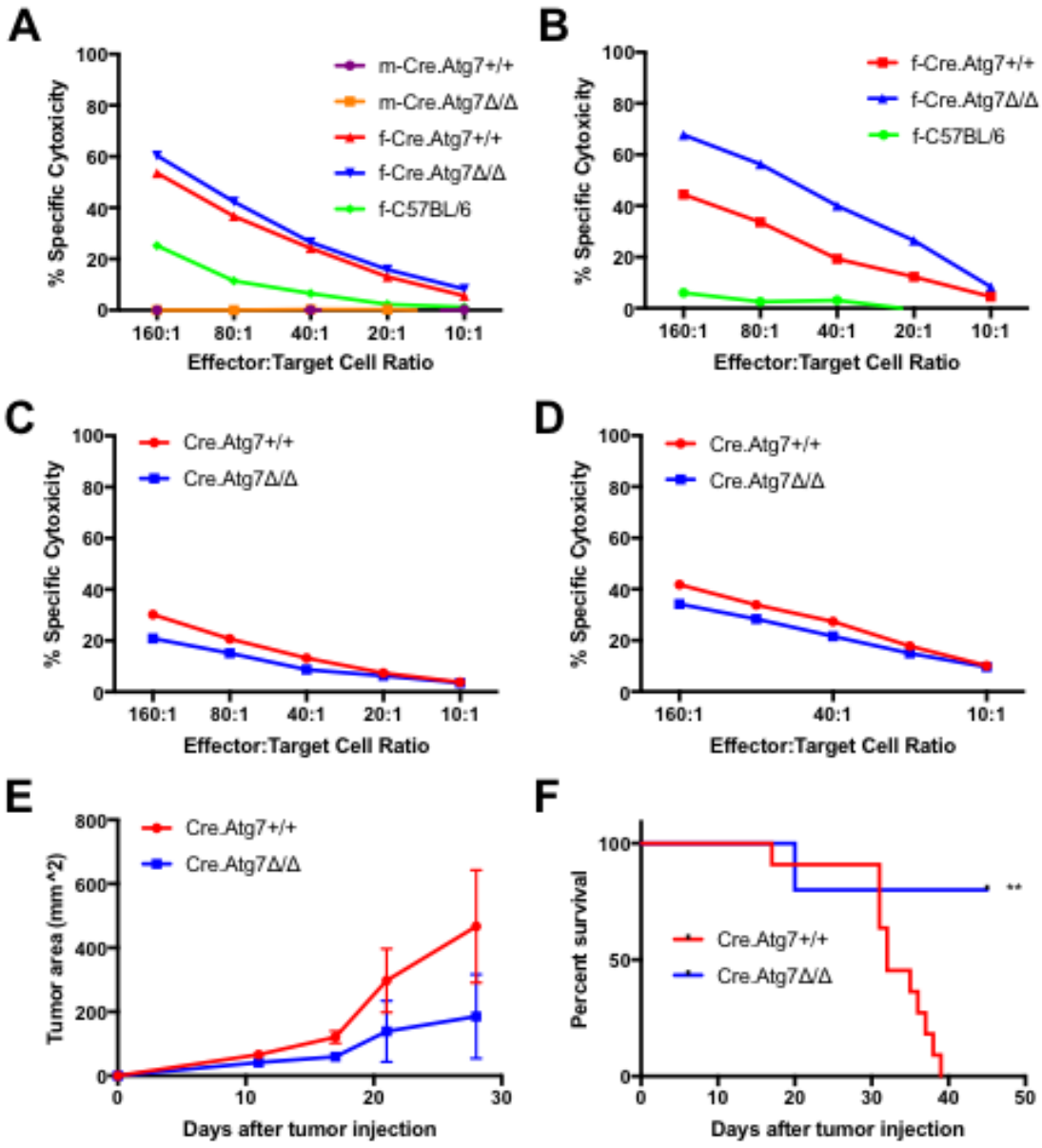

Figure 12. Cre.Atg7Δ/Δ are capable of generating specific anti-tumor immunity similar to Cre.Atg7+/+ and C57BL/6 mice. Male and female Cre.Atg7+/+ and Cre.Atg7Δ/Δ as well as fB6 were immunized i.p. with VV-HY (**A**), irradiated male

splenocytes (**B**), or injected s.c. into the left groin with MB49 tumors (**C-D**). Systemic CTL activity after re-stimulation with irradiated male splenocytes against MB49 (**A-C**) or YUMM1.7 target cells (**D**). MB49 tumor growth over time (**E**). Survival analysis of Cre.Atg7+/+ and Cre.Atg7Δ/Δ female mice injected s.c. with 2.5x10^5 MB49 cells in bilateral flanks, mice sacrificed when tumors reached 225mm^2 in area (**F**). (Mantel-Cox test; ** P<0.01).

MB49 is rejected by female Cre.Atg7Δ/Δ and tumor growth rescued by T-cell depletion.

Given our preliminary results showing decreased tumor growth and increased survival in Cre.Atg7Δ/Δ female mice, as well as unpublished reports from the White lab of seeing similar results in different cells lines, we next tested whether the decrease in MB49 growth in Cre.Atg7Δ/Δ was significant and immunogenic in nature. We injected 2.5x10^5 MB49 cells into bilateral flanks of female Cre.Atg7+/+ and Cre.Atg7Δ/Δ. Two days prior to tumor cell injection, T-cells were depleted by in-vivo i.p. injection of anti-CD4 (aCD4) and anti-CD8 (aCD8) monoclonal antibodies, with continual doses every 5 days throughout the experiment to maintain T cell depletion. Tumors in untreated Cre.Atg7Δ/Δ grew at the same rate as Cre.Atg7+/+ for the first two weeks, but by three weeks of growth had regressed in size, matching the expected time period for the development of adaptive T cell responses (**Figure 13A**). T cell depletion increased the size of tumors in both groups, rescuing tumor growth in Cre.Atg7Δ/Δ to the level of Cre.Atg7+/+ (**Figure 13B-D**). T-cell depletion was confirmed by flow cytometry analysis, and the tumors of Cre.Atg7Δ/Δ mice were shown to have increased infiltrating CD3+ and CD4+ T-cells (but not Tregs) compared to Cre.Atg7+/+ (**Figure 13E**). IHC

confirmed the CD4+ T-cell increase in Cre.Atg7Δ/Δ tumors (**Figure 13F**). These data confirmed that MB49 was rejected in Cre.Atg7Δ/Δ via an adaptive, T-cell driven immune response. This led us to investigate if this effect only occurred in the presence of the HY antigens, or would also be found when grown in male Cre.Atg7Δ/Δ mice.

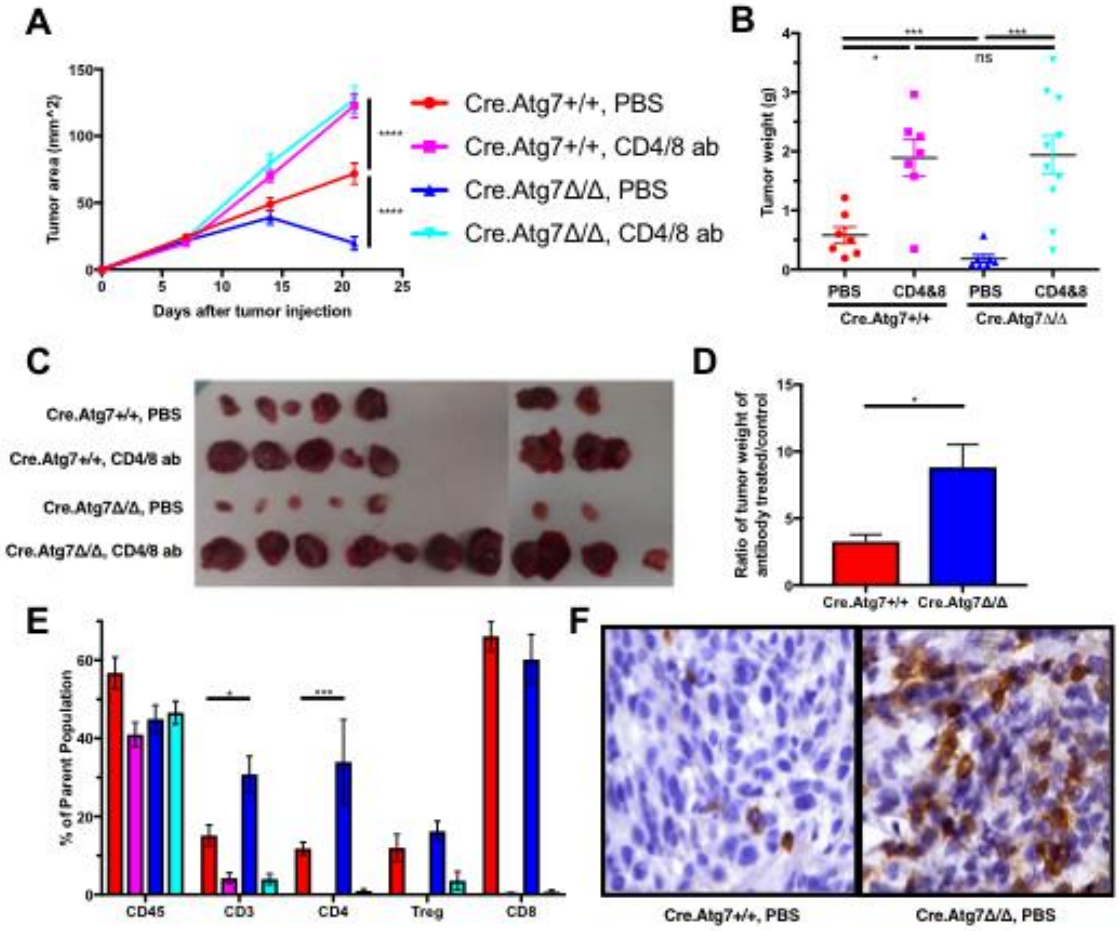

Figure 13. MB49 growth is inhibited in female Cre.Atg7Δ/Δ, rescued by systemic T-cell depletion. 2.5x10^5 MB49 cells were injected s.c. into bilateral flanks of female Cre.Atg7+/+ and Cre.Atg7Δ/Δ and measured over time (**A**), injected i.p. with aCD4 and aCD8 monoclonal antibodies at day -2 and every 5 days thereafter. At three weeks of

growth tumors were removed, weighed (**B**), and photographed (**C**). The ratio of the tumor weight of antibody-treated and PBS control groups was calculated (**D**). TILs measured and T-cell depletion validated via flow cytometry (**E**). IHC staining for CD4+ T-cells (**F**). (Turkey's multiple comparisons test; * P<0.05, *** P<0.001).

MB49 growth is decreased in male Cre.Atg7Δ/Δ, rescued by T-cell depletion.

Knowing that MB49 expresses HY antigens, we hypothesized that the effects seen when grown in female mice might be abrogated if grown in male mice, which as described above cannot respond to HY antigens. We found that when the experiments were repeated in male Cre.Atg7+/+ and Cre.Atg7Δ/Δ mice, T cell depletion again rescued tumor growth. However, compared to female mice, male Cre.Atg7Δ/Δ mice only slowed MB49 growth instead of rejecting it completely (**Figure 14A**). Treatment with aCD4 and aCD8 antibodies rescued Cre.Atg7Δ/Δ's tumors' sizes to Cre.Atg7+/+ levels (**Figure 14 B-D**). T-cell depletion was validated by flow cytometry (data not shown), and evaluation of infiltrating immune cells revealed no significant changes in immune cell populations beyond a slightly elevated proportion of live CD45+ cells (**Figure 14E**) and a non-significant increase in CD4+ T-cells. Further staining by IHC confirmed the slight increase in CD4+ T cells within the tumor (**Figure 14F**). The effects seen on MB49 when grown in male compared to female Cre.Atg7Δ/Δ mice indicate that targeting of HY antigens was necessary for complete tumor rejection—consistent with described differences in inherent immunogenicty—but even without targeting HY, male Cre.Atg7Δ/Δ had an improved immune response against MB49 than Cre.Atg7+/+.

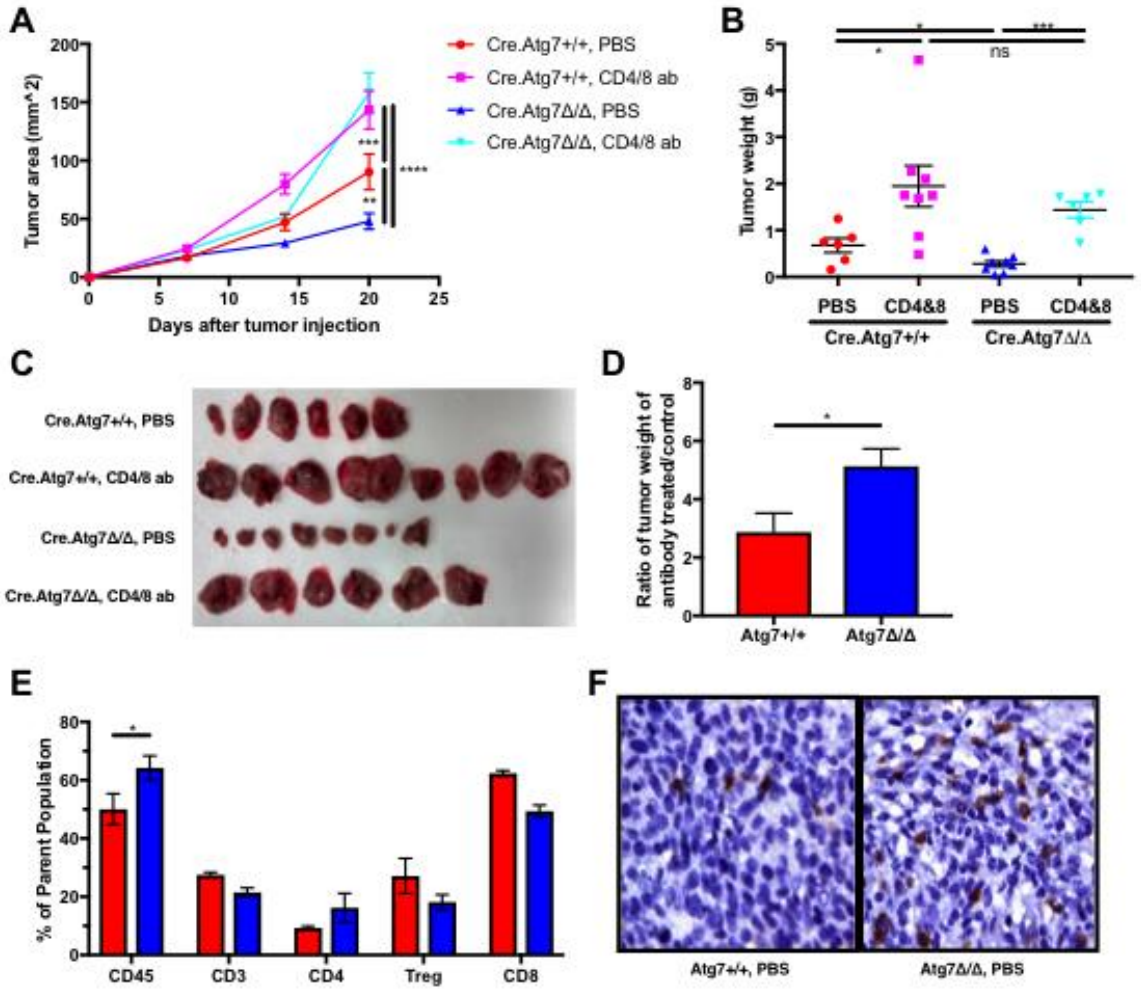

Figure 14. MB49 growth is inhibited in male Cre.Atg7Δ/Δ and rescued by systemic T-cell depletion. 2.5x10^5 MB49 cells were injected s.c. into bilateral flanks of male Cre.Atg7+/+ and Cre.Atg7Δ/Δ and measured over time (**A**), injected i.p. with aCD4 and aCD8 monoclonal antibodies at day -2 and every 5 days thereafter. At three weeks of growth tumors were removed, weighed (**B**), and photographed (**C**). The ratio of the tumor weight of antibody-treated and PBS control groups was calculated (**D**). TILs measured via flow cytometry (**E**). IHC staining for CD4+ T-cells (**F**). (Turkey's multiple

comparison's test (**A**), Mann-Whitney test (**B**), Welch's t test (**D**), and Sidak's multiple comparisons test (**E**); * P<0.05, ** P<0.01, *** P<0.001, **** P<0.0001).

No significant differences between Cre.Atg7+/+ and Cre.Atg7Δ/Δ at two weeks growth

Having seen that MB49 regresses almost completely by three weeks of growth in female Cre.Atg7Δ/Δ mice, we decided to repeat the experiment and harvest tissue at two weeks of growth, enough time for the development of adaptive immune response but when tumors were still present and similarly sized regardless of *Atg7* status, which would allow us to analyze immune cell infiltration by IHC and RNA expression of several hundred immune related genes and their associated pathways by Nanostring. 2.5x10^5 MB49 cells were injected bilaterally into the flanks of female Cre.Atg7+/+ and Cre.Atg7Δ/Δ mice two days after i.p. treatment with PBS control or aCD4 and aCD8 monoclonal antibody. Mice received additional antibody or PBS injections every 5 days, and tumor growth was measured by calipers (**Figure 15A**). At 14 days of growth there was no significant difference in MB49 tumor size between Cre.Atg7+/+ and Cre.Atg7Δ/Δ mice, except that CD4/8 treatment in Cre.Atg7+/+ mice had already begun to significantly increase growth (**Figure 15B**). Analysis by flow cytometry confirmed depletion of T-cells by the monoclonal antibody treatments, and revealed no significant differences between the control groups based on *Atg7* status (**Figure 15C**). As expected, splenocytes from antibody-treated mice were incapable of generating an effective anti-male CTL response and failed to lyse any MB49 cells (**Figure 15D**). In addition, there was no significant difference in CTL activity between the untreated groups. Most importantly, the tumors were still present in all groups, and of large enough size to allow

us to take sections for IHC and isolate RNA for gene expression analysis with Nanostring.

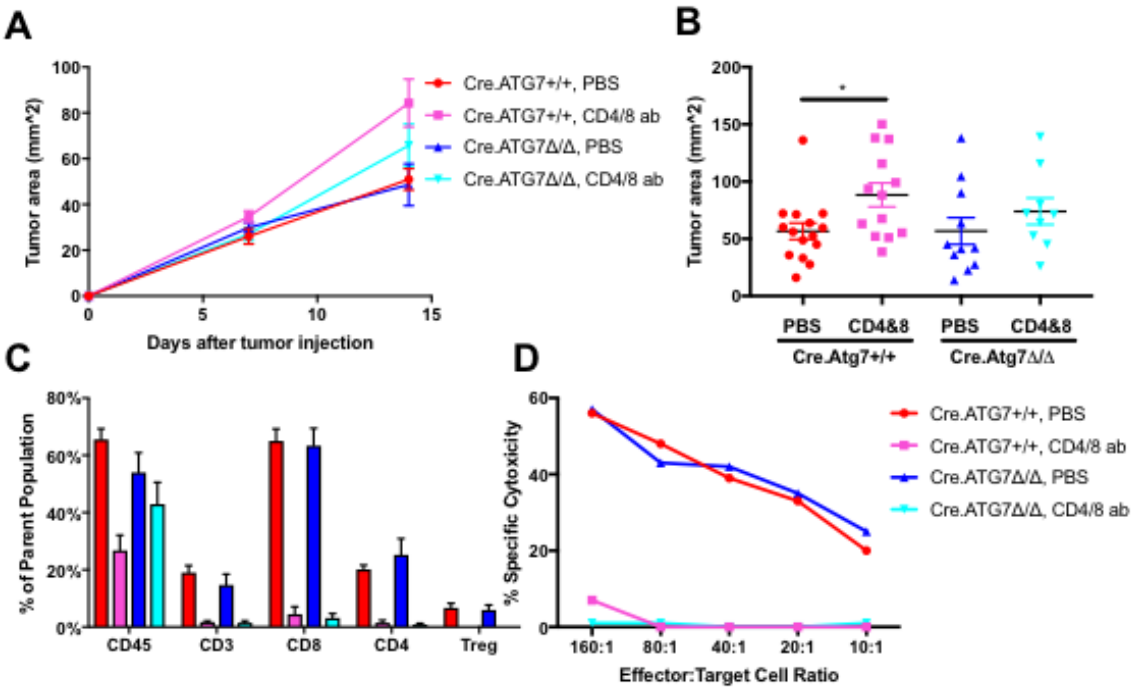

Figure 15. No significant difference between Cre.Atg7+/+ and Cre.Atg7Δ/Δ at two weeks of growth. 2.5x10^5 MB49 cells were injected s.c. into bilateral flanks of female Cre.Atg7+/+ and Cre.Atg7Δ/Δ mice and measured over time (**A**), injected i.p. with a-CD4 and a-CD8 monoclonal antibodies at day -2 and every 5 days thereafter. At two weeks of growth tumors were measured (**B**) and removed. TILs were measured via flow cytometry (**C**). Splenocytes from the mice were cultured *in vitro* for 5 days with irradiated male splenocytes and used in a CTL assay against MB49 target cells (**D**). (Welch's t test; * $P < 0.05$)

No difference in the number of Tregs in Cre.Atg7+/+ and Cre.Atg7Δ/Δ

To confirm the flow cytometry finding that there was no change in the number of Tregs, we performed IHC staining for the key Treg transcription factor FoxP3 on the two-week growth MB49 samples from Figure 15. Confirming results seen by flow cytometry, there was no apparent difference in the absolute number of FoxP3+ Tregs between Cre.Atg7+/+ and Cre.Atg7Δ/Δ mice (**Figure 16**). This indicated that the improved immune-mediated rejection of MB49 seen in Cre.Atg7Δ/Δ mice was not driven but a gross loss of Tregs.

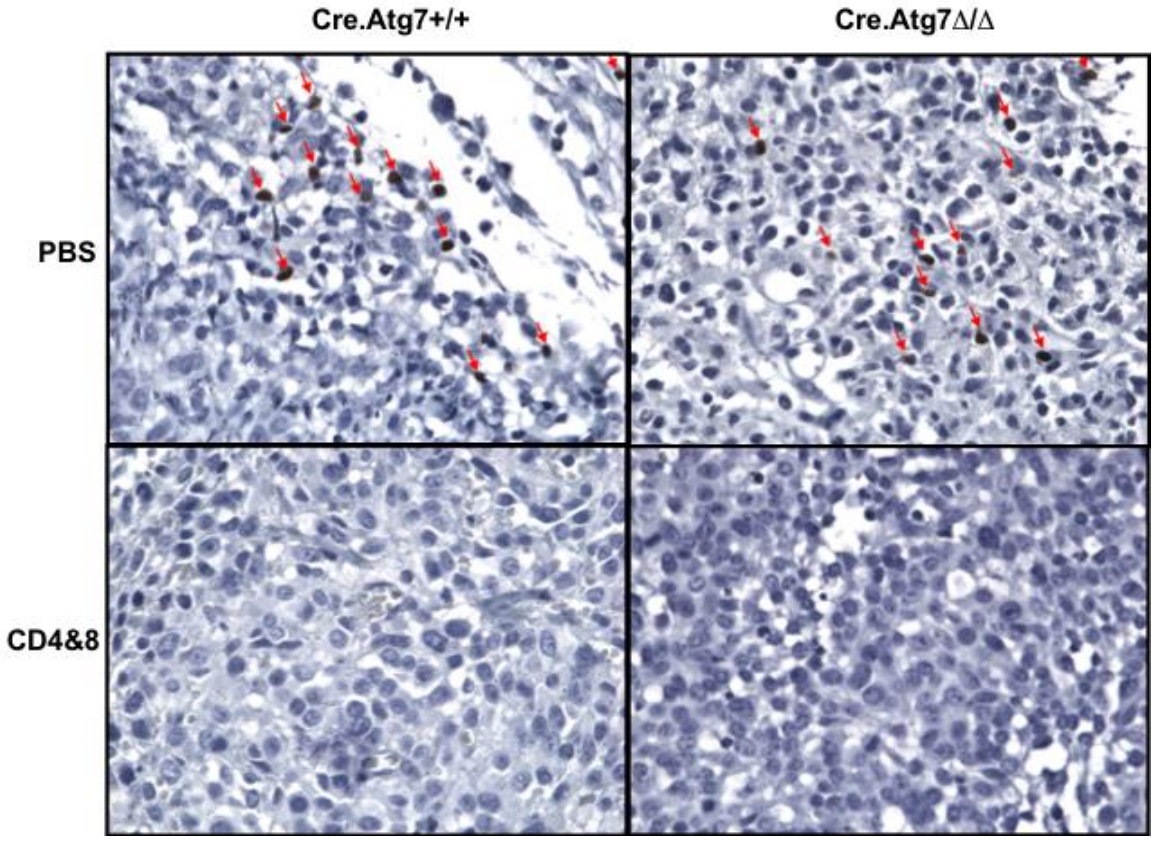

Figure 16. FoxP3 IHC of MB49 from Cre.Atg7+/+ and Cre.Atg7Δ/Δ mice at 14 days growth reveal similar numbers of Tregs. Tumors from both genotype of mice that had received either PBS or monoclonal antibody treatment were sectioned at stained for FoxP3, with positive cells indicated by red arrows.

Significant elevation in expression of immune-related genes in Cre.Atg7Δ/Δ tumors.

Atg7 status of the mice from Figure 15 was confirmed by DNA and protein immunoblotting (data not shown), two mice from each group were selected, and their tumors were taken for IHC and RNA isolation. Analysis of the isolated RNA from tumors using the Nanostring PanCancer Immune Profiling Panel revealed that tumors from Cre.Atg7Δ/Δ mice had gene expression consistent with upregulated immune responses in comparison to Cre.Atg7+/+ mice, and that the monoclonal antibody treatment had generally subdued the immune response (**Figure 17A**). This panel analyzed several hundred immune-associated genes, and grouped them into relevant immune pathways and cell types. Tumors from Cre.Atg7Δ/Δ mice had elevated pathway scores for all of the measured immune pathways, with depletion of T cells by treatment with aCD4 and aCD8 decreasing the scores of all the pathways, suggesting a link between T cell activity and signaling and these other pathways (**Figure 17B**). Analysis of gene expression patterns based on immune cell profiles also revealed that while tumors from Cre.Atg7Δ/Δ mice had equal or elevated scores for almost all immune cell populations (with largest increases in Mast cell, Neutrophil and Activated CD8 scores), they had decreased Treg signal (as determined by expression of key transcription factor FoxP3) (**Figure 17C**). The Nanostring panel includes several hundred genes, but given the known role of autophagy on innate immune pathways like STING, we focused on gene changes in innate pathways.

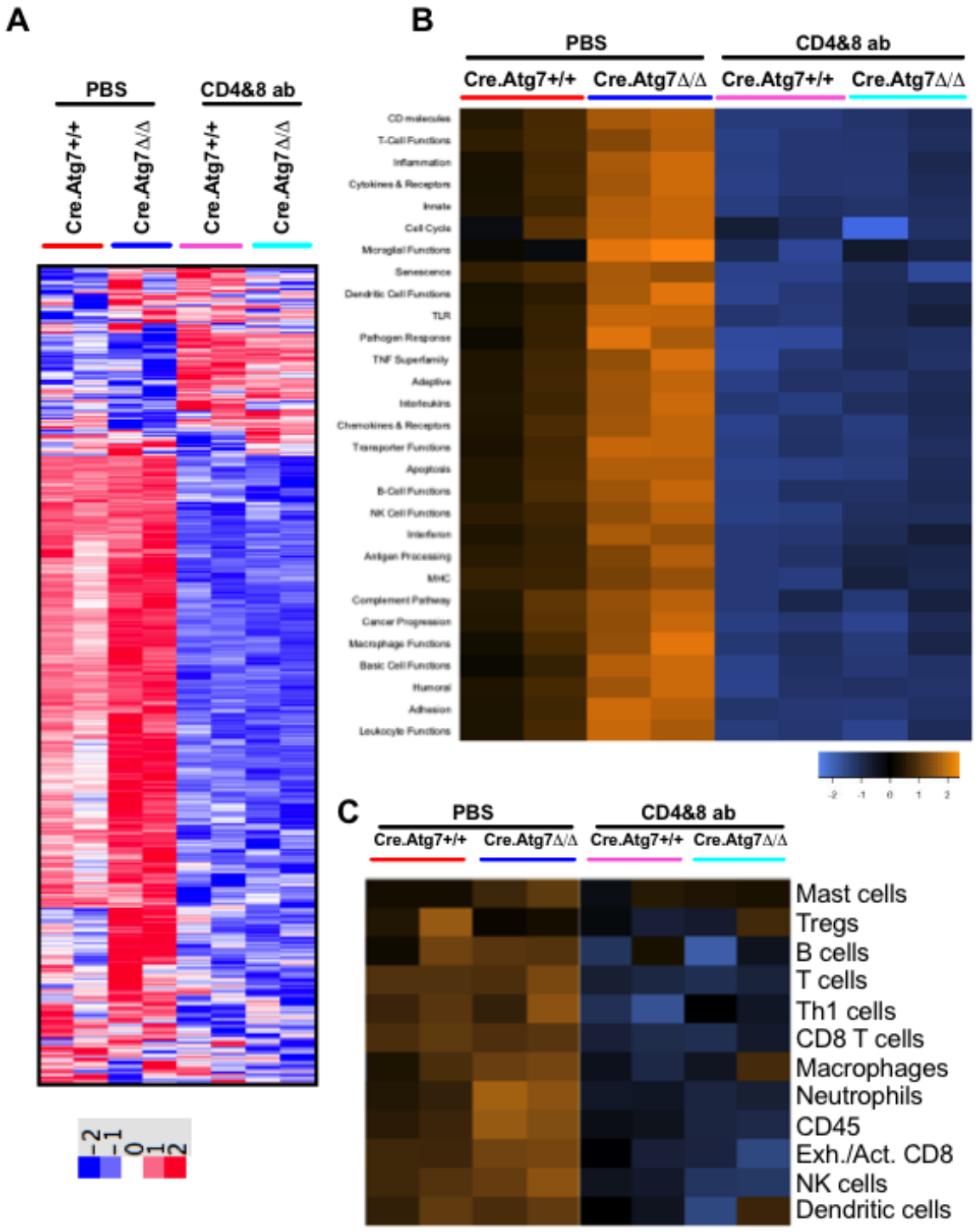

Figure 17. Nanostring analysis reveals general upregulation of immune response markers in Cre.Atg7Δ/Δ mice. Tumors from the mice in Figure 15 were removed and processed to isolate RNA before undergoing Nanostring protocol. Heat map of all the

immune-related genes (**A**). Aggregate gene scores for multiple different immune pathways (**B**). Pathway scores for different immune cell types (**C**).

Many innate immunity genes are upregulated in tumors from Cre.Atg7Δ/Δ mice

The Nanostring PanCancer Immune Profiling Panel contains several hundred genes, of which we found 100 to be differentially expressed and statistically significant between Cre.Atg7+/+ and Cre.Atg7Δ/Δ (**Table 1**). Knowing the role that autophagy has on innate immunity[44-46], and that autophagy deficiency can cause inflammation and upregulation of innate immunity[52-54], we looked at the Innate panel of genes generated by the Nanostring. We found 40 genes in that panel that were highly differentially expressed between Cre.Atg7+/+ and Cre.Atg7Δ/Δ, the majority of them upregulated in the autophagy-deficient mouse as expected (**Figure 18A-B**). Because other groups have shown that autophagy directly interacts with Toll-Like Receptors (TLR)[48,49], we focused in on the TLR pathway subpanel, and found 7 genes that were significantly upregulated in the tumors of Cre.Atg7Δ/Δ mice (**Figure 18C-D**). Many innate pathways work via IFN signaling, and our analysis found 6 different IFN-related genes that were upregulated in the tumors of Cre.Atg7Δ/Δ mice (**Figure 18E-F**). Finally, knowing that autophagy can provide important antigens for antigen presentation, we evaluated changes in the Antigen Processing panel and found 5 upregulated genes (**Figure 18G-H**). The differentially expressed and statistically significant genes that are changed in Cre.Atg7Δ/Δ mice indicate that the immune-mediated rejection of MB49 by Cre.Atg7Δ/Δ was likely driven by changes in innate immunity and inflammation that lead to improved adaptive responses. Specifically looking at the impact of the upregulation of TLR genes in the

Cre.Atg7Δ/Δ samples, we can see that they led to end effector changes like the increased production of pro-inflammatory cytokines IL-1ß and IL-12, as well as costimulatory molecules like CD86 (**Figure 18I**), that could mediate our observations of tumor growth in these mice.

Gene	Log2 fold change	P-value	Pathways
Chil3	2.5	0.00328	Basic Cell Functions
H2-Q10	2.43	0.00722	Adaptive, Antigen Processing, B-Cell Functions, MHC
Cxcr2	2.43	0.000156	Adaptive, CD molecules, Chemokines & Receptors, Cytokines & Receptors, Inflammation, Innate, Interleukins
Sell	2.36	0.000278	Adhesion, Apoptosis, CD molecules, T-Cell Functions
Il1b	2.26	0.00473	Adaptive, Chemokines & Receptors, Humoral, Inflammation, Innate, Interleukins, Macrophage Functions, Pathogen Response, T-Cell Functions, Transporter Functions
Cd1d1	2.22	0.000389	Antigen Processing, CD molecules, Innate, Interleukins, MHC, Macrophage Functions, T-Cell Functions
Bst1	2.19	0.00374	CD molecules, Humoral
Fpr2	2.12	0.000641	Adaptive, Basic Cell Functions, Inflammation
Tnfsf11	1.97	0.00603	CD molecules, Cytokines & Receptors, T-Cell Functions, TNF Superfamily , Transporter Functions
Arg2	1.91	0.00369	Basic Cell Functions
Nos2	1.82	0.00214	Adaptive, Apoptosis, Inflammation, Interferon, T-Cell Functions
Mefv	1.82	0.000293	Inflammation, Innate
Irak3	1.81	0.00476	Cytokines & Receptors, Innate, Interleukins
Il1rn	1.77	0.00393	Cytokines & Receptors, Inflammation, Interleukins
Csf3r	1.76	0.000622	Adhesion, CD molecules, Cytokines & Receptors
Tpsab1	1.74	0.000416	
Cd38	1.73	7.33E-05	Apoptosis, B-Cell Functions, CD molecules
Il1r2	1.64	0.00561	B-Cell Functions, CD molecules, Cytokines & Receptors, Interleukins
Csf2rb	1.64	0.000674	CD molecules, Cancer Progression, Cytokines & Receptors
Ifitm1	1.63	0.00975	CD molecules, Innate, Interferon
Egr3	1.6	0.000984	Apoptosis
Abca1	1.48	0.00892	Innate, Transporter Functions
Syk	1.47	0.00131	B-Cell Functions, Innate, Interleukins, Leukocyte Functions, Macrophage Functions, T-Cell Functions, Transporter Functions
Amica1	1.45	0.00446	Adhesion, Transporter Functions
Ctss	1.4	7.30E-05	Innate
Cfp	1.39	0.00085	Cancer Progression, Complement Pathway, Innate
Cd274	1.39	0.0018	CD molecules, T-Cell Functions
Mmp9	1.38	0.00123	Adhesion, Apoptosis, Cancer Progression
Cd53	1.37	0.00817	CD molecules
Cd14	1.37	0.00142	CD molecules, Cytokines & Receptors, Inflammation, Innate, Pathogen Response, Transporter Functions
Slc7a11	1.37	0.00689	Transporter Functions
Fcgr3	1.34	0.00123	Antigen Processing, CD molecules, MHC, Transporter Functions
Psen2	1.34	0.00414	Leukocyte Functions, T-Cell Functions
Cybb	1.29	0.00181	Innate, Transporter Functions

Ccr2	1.28	0.00349	Adaptive, CD molecules, Cancer Progression, Chemokines & Receptors, Cytokines & Receptors, Dendritic Cell Functions, Humoral, Inflammation, Interleukins, Macrophage Functions, T-Cell Functions
Mertk	1.28	0.000555	Adhesion, Apoptosis, NK Cell Functions, Transporter Functions
Pycard	1.25	0.00955	Apoptosis, Inflammation, Innate, Interleukins
Tlr2	1.25	0.00495	CD molecules, Inflammation, Innate, Leukocyte Functions, TLR
Cebpb	1.25	0.00636	Inflammation, Innate, T-Cell Functions
Igf2r	1.24	0.00286	Apoptosis, CD molecules, Transporter Functions
Ncr1	1.22	0.00657	CD molecules
Cd84	1.19	0.00366	Adhesion, CD molecules
Itgae	1.19	0.00599	Adhesion, CD molecules
Selplg	1.19	0.00243	Adhesion, CD molecules, Leukocyte Functions
Pik3cd	1.19	0.000425	Inflammation, Innate
Ccr1	1.18	0.00271	Adaptive, CD molecules, Chemokines & Receptors, Cytokines & Receptors, Dendritic Cell Functions, Inflammation, Innate, Leukocyte Functions, Transporter Functions
Slamf6	1.17	0.00341	CD molecules
Icam1	1.16	0.00209	Adaptive, Antigen Processing, CD molecules, Leukocyte Functions, T-Cell Functions, Transporter Functions
Clec5a	1.15	0.000447	Apoptosis, Cytokines & Receptors, Innate
Slamf7	1.14	0.00592	CD molecules, Innate, NK Cell Functions
Hck	1.14	0.000277	Inflammation, Innate
Tlr6	1.09	0.000627	Adaptive, CD molecules, Inflammation, Innate, Interleukins, Microglial Functions, Pathogen Response, T-Cell Functions, TLR
Cd69	1.09	0.00741	B-Cell Functions, Macrophage Functions
Slc11a1	1.08	0.00332	Adaptive, Antigen Processing, Transporter Functions
Ptprc	1.07	0.0056	B-Cell Functions, CD molecules, Cytokines & Receptors, T-Cell Functions
Ikzf1	1.07	0.00503	B-Cell Functions, NK Cell Functions, T-Cell Functions
Tlr7	1.07	0.000951	Chemokines & Receptors, Inflammation, Innate, Interleukins, Microglial Functions, Pathogen Response, TLR
Tnfrsf1b	1.05	0.0048	CD molecules, Inflammation, TNF Superfamily
Lcp1	0.989	0.000513	T-Cell Functions, Transporter Functions
Ncf4	0.982	0.00141	Basic Cell Functions, Innate
Cd200	0.961	0.00951	CD molecules
Cd180	0.935	0.00387	CD molecules, Inflammation, Innate
Ifnar2	0.934	0.00208	Cytokines & Receptors, Interferon
Ikbkg	0.92	0.00521	B-Cell Functions, Innate
Irf5	0.91	0.000636	Senescence
Ly9	0.88	0.00179	Adhesion, CD molecules
Entpd1	0.871	0.00849	CD molecules
Tlr1	0.864	0.00132	CD molecules, Inflammation, Innate, Interleukins, Macrophage Functions, TLR
Tlr4	0.86	0.00217	Adaptive, CD molecules, Chemokines & Receptors, Inflammation, Innate, Interleukins, Pathogen Response, T-Cell Functions, TLR
Lamp1	0.849	0.00179	CD molecules, Transporter Functions
Ly86	0.837	0.00198	Humoral, Inflammation, Innate, Pathogen Response
Cd97	0.835	0.00128	Adaptive, Adhesion, CD molecules, Inflammation, Innate
Itgb2	0.832	3.92E-05	CD molecules, Humoral, Inflammation, Leukocyte Functions, NK Cell Functions, T-Cell Functions, Transporter Functions
Abcg1	0.8	0.00636	Innate, Transporter Functions
Lyn	0.781	0.00397	B-Cell Functions, Cytokines & Receptors, Dendritic Cell Functions, Inflammation, Innate, Transporter Functions
Irak2	0.78	0.00828	Cytokines & Receptors, Innate, Interleukins, TLR
Hif1a	0.773	0.00154	Apoptosis, Cancer Progression

Jak2	0.737	0.00114	Adaptive, Cytokines & Receptors, Innate, Interleukins, T-Cell Functions
Cd48	0.661	0.00506	CD molecules, T-Cell Functions
Ly96	0.615	0.00181	Humoral, Inflammation, Innate, Pathogen Response
Nlrc5	0.608	0.00748	Innate, Interferon, MHC
Prkcd	0.577	0.000211	Apoptosis, B-Cell Functions, Senescence, Transporter Functions
Ifnar1	0.564	0.00405	Adaptive, Interferon, T-Cell Functions
Stat5b	0.512	0.00781	B-Cell Functions, Cell Cycle, Interleukins, NK Cell Functions, T-Cell Functions
Psen1	0.486	0.000323	Apoptosis, Leukocyte Functions, T-Cell Functions, Transporter Functions
Irf8	0.444	0.00165	Interferon, Interleukins, T-Cell Functions
Irf2	0.427	0.00806	Adhesion
Stat6	0.384	0.00429	Adaptive, Cytokines & Receptors, T-Cell Functions
Trp53	-0.483	0.00778	Apoptosis, Cell Cycle, Senescence, T-Cell Functions
Dock9	-0.534	0.0044	Basic Cell Functions
Birc5	-0.553	0.000207	Apoptosis, Cell Cycle, Cytokines & Receptors
Erbb2	-0.603	0.00462	Cancer Progression, Cytokines & Receptors
Axl	-0.617	0.00199	Inflammation, Innate, NK Cell Functions, Transporter Functions
Nup107	-0.703	0.00861	Transporter Functions
Mapk11	-0.737	0.00914	Basic Cell Functions, Innate
Nfkb2	-0.854	0.00484	Innate
Itgb4	-1.14	0.00596	Adhesion, CD molecules
Sigirr	-1.18	0.000302	Chemokines & Receptors, Cytokines & Receptors, Innate
Ccl24	-2.22	0.00593	Adaptive, Chemokines & Receptors, Cytokines & Receptors, Inflammation

Table 1. 100 immune-related genes are statistically significant and differentially expressed between Cre.Atg7+/+ and Cre.Atg7Δ/Δ. A positive Log2 fold change indicates that a gene is upregulated in tumor samples from Cre.Atg7Δ/Δ compared to Cre.Atg7+/+, and a negative Log2 fold change indicates it is downregulated. Only P <0.01 were considered significant. Genes are listed in order of differentially gene expression from most upregulated to most downregulated. Pathways the genes are part of were determined by the Nanostring panel and the nCounter analysis software.

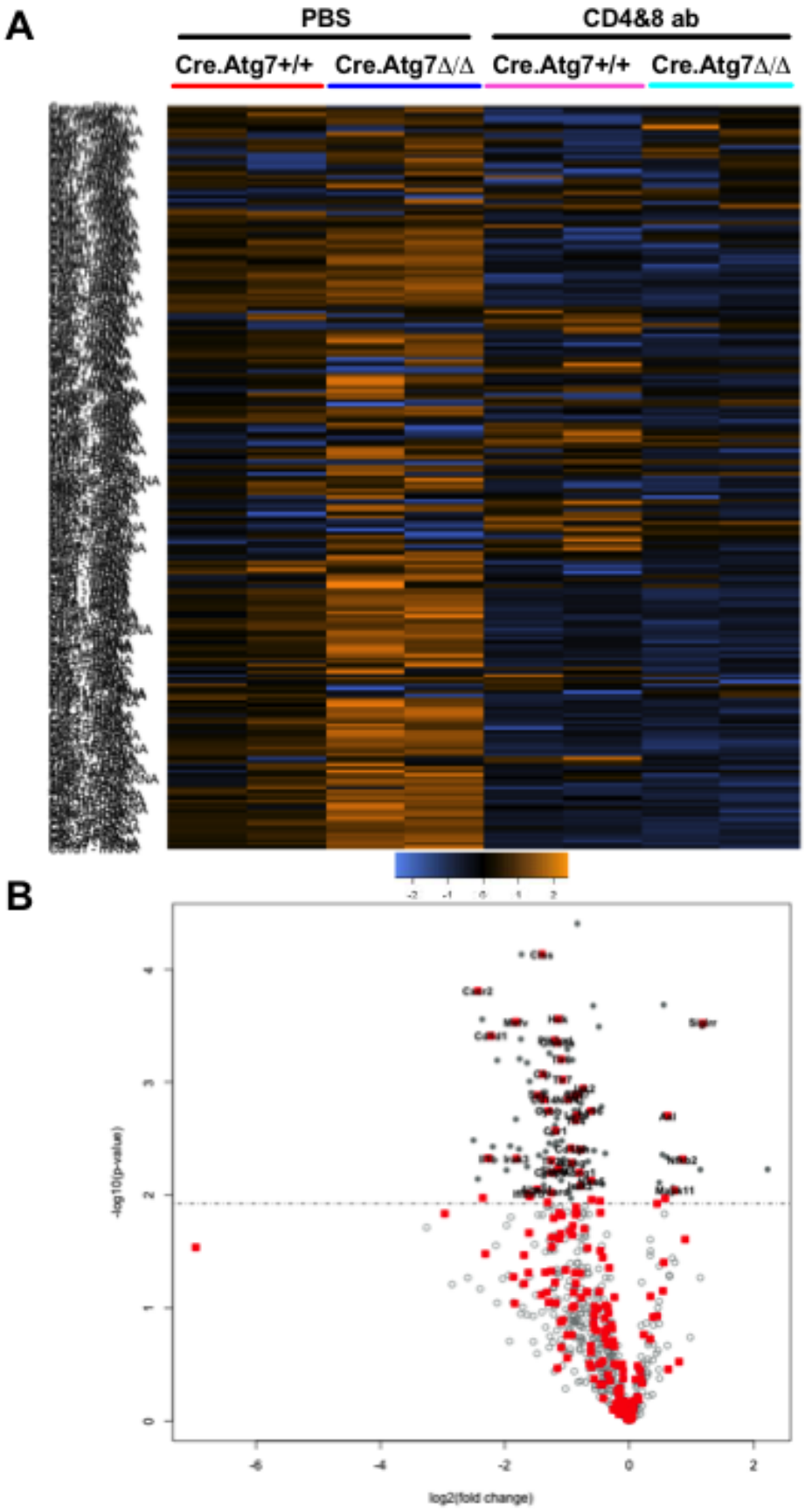
A
PBS
CD4&8 ab
Cre.Atg7+/+
Cre.Atg7Δ/Δ
Cre.Atg7+/+
Cre.Atg7Δ/Δ
B
-log10(p-value)
log2(fold change)

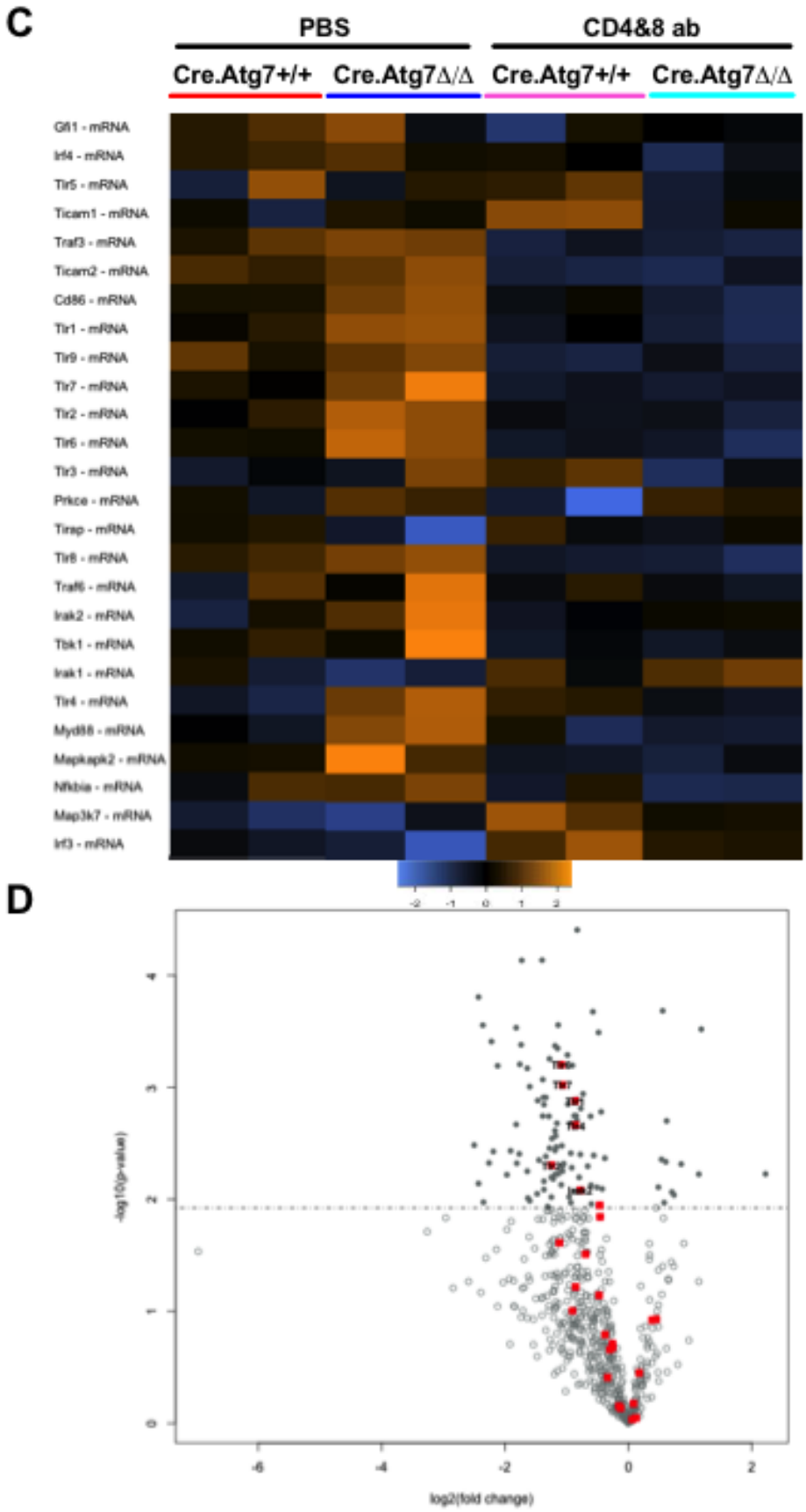
C
PBS
CD4&8 ab
Cre.Atg7+/+
Cre.Atg7Δ/Δ
Cre.Atg7+/+
Cre.Atg7Δ/Δ
Gfi1 - mRNA
Irf4 - mRNA
Tlr5 - mRNA
Ticam1 - mRNA
Traf3 - mRNA
Ticam2 - mRNA
Cd86 - mRNA
Tlr1 - mRNA
Tlr9 - mRNA
Tlr7 - mRNA
Tlr2 - mRNA
Tlr6 - mRNA
Tlr3 - mRNA
Prkce - mRNA
Tirap - mRNA
Tlr8 - mRNA
Traf6 - mRNA
Irak2 - mRNA
Tbk1 - mRNA
Irak1 - mRNA
Tlr4 - mRNA
Myd88 - mRNA
Mapkapk2 - mRNA
Nfkbia - mRNA
Map3k7 - mRNA
Irf3 - mRNA
-2
-1
0
1
2
D
-log10(p-value)
log2(fold change)
-6
-4
-2
0
2
0
1
2
3
4

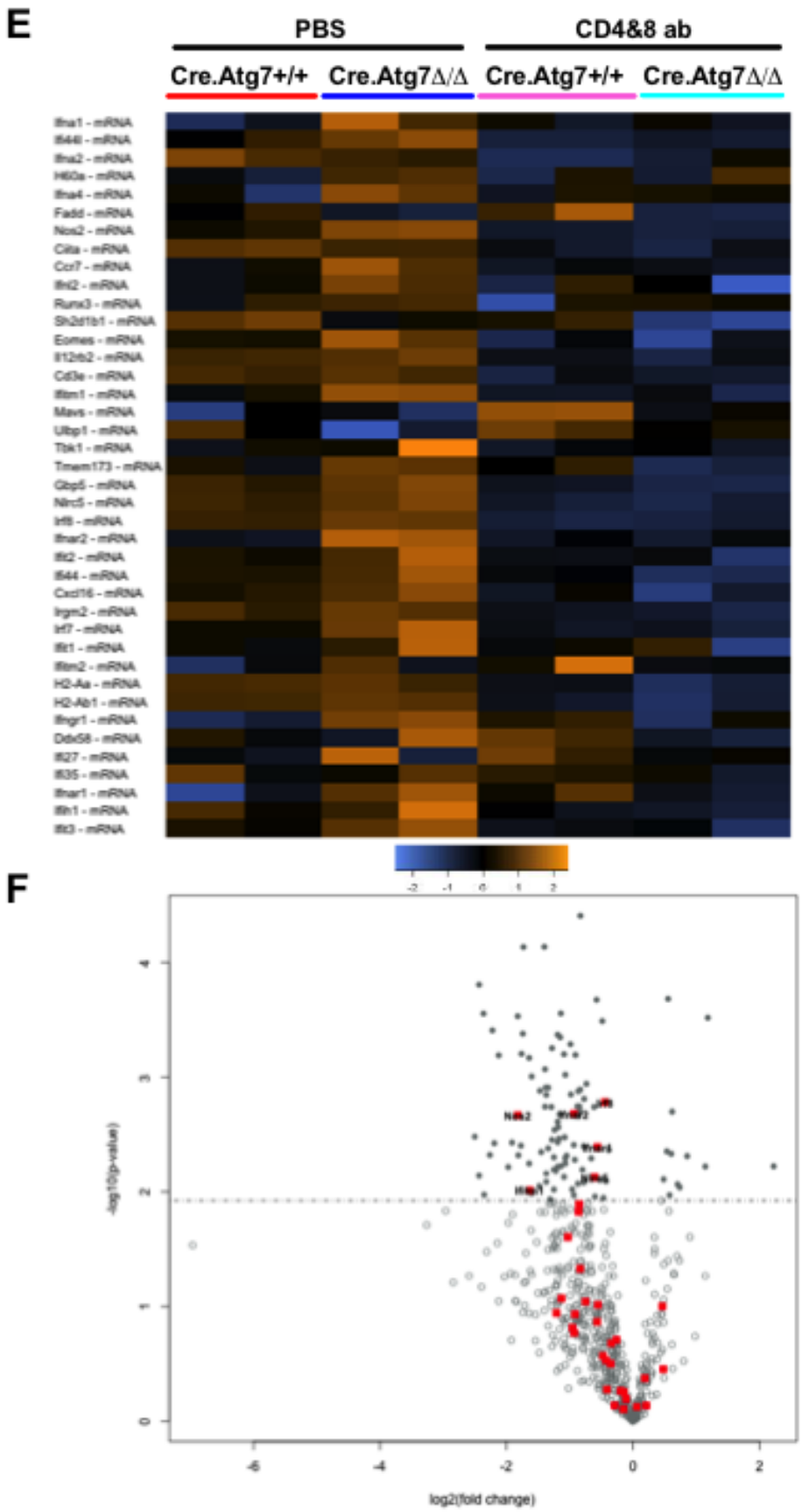
E
PBS
CD4&8 ab
Cre.Atg7+/+
Cre.Atg7Δ/Δ
Cre.Atg7+/+
Cre.Atg7Δ/Δ
Ifna1 - mRNA
Ifi44l - mRNA
Ifna2 - mRNA
H60a - mRNA
Ifna4 - mRNA
Fadd - mRNA
Nos2 - mRNA
Ciita - mRNA
Ccr7 - mRNA
Ifnl2 - mRNA
Runx3 - mRNA
Sh2d1b1 - mRNA
Eomes - mRNA
Il12rb2 - mRNA
Cd3e - mRNA
Ifitm1 - mRNA
Mavs - mRNA
Ulbp1 - mRNA
Tbk1 - mRNA
Tmem173 - mRNA
Gbp5 - mRNA
Nlrc5 - mRNA
Irf8 - mRNA
Ifnar2 - mRNA
Ifit2 - mRNA
Ifi44 - mRNA
Cxcl16 - mRNA
Irgm2 - mRNA
Irf7 - mRNA
Ifit1 - mRNA
Ifitm2 - mRNA
H2-Aa - mRNA
H2-Ab1 - mRNA
Ifngr1 - mRNA
Ddx58 - mRNA
Ifi27 - mRNA
Ifi35 - mRNA
Ifnar1 - mRNA
Ifih1 - mRNA
Ifit3 - mRNA
-2
-1
0
1
2
F
-log10(p-value)
log2(fold change)
-6
-4
-2
0
2
0
1
2
3
4

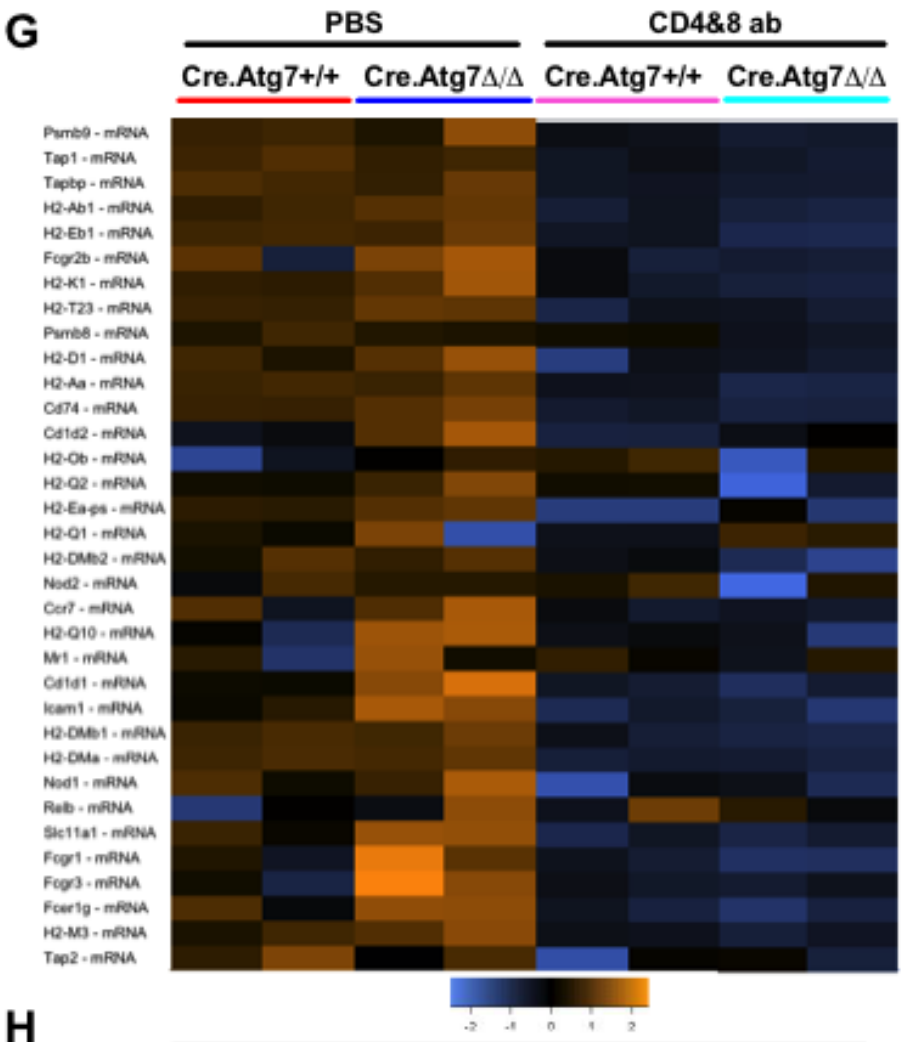
G
PBS
CD4&8 ab
Cre.Atg7+/+
Cre.Atg7Δ/Δ
Cre.Atg7+/+
Cre.Atg7Δ/Δ
Psmb9 - mRNA
Tap1 - mRNA
Tapbp - mRNA
H2-Ab1 - mRNA
H2-Eb1 - mRNA
Fcgr2b - mRNA
H2-K1 - mRNA
H2-T23 - mRNA
Psmb8 - mRNA
H2-D1 - mRNA
H2-Aa - mRNA
Cd74 - mRNA
Cd1d2 - mRNA
H2-Ob - mRNA
H2-Q2 - mRNA
H2-Ea-ps - mRNA
H2-Q1 - mRNA
H2-DMb2 - mRNA
Nod2 - mRNA
Ccr7 - mRNA
H2-Q10 - mRNA
Mr1 - mRNA
Cd1d1 - mRNA
Icam1 - mRNA
H2-DMb1 - mRNA
H2-DMa - mRNA
Nod1 - mRNA
Ralb - mRNA
Slc11a1 - mRNA
Fcgr1 - mRNA
Fcgr3 - mRNA
Fcer1g - mRNA
H2-M3 - mRNA
Tap2 - mRNA
-2
-1
0
1
2

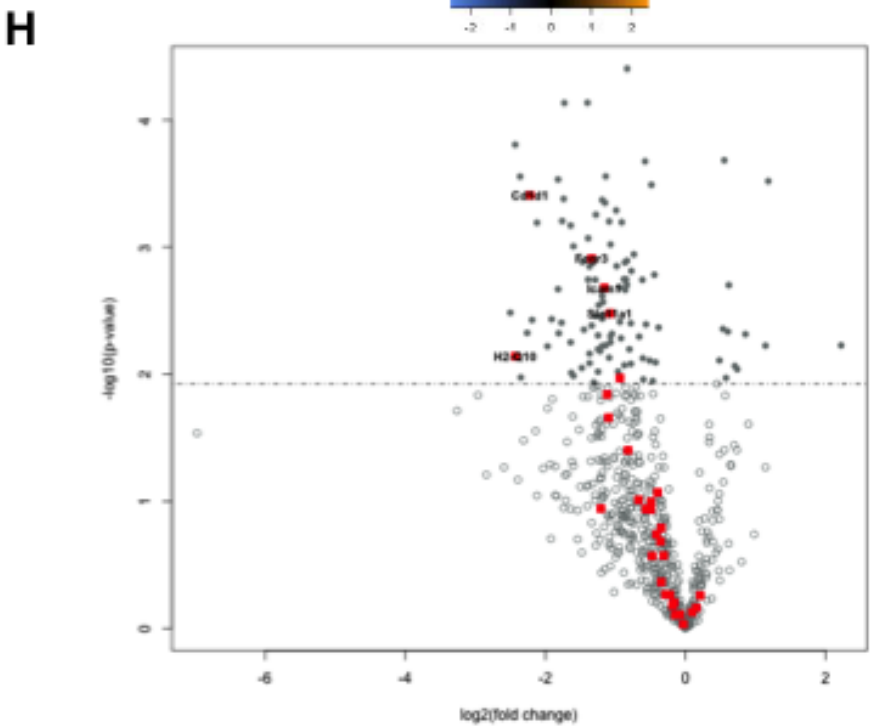
H
-log10(p-value)
log2(fold change)
-6
-4
-2
0
2
0
1
2
3
4

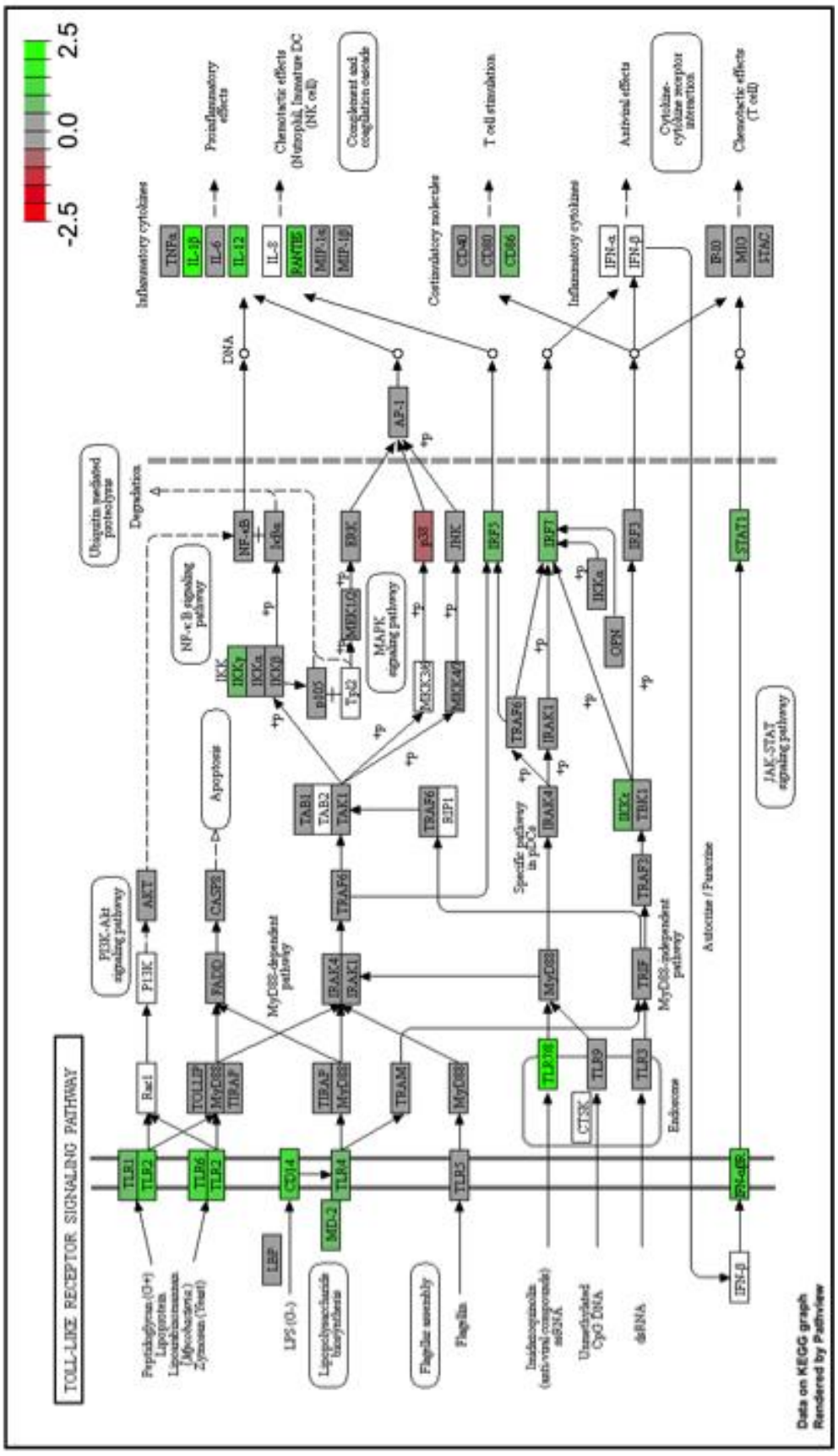
TOLL-LIKE RECEPTOR SIGNALING PATHWAY
-2.5
0.0
2.5
Data on KEGG graph
Rendered by Pathview

Figure 18. Many immunity genes are upregulated in tumor samples from Cre.Atg7Δ/Δ mice. Heatmaps and Volcano plots of genes from nCounter pathways: Innate (**A-B**), TLR (**C-D**), Interferon (**E-F**) and Antigen Processing (**G-H**). Heatmaps show relative increase in gene expression in orange and decrease in blue. The Volcano plots indicate pathway-related genes with red squares, upregulation in Cre.Atg7Δ/Δ compared to Cre.Atg7+/+ is shown in genes on the left side of the plot, and genes of statistical significance ($P < 0.01$ by the nCounter software) are above the dotted lines. Grey circles are other genes from the Nanostring that are not part of the analyzed pathway. A graphical representation of the TLR pathway and the genes upregulated (green) in Cre.Atg7Δ/Δ samples (**I**).

In vivo *depletion of Tregs by PC61 monoclonal antibody treatment causes regression of tumor in Cre.Atg7+/+ mice.*

The analysis of the gene expression of tumors borne by Cre.Atg7Δ/Δ having revealed a slightly decreased Treg signal, and previous work by the Lattime group having shown the important of Tregs in the parent MB49 model[113], we decided to confirm their findings in the Cre.Atg7 construct mice. Four days before injecting 2.5x10^5 MB49 cells into the bilateral flanks of Cre.Atg7+/+ and Cre.Atg7Δ/Δ mice, we injected 250 μg PC61 monoclonal antibody in 200 μL i.p, with continued doses every seven days thereafter. PC61 targets the CD25 receptor, the high-affinity IL-2 receport, and has been shown to preferentially deplete Tregs *in vivo*[Kohm 2006]. Cre.Atg7+/+ mice treated with PC61 had their tumors regress over time (**Figure 19A**), and by the end of the experiment they had shrunk to the level of the Cre.Atg7Δ/Δ mice's untreated tumors (**Figure 19B-C**).

PC61 treatment had a significantly larger effect on Cre.Atg7+/+ mice than Cre.Atg7Δ/Δ mice, suggesting the possibility that *Atg7* deficiency acted on MB49 tumor growth via a Treg-dependant mechanism (**Figure 19D**), possibly by the increased pro-inflammatory milieu as evidenced by the gene expression data.

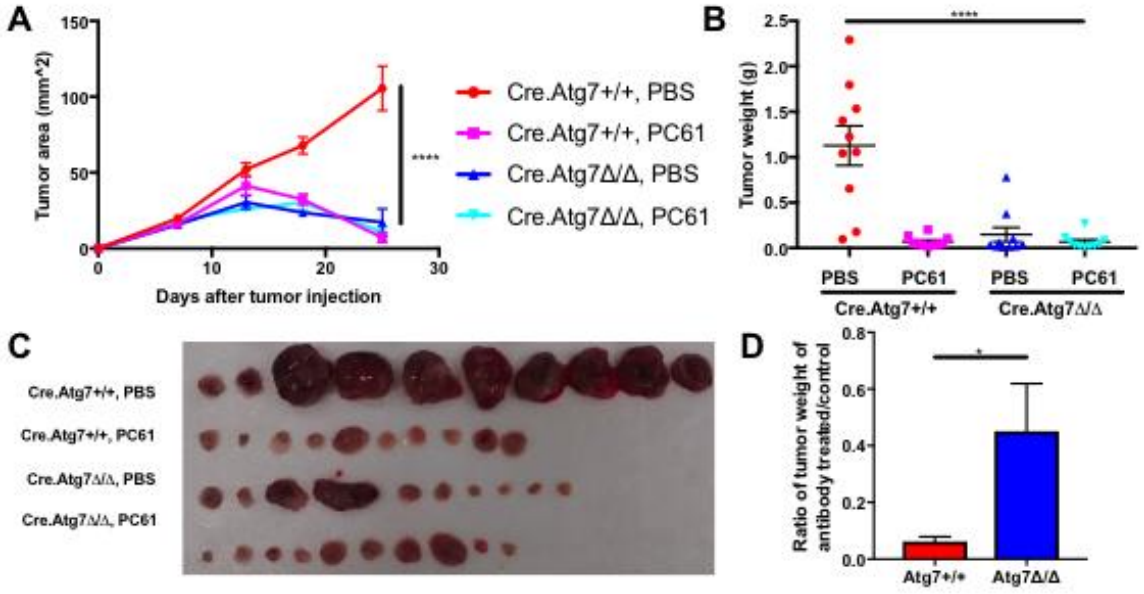

Figure 19. Depletion of Tregs by PC61 monoclonal antibody treatment causes MB49 rejection in female Cre.Atg7+/+ mice similar to untreated Cre.Atg7Δ/Δ. MB49 was injected s.c. into bilateral flanks of female mice of the indicated group, and tumor area was measured over time (**A**), with tumor weight measured at the end of the experiment (**B**) and pictures taken (**C**). PC61 monoclonal antibody was injected i.p. on day -4 and every 7 days after. The ratio of tumor weight between PBS controls and PC61 treated mice (**D**). (Turkey's multiple comparisons test (**A-B**) and Welch's t test (**D**); * P<0.05, **** P<0.0001).

CD4+ T have a larger effect in the immunogenic rejection MB49 in Cre.Atg7Δ/Δ than CD8+ T cells.

Previous work by the Lattime group had shown that in the absence of Tregs, the CD4+ T cell response was the most important element of MB49 immune rejection[113]. Our earlier monoclonal antibody experiments had only included combined aCD4 and aCD8 antibody treatments, so we decided to treat with the antibodies separately to evaluate the importance of each T-cell population. We treated MB49-bearing female Cre.Atg7Δ/Δ mice with either aCD4 monoclonal antibody, aCD8 monoclonal antibody, or both, and measured growth over time (**Figure 20A**). We found that depletion of CD4+ T cells had a larger impact on tumor growth than depletion of CD8+ T cells, but that it alone did not reconstitute the complete effect of depletion of both populations (**Figure 20B**). Depletion of CD4+ T cells also depleted Tregs, possibly creating mixed effects, but the increased tumor size in the aCD4 group indicates that the loss of effector cells outweighed any effects of loss of Tregs in Cre.Atg7Δ/Δ mice. This matched with what the Lattime group had previously seen and indicated that the CD4+ T cells were key in Cre.Atg7Δ/Δ immune rejection of MB49.

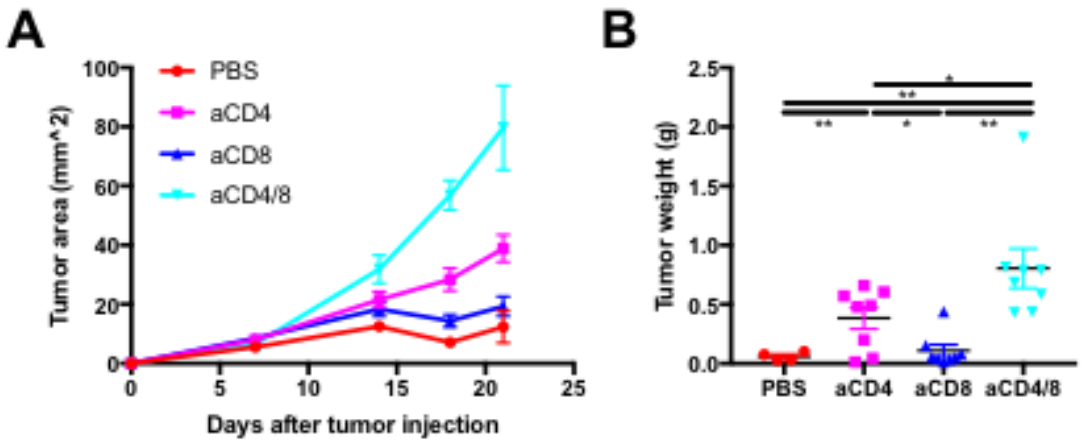

Figure 20. CD4+ T cell depletion has a larger impact on MB49 tumor growth in female Cre.Atg7Δ/Δ than CD8+ T cell depletion. 2.5x10^5 MB49 tumor cells were injected s.c. into bilateral flanks of female Cre.Atg7Δ/Δ mice. Two days prior and every five days thereafter 200 μg of each indicated antibody was injected in 100 μL PBS i.p. into the mice, and tumor area was measured over time (**A**). Tumors were excised and weighed at the end of the experiment (**B**). (Welch's t test; * P<0.05, ** P<0.01).

The decreased growth of YUMM1.1 in male Cre.Atg7Δ/Δ is not rescued by aCD4 and aCD8 antibody treatment.

Having determined that the growth of MB49 was impacted by host *Atg7* status in an immunogenic manner, we next sought to determine if this effect was replicated in other tumor cell lines. We injected 1x10^6 male murine melanoma YUMM1.1 cells into bilateral flanks of male Cre.Atg7+/+ and Cre.Atg7Δ/Δ mice two days after treating with aCD4 and aCD8 monoclonal antibodies, and tracked their growth (with repeated doses of antibody every five days) as we had with MB49 (**Figure 21A**). While there was a significant decrease in tumor area and weight in Cre.Atg7Δ/Δ mice, tumor growth was

not significantly rescued by T cell depletion (**Figure 21B-D**). T cell depletion was confirmed by flow cytometry, which showed no significant changes in the TILs (**Figure 21E**). The decrease in growth of YUMM1.1 in male Cre.Atg7Δ/Δ mice thus did not appear to be immunogenic in nature, which was not surprising given its low mutation burden and the lack of the surrogate HY antigens[124].

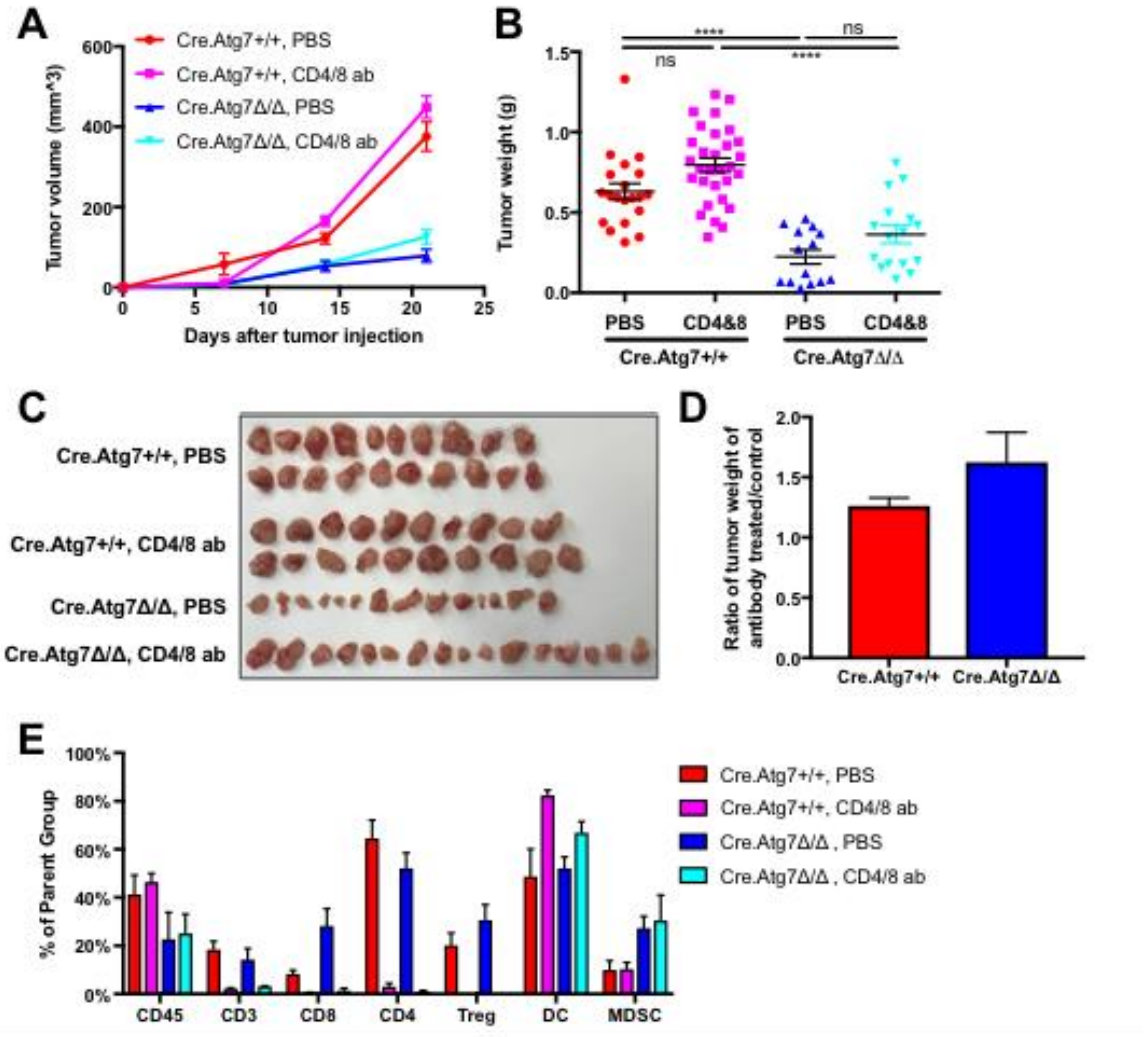

Figure 21. YUMM1.1 growth is decreased in male Cre.Atg7Δ/Δ but is not rescued by aCD4 and aCD8 antibody treatment. 1x10^6 YUMM1.1 cells were injected s.c. into

bilateral flanks of male Cre.Atg7+/+ and Cre.Atg7Δ/Δ mice and measured over time (**A**), injected i.p. with a-CD4 and a-CD8 monoclonal antibodies at day -2 and every 5 days thereafter. At three weeks of growth tumors were removed, weighed (**B**), and photographed (**C**). The ratio of the tumor weight of antibody-treated and PBS control groups was calculated (**D**). TILs measured via flow cytometry (**E**). (Turkey's multiple comparisons test; **** P<0.0001).

aCD4 and aCD8 antibody treatment rescue the growth of YUMM1.1 in female Cre.Atg7Δ/Δ mice.

Knowing that YUMM1.1 as a genetically induced tumor model contains less potential neo-antigens than MB49, especially when grown in male mice, we next tested the impact on YUMM1.1 growth in female mice, where we could make use of the surrogate HY antigens. Two days before injecting 1x10^6 YUMM1.1 cells into bilateral flanks of female Cre.Atg7+/+ and Cre.Atg7Δ/Δ mice, we treated with aCD4 and aCD8 monoclonal antibodies, giving another dose every five days. Tumor volume was decreased in Cre.Atg7Δ/Δ mice compared to Cre.Atg7+/+ mice, but significantly rescued by antibody treatment (**Figure 22A**). This rescue of tumor growth was even clearer when tumors were removed, weighed and photographed (**Figure 22B-D**), showing that there was no significant difference in tumor weight after antibody treatment between Cre.Atg7+/+ and Cre.Atg7Δ/Δ mice. T cell depletion was confirmed by flow cytometry (data not shown). These data indicate that in the presence of HY antigens, female Cre.Atg7Δ/Δ can drive a successful immune response against YUMM1.1 tumors.

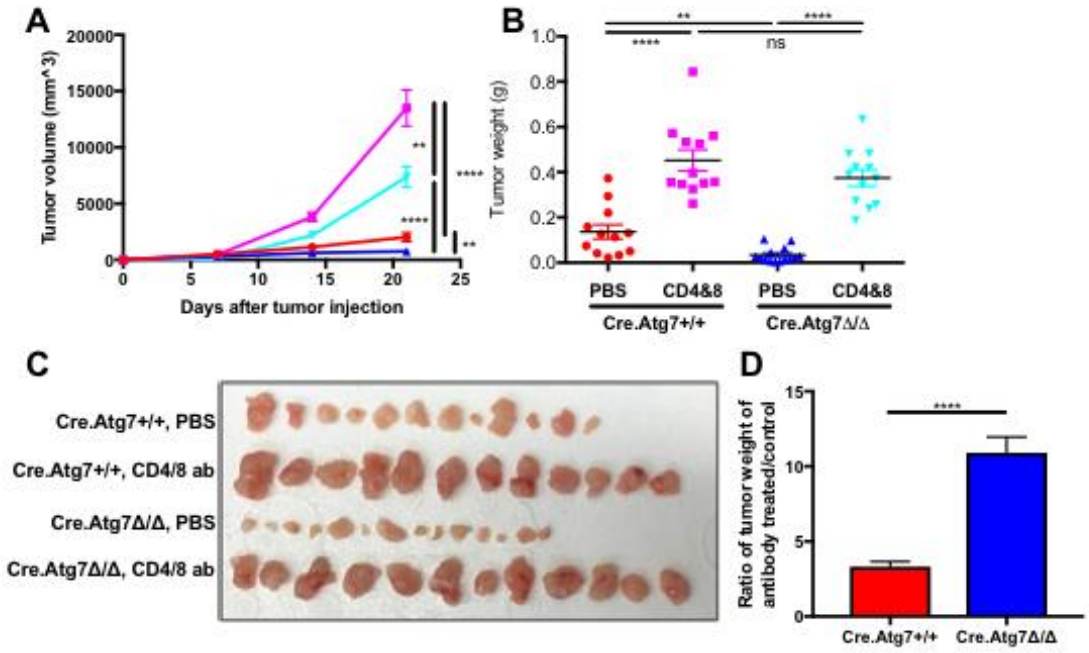

Figure 22. YUMM1.1 growth in Cre.Atg7Δ/Δ is rescued by aCD4 and aCD8 monoclonal antibody treatment. 1x10^6 YUMM1.1 cells were injected s.c. into bilateral flanks of female Cre.Atg7+/+ and Cre.Atg7Δ/Δ mice and measured over time (**A**), injected i.p. with a-CD4 and a-CD8 monoclonal antibodies at day -2 and every 5 days thereafter. At 3 weeks of growth tumors were removed, weighed (**B**), and photographed (**C**). The ratio of the tumor weight of antibody-treated and PBS control groups was calculated (**D**). (Unpaired t test; ** P<0.01, **** P<0.0001).

YUMM1.7 shows indications of immune mediated decrease in growth in Cre.Atg7Δ/Δ mice

Preliminary studies with another tumor line, YUMM1.7, showed promising results in Cre.Atg7Δ/Δ that indicate they may replicate the immune findings with MB49 and YUMM1.1. We found that YUMM1.7 grew significantly smaller in female Cre.Atg7Δ/Δ mice (**Figure 23A-B**), but not in male Cre.Atg7Δ/Δ mice (**Figure 23C-D**). No T cell depletions have yet been tested to confirm that this difference in growth is immunogenic, but in fB6, even though YUMM1.7 grows larger than YUMM1.1 (**Figure 23E**), it generates greater specific anti-tumor CTL (**Figure 23F**). While preliminary, this is similar to findings with YUMM1.1 and suggests Cre.Atg7Δ/Δ mice can generate a more effective anti-tumor immune response than Cre.Atg7+/+, contingent on the expression of a strong TAA like HY.

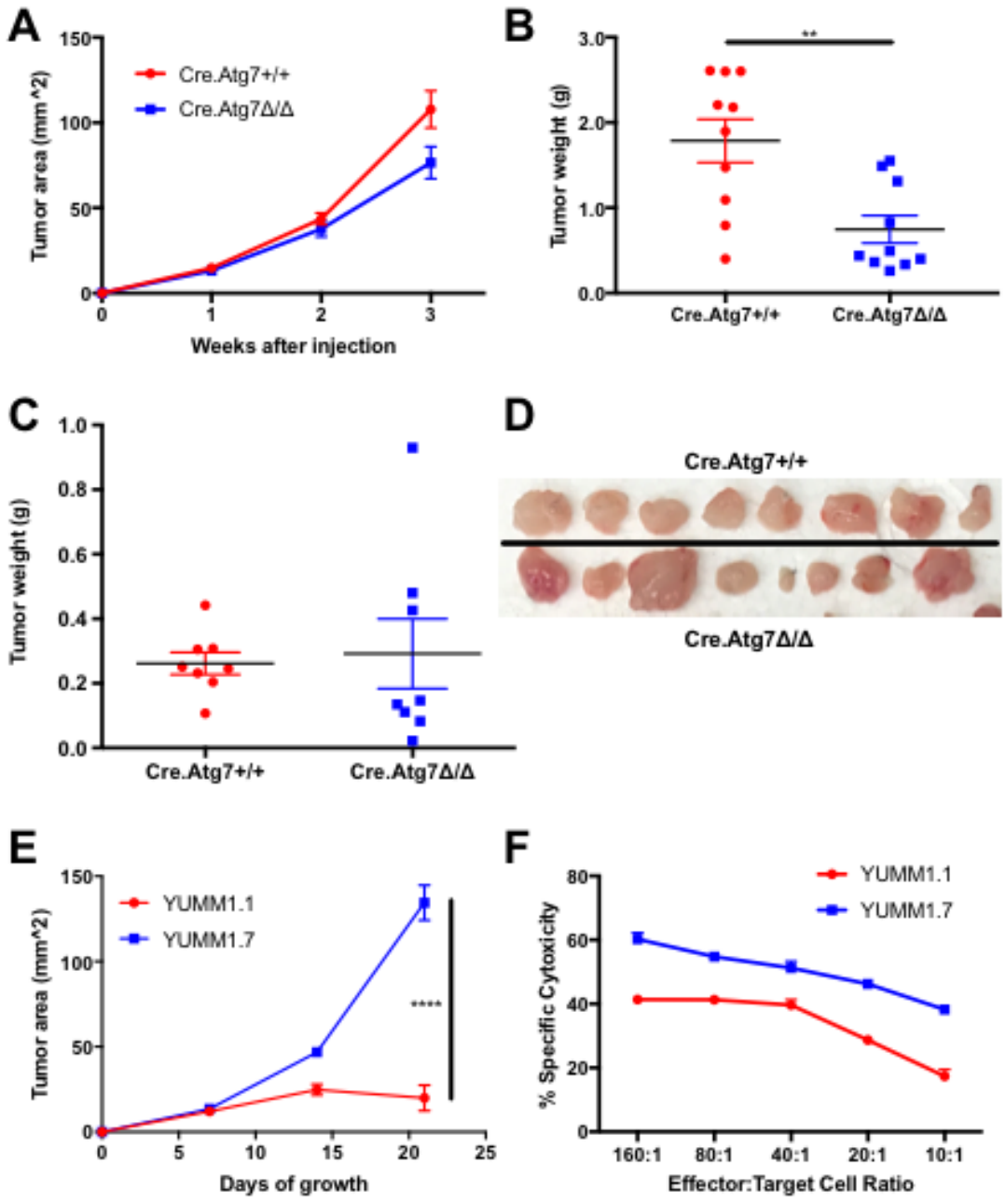

Figure 23. YUMM1.7 growth is suppressed in female Cre.Atg7Δ/Δ mice in a likely immunogenic manner. 1x10^5 YUMM1.7 cells were injected s.c. into bilateral flanks of female Cre.Atg7+/+ and Cre.Atg7Δ/Δ mice and measured over time (**A**) before being removed and weighed (**B**). 1x10^5 YUMM1.7 cells were injected s.c. into bilateral flanks of male Cre.Atg7+/+ and Cre. Atg7Δ/Δ mice for 21 days before being removed, weighed

(**C**) and photographed (**D**). 1x10^6 YUMM1.1 and 1x10^5 YUMM1.7 cells were injected into bilateral flanks of fB6 mice and measured over time (**E**). Their spleens were removed, restimulated with irradiated male splenocytes as part of a CTL assay against MB49 tumor cells (**F**). (Welch's t test (**B**) and Sidak's multiple comparisons test (**E**); ** $P<0.01$, **** $P<0.0001$).

DISCUSSION

The findings reported here provide additional evidence of the important role autophagy can play in the development of immune responses against cancer. We found a significant difference in immune response against one Atg7Δ/Δ MB49 clone but were unable to find any significant patterns based on *Atg7* status after testing several additional clones, with or without intratumoral vaccinia virus treatment. Whole body deletion of *Atg7* led to significantly reduced MB49 growth in both female and male mice that was immunologic in nature, while YUMM1.1 only generated a significant immune response when grown in female, not male mice. Finally, we attempted to characterize the female Cre.Atg7Δ/Δ immune response to MB49 and show how loss of Treg function could be the mechanism by which loss of *Atg7* led to MB49 rejection.

Clonal variability and hetereogeneity between MB49 CRISPR-Cas9 clones prevented any conclusions on potential immune differences based on Atg7 status.

The studies described in Chapter 1 of EXPERIMENTAL RESULTS demonstrate that while the Atg7Δ/Δ clone MB49-XD3 resulted in significantly elevated immune responses, there was no clear pattern of immune effects based on *Atg7* deletion when more clones were studied. Compared to Atg7+/+ clone MB49-XD1, MB49-XD3 induced a stronger immune response, leading to tumor rejection, increased specific anti-tumor CTL activity, and IFN-γ production (**Figure 4**). MB49-XD3 had fewer infiltrating Tregs and a larger proportion of CD4+ effector T cells than MB49-XD1, and a greatly decreased number of tumor cells expressing MHC-II *in vivo* (**Figure 5**). Intratumoral treatment with the VV-HY viral cocktail expressing GM-CSF and HY antigens decreased

tumor growth and increased anti-tumor CTL in MB49-XD1, but in MB49-XD3 it actually led to decreased CTL activity (**Figure 6**).

The generation and testing of additional Atg7+/+ and Atg7Δ/Δ MB49 clones by CRISPR-Cas9 revealed significant clonal variability in growth and the capacity to induce specific anti-tumor immune responses, but no pattern based on *Atg7* status emerged (**Figure 7**). Interestingly, when grown in mB6 instead of fB6, removing HY as a potential antigen, the three Atg7Δ/Δ MB49 clones tested grew significantly larger, but the 2 Atg7+/+ clones did not (**Figure 8**), indicating the possibility than in the absence of a strong surrogate antigen like HY, loss of tumor autophagy actually increased tumor growth and potentially weakened the immune response against other TAAs.

Since MHC-II expression on tumor cells can be used to induce activation of CD4+ T cells[115,125,126], and tumors are known to induce Tregs[127,128], we hypothesize that the downregulation of MHC-II on MB49-XD3 led to rejection by the immune system via decreased Treg signaling. While at first we thought it possible that this lack of MHC-II expression *in vivo* could have been a function of *Atg7* deletion in the clone, other Atg7Δ/Δ MB49 clones expressed significant amounts of MHC-II *in vivo* (**Figure 9**), such that the underlying mechanism by which MB49-XD3 downregulated MHC-II expression *in vivo* is more likely to be based on inherent clonal variability of the MB49 line. MB49 was generated via exposure to a carcinogen, a process known to generate many distinct mutations, and demonstrates significant heterogeneity in the cell line. The CRISPR-Cas9 process we utilized likely either selected for a subclone that was phenotypically distinct before *Atg7* was deleted or introduced off target mutations that altered MHC-II expression.

Indeed, further analysis of additional CRISP-Cas9 generated MB49 clones supported the clonal variability hypothesis, as there was no significant or consistent difference in Atg7+/+ MB49-XC31 and Atg7Δ/Δ MB49-XC49 with regards to tumor size or induced CTL (**Figure 9**). To rule out the possibility that our choice of injection site was impacting experimental variability, we switched from the groin to the flank of the mice. While there appeared to be less variability in size between mice within each group, there was still no clear pattern based on *Atg7* status, with significant clonal variability even between clones of the same genotype (**Figures 10-11**). In an attempt to remove the confounding issue of clonal variability, we generated new MB49 subclones by single-cell sorting. In the future we will select a few of these single-cell MB49 clones and perform CRISPR-Cas9 deletion of *Atg7* again, creating paired Atg7+/+ and Atg7Δ/Δ clones that arise from the same original cell. This will allow us to repeat these experiments without the clonal variability and with minimal genetic variability between compared clones to determine what—if any—effect deleting tumor *Atg7* has on the development of an anti-tumor immune response.

Whole body deletion of Atg7 leads to immune-mediated rejection of MB49, likely through decreased Treg function.

The studies described in Chapter 2 of EXPERIMENTAL RESULTS show that autophagy deficiency in the host can lead to a significant immunological response that can cause tumor regression and rejection. Previous work by many groups have shown the complicated role that autophagy can play in development of anti-tumor immune responses[65,129,130], facilitating presentation and cross-presentation of tumor antigens[131-133], production of and signaling by both type I and II interferons[51,134,135], as well as other

cytokines[136,137], as well as promoting survival and maturation of immune cells[68,72,138,139]. Our work indicated that in the context the tumor lines studied, global autophagy deficiency improved the immune outcome.

We first confirmed that the addition of the inducible Cre-recombinase construct to C57BL/6 mice did not grossly impair the ability of the mice to generate specific anti-HY immunity (**Figure 12**). Preliminary results and data from collaborators in the White lab indicated that, in fact, tumors often had suppressed growth in Cre.Atg7Δ/Δ mice. We determined that MB49—previously characterized by our lab as a strongly immunosuppressive tumor with a high mutation burden[116] that under proper conditions can generate a productive immune response[112]—followed the pattern seen by the White lab. MB49 completely regressed in female Cre.Atg7Δ/Δ mice (**Figure 13**) and had diminished growth in male Cre.Atg7Δ/Δ mice (**Figure 14**), but was rescued when T cells were depleted. Previous work by our lab (**Figure 1**) determined that MB49 evaded the immune response via the immune-inhibitory effects of Tregs, and that if Tregs were depleted by PC61 monoclonal antibody treatment, the resulting CD4+ T cell response could effectively reject the tumors[113]. We showed by flow cytometry that at 2 weeks of growth there was no difference in the frequency of Tregs in MB49 tumors grown in female Cre.Atg7+/+ or Cre.Atg7Δ/Δ (**Figure 15**), and confirmed that by IHC (**Figure 16**). Analysis of RNA expression by Nanostring showed a general upregulation of immune responses across multiple immune pathways, with a slight decrease in Treg signal in Cre.Atg7Δ/Δ (**Figure 17**). Many of the 100 significant and highly differentially expressed genes in Cre.Atg7Δ/Δ (**Table 1**) were related to innate immunity, demonstrating a possible causal link for MB49 regression via increased innate pro-

inflammatory responses that allowed for the generation of activated effector T cells instead of inhibitory Tregs (**Figure 18**). Depletion of Tregs by PC61 monoclonal treatment caused the tumors of Cre.Atg7+/+ mice to regress similar to Cre.Atg7Δ/Δ mice, supporting the hypothesis that deficient Treg function was central to the Cre.Atg7Δ/Δ immune response (**Figure 19**). Additionally, we found that CD4+ T cells were key to the rejection of MB49 in Cre.Atg7Δ/Δ mice (**Figure 20**). These results suggest that *Atg7* deficiency led to increased activation of innate immunity pathways and pro-inflammatory cytokine production that resulted in decreased activation or function of Tregs, allowing the development of a successful anti-MB49 immune response that caused tumor rejection.

Functional autophagy has been shown by other groups to be important to Treg health and function. Specific disruption of *Atg7* in FoxP3+ Tregs led to a profound loss of Tregs in mice[77], and increased tumor rejection[76]. Our model differs significantly from that of these other groups in that loss of *Atg7* is global instead of Treg-specific and induced only one week before tumor inoculation, which may explain why we found no difference in the number of Tregs in the spleens or tumors of the Cre.Atg7Δ/Δ mice. Preliminary results of ongoing work in our lab indicate that the Tregs from Cre.Atg7Δ/Δ mice maintain the capacity to produce IL-10 when broadly stimulated *in vitro* by PMA/Ionomycin (data not shown) or CD3/CD28 microbeads. This may indicate that the Treg function may not be directly impacted by loss of *Atg7*, but may instead be indirectly impacted by alterations in innate immunity such as antigen presentation and cytokine production, or by tumor or host immune metabolism or some other mechanism.

YUMM lines replicate some of the key results seen with MB49 in Cre.Atg7Δ/Δ.

Having shown that MB49 growth was suppressed via immune-mediated rejection in Cre.Atg7Δ/Δ mice, we next showed that this effect could be recapitulated with other cell lines. YUMM1.1 and YUMM1.7 differ from MB49 significantly in that they are a genetically induced cell lines with a few key driver mutations[118], with an overall low mutation burden, but they share expression of the HY surrogate antigen. When YUMM1.1 was implanted in male Cre.Atg7Δ/Δ mice, tumor growth was inhibited, but was not rescued by T cell depletion (**Figure 21**). However, when implanted into female Cre.Atg7Δ/Δ mice, T cell depletion was sufficient to rescue tumor growth (**Figure 22**). Preliminary experiments with YUMM1.7 reveal similar results, with decreased growth only in female Cre.Atg7Δ/Δ mice (**Figure 23**). These results indicate that in the presence of the strong antigen HY, Cre.Atg7Δ/Δ can improve immune-mediated suppression of YUMM1.1, but without a strong antigen any effect on tumor growth is non-immunogenic.

This would also explain why male Cre.Atg7Δ/Δ has a significant immune-mediated effect on the growth of MB49 but not YUMM1.1, as the MB49 line contains many mutations and potential neoantigens beyond HY, while YUMM1.1 and YUMM1.7 contain few. High numbers of mutations, and thus neoantigens, have been shown by many groups to correlate to successful cancer immunotherapy and are theorized to provide many neo-epitopes for the adaptive immune system to target[124,140-142]. Based on these observations, research into the effects on the immune response against YUMM1.1

and YUMM1.7 clones mutagenized with ultraviolet radiation are being planned by our group in collaboration with the White lab.

Future directions based on these studies

Our work in this dissertation can be broken down into three key findings. We found that tumor autophagy defects in MB49 may lead to improved immune responses, but clonal variability needs to be controlled for. We demonstrated that inducible deletion of *Atg7* and disruption of autophagy caused an immune-mediated suppression of MB49 growth that was likely caused by modulation innate immunity impacting Treg function. And finally we showed that this effect could be seen in additional tumor lines beyond MB49, with both YUMM1.1 and YUMM1.7 showing suppressed growth in Cre.Atg7Δ/Δ female mice. Future studies based on this work will build off of these three key findings.

The MB49 CRISPR-Cas9 clones studied in this work were generated from a heterogenous cell line with many mutations. Single-cell subclones have already been generated, and the CRISPR-Cas9 protocol to delete *Atg7* can be repeated with them to generate paired sets of Atg7+/+ and Atg7Δ/Δ MB49 clones derived from the same single cell, and thus with as similar a genotype as possible but for the *Atg7* locus. Use of these paired sets would eliminate the confounding clonal variability we saw in the results of Chapter 1 of EXPERIMENTAL RESULTS. Future experiments could determine whether the deletion of *Atg7* in these MB49 clones causes a significant and consistent difference in their capacity to grow *in vitro* and *in vivo*. In the event of a pattern of changed growth in Atg7Δ/Δ clones, the identity of key immune cell populations affecting tumor growth could be identified by flow cytometry and IHC. Treating with monoclonal antibodies to eliminate CD4+ and/or CD8+ cells, or to eliminate Tregs, could connect those important

populations to Atg7Δ/Δ tumor growth. While previous work by our lab showed that functional autophagy is not required for VV replication and maturation[99], others have shown how autophagy defects impact the STING pathway[143]. It will be important to determine if Atg7Δ/Δ tumor cells are more or less amenable to OV therapy. The ultimate goal of these studies would be to use the Atg7Δ/Δ MB49 cells as a model for the combination of autophagy modulation treatments with immunotherapy.

Our findings that global disruption of *Atg7* led to immune-mediated rejection of MB49 serves as a basis for several future avenues of study. First, 100 significant differentially expressed genes were discovered via Nanostring in the tumors of Cre.Atg7Δ/Δ mice, many of them related to innate immunity. Identifying specific genes for further study such as TLR genes will allow for investigation into the mechanisms of the immune-mediated rejection of MB49. Based on the finding of decreased genetic signal for Tregs, continued work to determine how Tregs are impacted in Cre.Atg7Δ/Δ mice can be done by isolating and using them in a Treg suppression assay[144]. Isolating CD11c+ dendritic cells and priming them with tumor-specific antigen peptides to use as APCs instead of broad stimulation with CD3/CD28 latex beads in a T cell Proliferation assay would allow us to determine if *Atg7* deletion grossly impacts the ability of T cells to proliferate or only in response to recognize specific antigens. The same could be activate Tregs and stimulate IL-10 and TGF-β production to determine if *Atg7* deletion impacts the capacity of Tregs to be stimulated globally or by specific antigens. Furthermore, to investigate the possibility that Tregs are only indirectly impacted by *Atg7* deletion, with the primary cause being change in antigen presentation, CD11c-Cre mice[145] could be obtained and crossbred with Atg7flox/flox mice. In our work presented

here, host autophagy was disrupted while tumor autophagy remained intact, an unrealistic condition that would not be present in patients potentially treated with autophagy inhibitors. Atg7Δ/Δ MB49 clones could be injected into Cre.Atg7Δ/Δ mice, or in order to more closely model potential therapy conditions, autophagy inhibitors like hydroxychloroquine, bafilomycin A1 or 3-methyladenine could be used[43,146]. By evaluating the impacts on anti-tumor immunity in a variety of autophagy-deficient models we can hope to gain a more complete understanding of the complex role autophagy plays.

Our findings regarding YUMM1.1 and YUMM1.7 growth and generation of immunity in Cre.Atg7Δ/Δ mice lead to several remaining questions. YUMM1.7 has yet to be examined with monoclonal antibodies depleting T cells to fully confirm that the change in growth seen in Cre.Atg7Δ/Δ is indeed immunogenic, nor have we determined if Tregs (or perhaps MDSCs) are important in YUMM1.1 or YUMM1.7 immune evasion. Another question to be answered is whether mutagenizing these YUMM lines with UV-irradiation will cause them to be more immunogenic, and in the case of growth in Cre.Atg7Δ/Δ mice, more fully replicate the findings seen with MB49. Preliminary ongoing work with these YUMM-UV lines is supportive of this hypothesis. Finally, having seen immunogenic differences in all three of these tumor lines, finding additional tumor lines to study to determine if this is only seen in certain tumors, such as those with significant antigens like HY or that contain many neoantigens.

The studies described in this dissertation provide additional evidence that autophagy plays critical roles in the development of anti-tumor immunity. The models presented here provide numerous options for future research aimed at more fully

understanding how disrupting autophagy can be used to treat cancer, and how the interplay between autophagy's effects on tumor metabolism and its impact on the generation of anti-tumor immunity can best be balanced.

CONCLUSIONS

Based on the findings presented in this dissertation, we make the following conclusions:

1. Subcutaneous injection of the Atg7Δ/Δ tumor cell line MB49-XD3 resulted in tumor rejection and increased specific anti-tumor CTL activity and IFN-γ production, likely because of the decreased expression of MHC-II *in vivo*. However, analysis of additional Atg7Δ/Δ clones did not replicate this finding, and this clonal variability prevents the drawing of any conclusion based on *Atg7* status.

2. Host autophagy deficiency caused by the acute inducible deletion of *Atg7* does not grossly impact the capacity to be immunized against the HY antigen and generate specific CTL activity. This suggests that in the timeframe of our immune experiments we can confidently use the Cre.Atg7Δ/Δ mouse model to characterize anti-tumor immunity.

3. Female Cre.Atg7Δ/Δ but not Cre.Atg7+/+ mice reject MB49 tumors by three weeks of growth, but i.p. injection with aCD4 and aCD8 monoclonal antibodies fully rescues growth. Analysis by flow cytometry and IHC revealed a significant increase in tumor-infiltrating CD4+ T cells in Cre.AtgΔ/Δ mice. We thus conclude that global *Atg7* disruption caused an immunogenic rejection of MB49.

4. MB49 growth is significantly suppressed in male Cre.Atg7Δ/Δ compared to Cre.Atg7+/+, with i.p. injection with aCD4 and aCD8 monoclonal antibodies fully rescuing tumor growth. Compared to growth in female Cre.Atg7Δ/Δ the tumor grew larger and did not have as significant an elevation of CD4+

infiltrating T cells as determined by flow cytometry and IHC. From this we can conclude that in the even absence of the strong HY antigen, *Atg7* disruption can have a significant effect on anti-MB49 immunity, likely through targeting of TAAs.

5. The size of the Treg population was unchanged in the spleens and tumors of Cre.Atg7+/+ and Cre.Atg7Δ/Δ mice as measured by flow cytometry and IHC, but Nanostring analysis of RNA expression showed a slight decrease in the Treg signal profile in Cre.Atg7Δ/Δ mice's tumors, and depletion of Tregs *in vivo* by i.p. injection of PC61 monoclonal antibody caused the rejection of MB49 tumors in Cre.Atg7+/+ mice. Preliminary analyses of inducible *ex vivo* Treg function showed no difference between Cre.Atg7+/+ and Cre.Atg7Δ/Δ. In addition, we showed that CD4+ T cells were more crucial than CD8+ T cells to support the rejection of MB49 in Cre.Atgy7Δ/Δ. These data support the conclusion that *Atg7* disruption altered Treg-driven immune escape, allowing a productive CD4+ effector T cell anti-tumor response, but further studies will be necessary to confirm this finding and determine the precise mechanism by which this occurs.

6. Analysis of the differential expression of several hundred immune related genes in the MB49 tumors of Cre.Atg7Δ/Δ mice revealed 100 statistically significant genes with highly altered expression. Many of them are related to innate immunity, TLRs, IFN and antigen presentation, confirming the work of others that autophagy deficiency can impact these pathways. More work needs to be done to fully identify and test all the genes involved, but these data support the conclusion that host autophagy deficiency led to an increase in innate immunity

that led to the upregulation of pro-inflammatory cytokines that altered the immune response to MB49, overcoming immune invasion by the tumor and driving specific and production anti-MB49 immunity.

7. YUMM1.1 tumor growth was inhibited in both male and female Cre.ATg7Δ/Δ mice, but was found to only be mediated by adaptive immunity when grown in female mice. In male mice, treatment with aCD4 and aCD8 monoclonal antibodies made no significant difference in tumor growth, but in female mice T cell depletion fully rescued growth in Cre.Atg7Δ/Δ mice. From this we conclude that *Atg7* disruption can improve anti-tumor immune responses only if a strong enough antigen is present.

SUMMARY

In the studies presented in this dissertation, we found that some Atg7Δ/Δ MB49 clones had significantly improved induction of specific anti-tumor immunity when grown in immunocompetent C57BL/6 mice, but that ultimately clonal variability was too much of an issue to draw broader conclusions about the role of tumor autophagy in the development of immune responses. The clone with the most impressive responses, MB49-XD3, differed significantly from other clones in that it did not express MHC-II *in vivo*, which likely led to a change in the ability of the tumor to activate immune escape mechanisms like Tregs. These changes causes a significant improvement increase in infiltration of CD4+ T cells, increased IFN-γ production and heightened CD8+ CTL activity.

We also examined whether global host autophagy deficiency would alter the development of systemic immune responses against MB49. Measurement of tumor growth revealed significant rejection of tumors by Cre.Atg7Δ/Δ mice that was rescued by depletion of effector T cells. Immunohistochemistry revealed significantly increased infiltrate of CD4+ T cells into the tumors of Cre.Atg7Δ/Δ mice. Analysis of tumor RNA expression indicated a broad upregulation of immune genes and increase innate immunity and pro-inflammatory cytokines, with a decreased Treg signal, though no gross changes in Treg number were detected systemically or in the tumor. Depletion of Tregs systemically led to the rejection of MB49 tumor even in Cre.Atg7+/+ mice. Preliminary experiments with additional cell lines replicate several of the key findings in MB49.

These results demonstrate the importance of autophagy in the development of anti-tumor immunity, and indicate that systemic autophagy inhibition may not only be a

viable chemotherapeutic option for cancer treatment, but can possibly lead to improved development of anti-tumor immunity.

BIBLIOGRAPHY

1 Mizushima, N. The pleiotropic role of autophagy: from protein metabolism to bactericide. *Cell Death and Differentiation* **12**, 1535-1541 (2005).

2 Klionsky, D. & Emr, S. Autophagy as a regulated pathway of cellular degradation. *Science* **290**, 1717-1721 (2000).

3 Klionsky, D. The molecular machinery of autophagy: unanswered questions. *J Cell Sci* **118**, 7-18 (2005).

4 Mizushima, N. & Komatsu, M. Autophagy: renovation of cells and tissues. *Cell* **147**, 728-741 (2011).

5 Yang, Z. & Klionsky, D. J. Mammalian autophagy: core molecular machinery and signaling regulation. *Curr Opin Cell Biol* **22**, 124-131 (2010).

6 Kroemer, G. & Jäättelä, M. Lysosomes and autophagy in cell death control. *Nat Rev Cancer* **5**, 886-897 (2005).

7 White, E. Deconvoluting the context-dependent role for autophagy in cancer. *Nat Rev Cancer* **12**, 401-410 (2011).

8 Clague, M. J. & Urbé, S. Ubiquitin: Same Molecule, Different Degradation Pathways. *Cell* **143**, 682-685 (2010).

9 Johansen, T. & Lamark, T. Selective autophagy mediated by autophagic adapter proteins. *Autophagy* **7**, 279-296 (2011).

10 Kroemer, G., Mariño, G. & Levine, B. Autophagy and the integrated stress response. *Mol cell* **40**, 280-293 (2010).

11 He, C. & Klionsky, D. J. Regulation Mechanisms and Signaling Pathways of Autophagy. *Annual Review of Genetics* **43**, 67-93 (2009).

12 Mizushima, N., Yamamoto, A., Matsui, M., Yoshimori, T. & Ohsumi, Y. In Vivo Analysis of Autophagy in Response to Nutrient Starvation Using Transgenic Mice Expressing a Fluorescent Autophagosome Marker. *Molecular Biology of the Cell* **15**, 1101-1111 (2004).

13 Mathew, R. & White, E. Autophagy in Tumorigenesis and Energy Metabolism: Friend by Day, Foe by Night. *Curr Opin Genet Dev* **21**, 113-119 (2011).

14 Rabinowitz, J. D. & White, E. Autophagy and Metabolism. *Science* **330**, 1344-1348 (2010).

15 Degenhardt, K. *et al.* Autophagy promotes tumor cell survival and restricts necrosis, inflammation, and tumorigenesis. *Cancer Cell* **10**, 51-64 (2006).

16 Levine, B. & Kroemer, G. Autophagy in the Pathogenesis of Disease. *Cell* **132**, 24-42 (2008).

17 Yang, Z., Goronzy, J. J. & Weyand, C. M. Autophagy in autoimmune disease. *J Mol Med* **93**, 704-717, doi:10.1007/s00109-015-1297-8 (2015).

18 Mizushima, N., Levine, B., Cuervo, A. M. & Klionsky, D. J. Autophagy fights disease through cellular self-digestion. *Nature* **451**, 1069-1075 (2008).

19 Nakai, A. *et al.* The role of autophagy in cardiomyocytes in the basal state and in response to hemodynamic stress. *Nature Medicine* **13**, 619-624 (2007).

20 Xie, Z. & Klionsky, D. J. Autophagosome formation: core machinery and adaptations. *Nature Cell Biology* **9**, 1102-1109 (2007).

21 Nishida, Y. *et al.* Discovery of Atg5/Atg7-independent alternative macroautophagy. *Nature* **461**, 654-658 (2009).

22 Juenemann, K. & Reits, E. A. Alternative Macroautophagic Pathways. *International Journal of Cell Biology* **2012**, 8 (2012).

23 Chang, T.-K. *et al.* Uba1 functions in Atg7- and Atg3-independent autophagy. *Nature Cell Biology* **15**, 1067-1078 (2013).

24 Mizushima, N., Yoshimori, T. & Ohsumi, Y. The Role of Atg Proteins in Autophagosome Formation. *Annual Review of Cell and Developmental Biology* **27**, 107-132 (2011).

25 Komatsu, M. *et al.* Impairment of starvation-induced and constitutive autophagy in Atg7-deficient mice. *J Cell Bio* **169**, 425-434 (2005).

26 Jin, S. & White, E. Role of Autophagy in Cancer: Management of Metabolic Stress. *Autophagy* **3**, 28-31 (2007).

27 White, E. & DiPaola, R. S. The Double-edged Sword of Autophagy Modulation in Cancer. *Clin Cancer Res* **15**, 5308-5316 (2009).

28 Mathew, R. *et al.* Autophagy Suppresses Tumorigenesis Through Elimination of p62. *Cell* **137**, 1062-1075 (2009).

29 Balkwill, F. & Coussens, L. M. Cancer: An inflammatory link. *Nature* **431**, 405-406 (2004).

30 Mathew, R. *et al.* Autophagy suppresses tumor progression by limiting chromosomal instability. *Genes Dev* **21**, 1367-1381 (2007).

31 Karantza-Wadsworth, V. *et al.* Autophagy mitigates metabolic stress and genome damage in mammary tumorigenesis. *Genes Dev* **21**, 1621-1635 (2007).

32 Crotzer, V. L. & Blum, J. S. Autophagy and its role in MHC-mediated antigen presentation. *J Immunol* **182**, 3335-3341 (2009).

33 Crotzer, V. L. & Blum, J. S. Autophagy and adaptive immunity. *Immunology* **131**, 9-17 (2010).

34 Chen, N. & Karantza, V. Autophagy as a therapeutic target in cancer. *Cancer Biol Ther* **11**, 157-168 (2011).

35 Kimmelman, A. C. The dynamic nature of autophagy in cancer. *Genes Dev* **36**, 1999-2010 (2011).

36 Guo, J. Y. *et al.* Autophagy suppresses progression of K-ras-induced lung tumors to oncocytomas and maintains lipid homeostasis. *Genes & Dev* **27**, 1447-1461 (2013).

37 Guo, J. Y. & White, E. Autophagy is required for mitochondrial function, lipid metabolism, growth, and fate of KRASG12D-driven lung tumors. *Autophagy* **9**, 1636-1638 (2013).

38 Yang, S. *et al.* Pancreatic cancers require autophagy for tumor growth. *Genes Dev* **25**, 717-729 (2011).

39 Kenific, C., Thorburn, A. & Debnath, J. Autophagy and Metastasis: Another double-edged sword. *Curr Opin Cell Biol* **22**, 241-245 (2010).

40 Mulcahy-Levy, J. M. & Thorburn, A. Targeting Autophagy During Cancer Therapy to Improve Clinical Outcomes. *Pharmacol Ther* **131**, 130-141 (2011).

41 Poklepovic, A. & Gewirtz, D. A. Outcome of early clinical trials of the combination of hydroxychloroquine with chemotherapy in cancer. *Autophagy* **10**, 1478-1480, doi:10.4161/auto.29428 (2014).

42 Rosich, L. *et al.* Counteracting Autophagy Overcomes Resistance to Everolimus in Mantle Cell Lymphoma. *Clinical Cancer Research* **18**, 5278 (2012).

43 Chude, C. & Amaravadi, R. Targeting Autophagy in Cancer: Update on Clinical Trials and Novel Inhibitors. *Int J Mol Sci* **18**, doi:10.3390/ijms18061279 (2017).

44 Deretic, V., Saitoh, T. & Akira, S. Autophagy in infection, inflammation and immunity. *Nature Reviews Immunology* **13**, 722-737 (2013).

45 Münz, C. Regulation of innate immunity by the molecular machinery of macroautophagy. *Cell Microbiol* **16**, 1627-1636 (2014).

46 Netea-Maier, R., Plantinga, T., van de Veerdonk, F., Smit, J. & Netea, M. Modulation of inflammation by autophagy: Consequences for human disease. *Autophagy* **12**, 245-260 (2016).

47 Műzes, G., Constantinovits, M., Fűri, I., Tulassay, Z. & Sipos, F. Interaction of autophagy and Toll-like receptors: a regulatory cross-talk--even in cancer cells? *Curr Drug Targets* **15**, 743-752 (2014).

48 Delgado, M. A., Elmaoued, R. A., Davis, A. S., Kyei, G. & Deretic, V. Toll-like receptors control autophagy. *EMBO J* **27**, 1110-1121 (2008).

49 Rey-Jurado, E., Riedel, C., González, P., Bueno, S. & Kalergis, A. Contribution of autophagy to antiviral immunity. *FEBS Lett* **589**, 3461-3470 (2015).

50 Deretic, V. *et al.* Immunologic manifestations of autophagy. *J Clin Invest* **125**, 75-84 (2015).

51 Lee, H., Lund, J., Ramanathan, B., Mizushima, N. & Iwasaki, A. Autophagy-dependent viral recognition by plasmacytoid dendritic cells. *Science* **315**, 1398-1401 (2007).

52 Joven, J., Guirro, M., Mariné-Casadó, R., Rodríguez-Gallego, E. & Menéndez, J. Autophagy is an inflammation-related defensive mechanism against disease. *Adv Exp Med Biol* **824**, 43-59 (2014).

53 Levine, B., Mizushima, N. & Virgin, H. W. Autophagy in immunity and inflammation. *Nature* **469**, 323-335 (2011).

54 Woo, S. *et al.* Autophagy in tumor cells and the host STING pathway are critical for innate immune sensing of tumors and bridging to an adaptive immune response (P2183). *J Immunol* **190**, 1 Supplement (2013).

55 English, L. *et al.* Autophagy enhances the presentation of endogenous viral antigens on MHC class I molecules during HSV-1 infection. *Nature Immunology* **10**, doi:10.1038/ni.1720 (2009).

56 Lee, H. *et al.* In vivo requirement for Atg5 in antigen presentation by dendritic cells. *Immunity* **32**, 227-239 (2010).

57 Romao, S. *et al.* Autophagy proteins stabilize pathogen-containing phagosomes for prolonged MHC II antigen processing. *J Cell Bio* **203**, 757-766 (2013).

58 Joffre, O., Segura, E., Savina, A. & Amigorena, S. Cross-presentation by dendritic cells. *Nat Rev Immunol* **12**, 557-569 (2012).

59 Justine D Mintern, C. M., Wei Jin Chin, Scott E Panozza, Elodie Segura, Natalie L Patterson, Peter Zeller, Dorothee Bourges, Sammy Bedoui, Paul J McMillan, Adi Idris, Cameron J Nowell, Andrew Brown, Kristen J Radford, Angus PR Johnston & Villadangos, J. A. Differential use of autophagy by primary dendritic cells specialized in crosspresentation. *Autophagy* **11**, 906-917, doi:10.1080/15548627.2015.1045178 (2015).

60 Mintern, J., Macri, C. & Villadangos, J. Modulation of antigen presentation by intracellular trafficking. *Curr Opin Immunol* **34**, 16-21 (2015).

61 Spel, L., Boelens, J., Nierkens, S. & Boes, M. Antitumor immune responses mediated by dendritic cells: How signals derived from dying cancer cells drive antigen cross-presentation. *Oncoimmunology* **2**, e26403 (2013).

62 Segura, E. & Amigorena, S. Cross-Presentation in Mouse and Human Dendritic Cells. *Adv Immunol* **5**, 1-31 (2015).

63 Münz, C. Autophagy and antigen presentation. *Cellular Microbiology* **8**, 891-898 (2006).

64 Schiavoni, G., Mattei, F. & Gabriele, L. Type I Interferons as Stimulators of DC-Mediated Cross-Priming: Impact on Anti-Tumor Response. *Front Immunol* **4** (2013).

65 Shibutani, S. T., Saitoh, T., Nowag, H., Münz, C. & Yoshimori, T. Autophagy and autophagy-related proteins in the immune system. *Nature Immunology* **16**, 1014-1024 (2015).

66 Pua, H. H., Dzhagalov, I., Chuck, M., Mizushima, N. & He, Y.-W. A critical role for the autophagy gene Atg5 in T cell survival and proliferation. *The Journal of Experimental Medicine* **204**, 25-31, doi:10.1084/jem.20061303 (2006).

67 Chen, M., Kodali, S., Jang, A., Kuai, L. & Wang, J. Requirement for Autophagy in the Long-Term Persistence but not Initial Formation of Memory B cells. *J Immunol* **194**, 2607-2615 (2015).

68 Chen, M. *et al.* Essential Role for Autophagy in the Maintenance of Immunological Memory Against Influenza Infection. *Nat Med* **20**, 503-510 (2014).

69 Cenci, S. Autophagy, a new determinant of plasma cell differentiation and antibody responses. *Molecular Immunology* **62**, 289-295 (2014).

70 Puleston, D. J. *et al.* Autophagy is a critical regulator of memory CD8+ T cell formation. *eLife* **3**, e03706 (2014).

71 Bronietzki, A. W., Schuster, M. & Schmitz, I. Autophagy in T-cell development, activation and differentiation. *Immunology and Cell Biology* **93**, 25-34 (2015).

72 Xu, X. *et al.* Autophagy is essential for effector CD8 T cell survival and memory formation. *Nat Immunol* **15**, 1152-1161 (2014).

73 Hubbard, V. M. *et al.* Macroautophagy Regulates Energy Metabolism during Effector T Cell Activation. *J Immunol* **185**, 7349-7357 (2010).

74 Schlie, K. *et al.* Survival of Effector CD8+ T Cells during Influenza Infection Is Dependent on Autophagy. *J Immunol* **194**, 4277-4286 (2015).

75 Shitara, K. & Nishikawa, H. Regulatory T cells: a potential target in cancer immunotherapy. *Ann N Y Acad Sco*, doi:10.1111/nyas.13625 (2018).

76 Wei, J. *et al.* Autophagy enforces functional integrity of regulatory T cells by coupling environmental cues and metabolic homeostasis. *Nat Immunol* **17**, 277-285 (2016).

77 Le Texier, L. *et al.* Autophagy-dependent regulatory T cells are critical for the control of graft-versus-host disease. *JCI Insight* **1**, e86850 (2016).

78 Bartlett, D. L. *et al.* Oncolytic viruses as therapeutic cancer vaccines. *Mol Cancer* **12** (2013).

79 Elsedawy, N. & Russell, S. Oncolytic vaccines. *Expert Rev Vaccines* **12**, 1155-1172 (2013).

80 Russell, S. & Peng, K. Viruses as anticancer drugs. *Trends Pharmacol Sci* **28**, 326-333 (2007).

81 Workenhe, S. & Mossman, K. Oncolytic virotherapy and immunogenic cancer cell death: sharpening the sword for improved cancer treatment strategies. *Mol Ther* **22**, 251-256 (2014).

82 Guo, Z., Liu, Z. & Bartlett, D. Oncolytic Immunotherapy: Dying the Right Way is a Key to Eliciting Potent Antitumor Immunity. *Front Oncol* **4** (2014).

83 Lichty, B., Breitbach, C., Stojdl, D. & Bell, J. Going viral with cancer immunotherapy. *Nat Rev Cancer* **14**, 559-567 (2014).

84 Overwijk, W. *et al.* gp100/pmel 17 is a murine tumor rejection antigen: induction of "self"-reactive, tumoricidal T cells using high-affinity, altered peptide ligand. *J Exp Med* **188**, 277-286 (1998).

85 Bronte, V. *et al.* Genetic vaccination with "self" tyrosinase-related protein 2 causes melanoma eradication but not vitiligo. *Cancer Res* **60**, 253-258 (2000).

86 Harrington, K. *et al.* Clinical development of talimogene laherparepvec (T-VEC): a modified herpes simplex virus type-1-derived oncolytic immunotherapy. *Expert Rev Anticancer Ther*, 12 (2015).
87 Zhang, S. Turning killer into cure -- the story of oncolytic herpes simplex viruses. *Discov Med* **20**, 303-309 (2015).
88 Koplan, J. & Marton, K. Smallpox vaccination revisited. Some observations on the biology of vaccinia. *Am J Trop Med Hyg* **24**, 656-663 (1975).
89 Willis, N. Edward Jenner and the eradication of smallpox. *Scott Med J* **42**, 118-121 (1997).
90 Hruby, D. Vaccinia virus: a novel approach for molecular engineering of peptide vaccines. *Semin Hematol* **30**, 35-43 (1993).
91 Guse, K., Cerullo, V. & Hemminki, A. Oncolytic vaccinia virus for the treatment of cancer. *Expert Opin Biol Ther* **11**, 595-608 (2011).
92 Gomella, L. *et al.* Phase i study of intravesical vaccinia virus as a vector for gene therapy of bladder cancer. *J Urol* **166**, 1291-1295 (2001).
93 Breitbach, C. *et al.* Pexa-Vec double agent engineered vaccinia: oncolytic and active immunotherapeutic. *Curr Opin Virol* **13**, 49-54 (2015).
94 Cripe, T. *et al.* Phase 1 study of intratumoral Pexa-Vec (JX-594), an oncolytic and immunotherapeutic vaccinia virus, in pediatric cancer patients. *Mol Ther* **23**, 602-608 (2015).
95 Tsang, K. *et al.* Generation of human cytotoxic T cells specific for human carcinoembryonic antigen epitopes from patients immunized with recombinant vaccinia-CEA vaccine. *J Natl Cancer Inst* **87**, 982-990 (1995).
96 Kim, M. K. *et al.* Oncolytic and Immunotherapeutic Vaccinia Induces Antibody-Mediated Complement-Dependent Cancer Cell Lysis in Humans. *Science Translational Medicine* **5**, 185ra163 (2013).
97 Thorne, S. Immunotherapeutic potential of oncolytic vaccinia virus. *Front Oncol* **4** (2014).
98 Whilding, L. M. *et al.* Vaccinia Virus Induces Programmed Necrosis in Ovarian Cancer Cells. *Mol Ther* **21**, 2074-2086 (2013).
99 Zhang, H. *et al.* Cellular autophagy machinery is not required for vaccinia virus replication and maturation. *Autophagy* **2**, 91-95 (2006).
100 Lewis, J. D., Shearer, M. H., Kennedy, R. C. & Bright, R. K. Surrogate Tumor Antigen Vaccination Induces Tumor-Specific Immunity and the Rejection of Spontaneous Metastases. *Cancer Res* **65**, 2938-2946 (2005).
101 Janelle, V. *et al.* The Strength of the T Cell Response Against a Surrogate Tumor Antigen Induced by Oncolytic VSV Therapy Does Not Correlate With Tumor Control. *Mol Ther* **22**, 1198-1210 (2014).
102 Bellone, M. *et al.* Relevance of the Tumor Antigen in the Validation of Three Vaccination Strategies for Melanoma. *J Immunol* **165**, 2651-2656 (2000).
103 Janelle, V. & Lamarre, A. How Informative is the Immune Response Against Surrogate Tumor Antigens to Assess Antitumor Immunity? *Front Oncol* **4** (2014).
104 Rary, J., Cummings, D., Jones, H. J. & Rock, J. Assignment of the H-Y antigen gene to the short arm of chromosome Y. *J Hered* **70**, 78-80 (1979).
105 Scott, D. *et al.* Identification of a mouse male-specific transplantation antigen, H-Y. *Nature* **376**, 695-698 (1995).

106 Scott, D., Ehrmann, I., Ellis, P., Chandler, P. & Simpson, E. Why do some females reject males? The molecular basis for male-specific graft rejection. *J Mol Med* **75**, 103-114 (1997).
107 Simpson, E., Scott, D. & Chandler, P. THE MALE-SPECIFIC HISTOCOMPATIBILITY ANTIGEN, H-Y: A History of Transplantation, Immune Response Genes, Sex Determination and Expression Cloning. *Annu Rev Immunol* **15**, 39-61 (1997).
108 James, E. *et al.* HY peptides modulate transplantation responses to skin allografts. *International Immunology* **14**, 1333-1342 (2002).
109 Scott, D. *et al.* Dendritic cells permit identification of genes encoding MHC class II-restricted epitopes of transplantation antigens. *Immunity* **12**, 711-720 (2000).
110 Vogt, M. *et al.* UTY gene codes for an HLA-B60-restricted human male-specific minor histocompatibility antigen involved in stem cell graft rejection: characterization of the critical polymorphic amino acid residues for T-cell recognition. *Blood* **96**, 3126-3132 (2000).
111 Vogt, M. *et al.* The DBY gene codes for an HLA-DQ5-restricted human male-specific minor histocompatibility antigen involved in graft-versus-host disease. *Blood* **99**, 3027-3032 (2002).
112 Yang, A., Monken, C. & Lattime, E. Intratumoral vaccination with vaccinia-expressed tumor antigen and granulocyte macrophage colony-stimulating factor overcomes immunological ignorance to tumor antigen. *Cancer Res* **63**, 6956-6961 (2003).
113 Gabriel, E. *Modulation of Regulatory T cells overcomes systemic anergy to tumor-associated antigen and enhances the antitumor effects of recombinant vaccinia virus vaccines* PhD thesis, University of Medicine and Dentistry of New Jersey, (2007).
114 Halak, B., Maguire, H. J. & Lattime, E. Tumor-induced interleukin-10 inhibits type 1 immune responses directed at a tumor antigen as well as a non-tumor antigen present at the tumor site.

. *Cancer Res* **59**, 911-917 (1999).
115 Lattime, E., Gomella, L. & McCue, P. Murine Bladder Carcinoma Cells Present Antigen to BCG-specific CD4+ T-Cells. *Cancer Res* **52**, 4286-4290 (1992).
116 Yang, A. & Lattime, E. Tumor-induced interleukin 10 suppresses the ability of splenic dendritic cells to stimulate CD4 and CD8 T-cell responses. *Cancer Res* **63**, 2150-2157 (2003).
117 Karsli-Uzunbas, G. *et al.* Autophagy is required for glucose homeostasis and lung tumor maintenance. *Cancer Discov* **4**, 914-927 (2014).
118 Meeth, K., Wang, J., Micevic, G., Damsky, W. & Bosenberg, M. The YUMM lines: a series of congenic mouse melanoma cell lines with defined genetic alterations. *Pigment cell & melanoma research* **29**, 590-597 (2016).
119 Ruzankina, Y. *et al.* Deletion of the developmentally essential gene ATR in adult mice leads to age-related phenotypes and stem cell loss. *Cell Stem Cell* **1**, 131-126, doi:10.1016/j.stem.2007.03.002 (2007).
120 de Vries, C. *Characterization of systemic immune escape and the anti-tumor effectos of a recombinant vaccinia cirus expressing Her2/neu in a mouse model of Her2/neu-overexpressing breast cancer* PhD thesis, University of Medicine and Dentistry of New Jersey, (2013).
121 Nikitczuk, K., Schloss, R., Yarmush, M. & Lattime, E. PLGA-polymer encapsulating tumor antigen and CpG DNA administered into the tumor microenvironment elicits a systemic antigen-specific IFN-γ response and enhances survival. *J Cancer Ther* **4**, 280-290 (2013).

122 Ran, F. *et al.* Genome engineering using the CRISPR-Cas9 system. *Nature Protocols* **8**, 2281-2308, doi:10.1038/nprot.2013.143 (2013).

123 Vandesompele, J. *et al.* Accurate normalization of real-time quantitative RT-PCR data by geometric averaging of multiple internal control genes. *Genome Biol* **3** (2002).

124 Wang, J. *et al.* UV-induced somatic mutations elicit a functional T cell response in the YUMMER1.7 mouse melanoma model. *Pigment Cell Melanoma Res* **30**, 428-435 (2017).

125 Accolla, R. *et al.* Boosting the MHC Class II-Restricted Tumor Antigen Presentation to CD4+ T Helper Cells: A Critical Issue for Triggering Protective Immunity and Re-Orienting the Tumor Microenvironment Toward an Anti-Tumor State. *Front Oncol* **4**, doi:10.3389/fonc.2014.00032 (2014).

126 Thibodeau, J., Bourgeois-Daigneault, M. & Lapointe, R. Targeting the MHC Class II antigen presentation pathway in cancer immunotherapy. *Oncoimmunology* **1**, 908-916 (2012).

127 Curiel, T. Tregs and rethinking cancer immunotherapy. *J Clin Invest* **117**, 1167-1174 (2007).

128 Knutson, K., Disis, M. & Salazar, L. CD4 regulatory T cells in human cancer pathogenesis. *Cancer Immunol Immunother* **56**, 271-285 (2007).

129 Ma, Y., Galluzzi, L., Zitvogel, L. & Kroemer, G. Autophagy and cellular immune responses. *Immunity* **39**, 211-227 (2013).

130 Zhong, Z., Sanchez-Lopez, E. & Karin, M. Autophagy, Inflammation, and Immunity: A Troika Governing Cancer and Its Treatment. *Cell* **166**, 288-298 (2016).

131 Schmid, D., Pypaert, M. & Münz, C. Antigen-loading compartments for major histocompatibility complex class II molecules continuously receive input from autophagosomes. *Immunity* **26**, 79-92 (2007).

132 Li, Y. *et al.* Efficient Cross-presentation Depends on Autophagy in Tumor Cells. *Cancer Res* **68**, 6889-6895 (2008).

133 Li, B. *et al.* Autophagy facilitates major histocompatibility complex class I expression induced by IFN-γ in B16 melanoma cells. *Cancer Immunol Immunother* **59**, 313-321 (2010).

134 Henault, J. *et al.* Noncanonical Autophagy Is Required for Type I Interferon Secretion in Response to DNA-Immune Complexes. *Immunity* **37**, 986-997 (2012).

135 Chang, Y. *et al.* Autophagy Facilitates IFN-γ-induced Jak2-STAT1 Activation and Cellular Inflammation. *J Biol Chem* **285**, 28715-28722, doi:10.1074/jbc.M110.133355 (2010).

136 Saitoh, T. *et al.* Loss of the autophagy protein Atg16L1 enhances endotoxin-induced IL-1beta production. *Nature* **456**, 264-268 (2008).

137 Nakahira, K. *et al.* Autophagy proteins regulate innate immune responses by inhibiting the release of mitochondrial DNA mediated by the NALP3 inflammasome. *Nat Immunol* **12**, 222-230 (2011).

138 Pua, H., Dzhagalov, I., Chuck, M., Mizushima, N. & He, Y. A critical role for the autophagy gene Atg5 in T cell survival and proliferation. *J Exp Med* **204**, 25-31 (2007).

139 Mortensen, M. *et al.* The autophagy protein Atg7 is essential for hematopoietic stem cell maintenance. *J Exp Med* **208**, 455-467 (2011).

140 Ilyas, S. & Yang, J. Landscape of Tumor Antigens in T Cell Immunotherapy. *J Immunol* **195**, 5117-5122 (2015).

141 Finnigan, J. J., Rubinsteyn, A., Hammerbacher, J. & Bhardwaj, N. Mutation-Derived Tumor Antigens: Novel Targets in Cancer Immunotherapy. *Oncology (Williston Park)* **29**, 970-972, 974-975 (2015).

142 Lu, Y. & Robbins, P. Cancer immunotherapy targeting neoantigens. *Seminars in Immunology* **28**, 22-27 (2016).
143 Saitoh, T. *et al.* Atg9a controls dsDNA-driven dynamic translocation of STING and the innate immune response. *Proc Natl Acad Sci U S A* **106**, 20842-20846 (2009).
144 Collison, L. & Vignali, D. In vitro Treg suppression assays. *Methods Mol Biol* **707**, 21-37 (2011).
145 Caton, M., Smith-Raska, M. & Reizis, B. Notch-RBP-J signaling controls the homeostasis of CD8- dendritic cells in the spleen. *J Exp Med* **204**, 1653-1664 (2007).
146 Pasquier, B. Autophagy inhibitors. *Cell Mol Life Sci* **73**, 985-1001 (2016).

ABBREVIATIONS

2-ME – 2-mercaptoethanol

ACK - ammonium chloride buffer

APCs – Antigen-presenting cells

DCs – Dendritic cells

fB6 – Female C57BL/6J mice

FBS – Fetal bovine serum

GM-CSF – granulocyte macrophage colony-stimulating factor

i.p. – intraperitoneally

KLH - keyhole limpet hemocyanin

mB6 – Male C57BL/6J mice

MDSCs – myeloid-derived suppressor cells

OVs – Oncolytic viruses

PFUs – plaque-forming units

s.c. – subcutaneously

TAAs – Tumor associated antigens

TAM - Tamoxifen

TCM – T cell media

TILs – Tumor infiltrating lymphocytes

Tregs – regulatory T cells

VV – Vaccinia Virus